NASA TECHNICAL MEMORANDUM

NASA TM X-73653

NASA TM X-73653

(NASA-TM-X-73653) INTERACTIVE CALCULATION PROCEDURE FOR SUPERSONIC FLOWS Ph.D. Thesis - Case Western Reserve Univ., 1976. Final Report (NASA) 170 p HC A08/MF A01 CSCL 20D

N77-23408

Unclas
G3/34 29075

INTERACTIVE CALCULATION PROCEDURE FOR SUPERSONIC FLOWS

by Yehuda Tassa, Bernhard H. Anderson,
and Eli Reshotko
Lewis Research Center
Cleveland, Ohio 44135

May 1977

1. Report No.	2. Government Accession No.	3. Recipient's Catalog No.
NASA TM X-73653		

4. Title and Subtitle	5. Report Date
INTERACTIVE CALCULATION PROCEDURE FOR SUPERSONIC FLOWS	April 1977
	6. Performing Organization Code

7. Author(s)	8. Performing Organization Report No.
Yehuda Tassa, Case Western Reserve University; Bernhard H. Anderson, NASA Lewis Research Center; and Eli Reshotko, Case Western Reserve University	FTAS/TR-76-125
	10. Work Unit No.

9. Performing Organization Name and Address	11. Contract or Grant No.
Case Western Reserve University 2040 Adelbert Road Cleveland, Ohio 44106	NGR 36-027-064
	13. Type of Report and Period Covered
12. Sponsoring Agency Name and Address	Technical Memorandum
National Aeronautics and Space Administration Washington, D.C. 20546	14. Sponsoring Agency Code

15. Supplementary Notes

Report was submitted as a thesis by the first author in partial fulfillment of the requirements for the degree Doctor of Philosophy at Case Western Reserve University in August 1976. Final report. Project Manager, Allan R. Bishop, Wind Tunnel and Flight Division, NASA Lewis Research Center, Cleveland, Ohio.

16. Abstract

An interactive procedure has been developed for supersonic viscous flows that can be used for either two-dimensional or axisymmetric configurations. The procedure is directed to supersonic internal flows as well as those supersonic external flows that require consideration of mutual interaction between the outer flow and the boundary layer flow. The flow field is divided into two regions: (a) an inner region which is highly viscous and mostly subsonic and (b) an outer region where the flow is supersonic and in which viscous effects are small but not negligible. For the outer region a numerical solution is obtained by applying the method of characteristics to a system of equations which includes viscous and conduction transport terms only normal to the streamlines. The inner region is treated by a system of equations of the boundary layer type that includes higher order effects such as longitudinal and transverse curvature and normal pressure gradients. These equations are coupled and solved simultaneously in the physical coordinates by using an implicit finite difference scheme. This system can also be used to calculate laminar and turbulent boundary layers using a scalar eddy viscosity concept. In the interactive mode, the two regions are coupled interactively along a matching line where the Mach number is of the order of 1.2. Numerical results for the outer region in the noninteractive mode agree very well with experiments and other numerical results. For the inner region stable and convergent solutions have been obtained for compressible boundary layers over flat plate and axisymmetric configurations. Agreement with available exact solutions is very good. In the interactive mode results were obtained for the axisymmetric waisted body configuration of Winter, Smith, and Rotta assuming laminar flow. The numerical results indicate a slight but noticeable effect on the pressure distribution when compared with the results of noninteractive characteristics solutions.

17. Key Words (Suggested by Author(s))	18. Distribution Statement
Axisymmetric; Supersonic; Viscous; Boundary layer; Turbulent; Laminar	Unclassified - unlimited STAR Category 34

19. Security Classif. (of this report)	20. Security Classif. (of this page)	21. No. of Pages	22. Price*
Unclassified	Unclassified	169	A08

* For sale by the National Technical Information Service, Springfield, Virginia 22161

TABLE OF CONTENTS

LIST OF FIGURES

CHAPTER I

INTRODUCTION

It has been recognized for some time that proper calculation of supersonic internal and external flows requires consideration of the mutual interaction between the highly viscous region near the surface and the weakly viscous region away from the surface. For supersonic internal flows such as in mixed compression inlets or in exit nozzles it is furthermore desirable to be able to track the shock structure even into the boundary layer to properly incorporate design features such as for example boundary layer control.

Over the past decade much interest and effort have been devoted to viscous-inviscid interaction analyses. However, most of these methods have failed adequately to predict experimental data on configurations with significant curvatures or in situations such as at high Mach numbers where the boundary layer is relatively thick. Generally there are two reasons for this failure: a) The interaction procedure between the inviscid supersonic region and the highly viscous layer near the wall may have some impropriety, and b) the description of the viscous layer in the classical boundary layer manner is inadequate when curvature effects are important.

There are several approaches for attacking the viscous-inviscid interaction problem in supersonic flow. The ultimate approach would be to solve the time dependent Navier-Stokes equations for the whole

flow field thus eliminating the patching procedure between the viscous region near the surface and the inviscid region away from the wall. However since the Navier-Stokes equations are spatially elliptic it is unfeasible and impractical from the points of view of both computer storage and running time. The objective of the present work is to develop a viscous-inviscid interactive procedure in supersonic flow that represents an intermediate development between past treatments and exact solution of the Navier-Stokes equations. The interactive flow analysis developed herein is based on dividing the flow field into regions where in one region the flow is supersonic with a dominant inviscid character and is treated by a hyperbolic system of equations, while the second region where the flow is highly viscous is treated by a parabolic set of equations. In both regions forward marching techniques can be used thus considerably reducing storage and time requirements. However when replacing the Navier-Stokes equations that are elliptic with sets of equations that are hyperbolic and parabolic in character, there is no capability of directly dealing with upstream influence effects. Hence the present procedure cannot handle flow separation or strong shock interactions where the elliptic behavior is important.

A. Applicable Earlier Work

The interaction methods that have been developed for supersonic flow all consider the flow field to consist of two regions. Generally these regions are a boundary layer or equivalent viscous layer and an external supersonic region. The methods however differ in the

complexity of the modeling assumptions for each of the regions and in the coupling procedures for effecting interaction.

An early but most significant formulation of an interaction procedure for supersonic flows was by Crocco and Lees (reference 1). In their work they related the pressure distribution of the external supersonic flow to the local slope of the displacement thickness of the viscous region using the Prandtl-Meyer relation which is a one-family characteristics procedure. The viscous layer in the Crocco-Lees procedure is based on the classical boundary layer approximation but was treated as a mixing layer using a specially-developed momentum integral procedure. Lees and Reeves (reference 2) extended the Crocco-Lees method by additionally employing a moment of momentum integral equation to improve the treatment of entrainment. The extension of the Lees-Reeves integral interaction procedure to include consideration of heat transfer was by Klineberg and Lees (reference 3).

Reyhner and Flugge-Lotz (reference 4) improved the treatment of the viscous portion of the interaction analysis by applying a full finite difference technique to solution of the compressible laminar boundary layer equations in the physical plane. The boundary layer is treated in the classical limit with the normal pressure gradient taken as zero. As with the earlier described procedures, the coupling between pressure and local streamline deflection at the edge of the boundary layer is through the Prandtl-Meyer relation.

Miller (reference 5) argues however that the inviscid flow must be calculated by a two-family characteristics method in order to

obtain a mathematically well-posed supersonic interactive problem, and thus eliminate the saddle point type singularity that is introduced by using the Prandtl-Meyer relation which is a one-family characteristics solution.

Ferri and Dash (reference 6) improved the treatment of viscous-inviscid interactions in supersonic flow in two ways: first, by applying a higher approximation for the boundary layer that includes normal pressure gradient and longitudinal curvature effects, and second, by using a two-family rotational characteristics scheme in the outer region that allows for entropy changes due to viscous effects. The pressure distribution across the viscous region was assumed to be a polynomial of fourth degree uncoupled from the rest of the system. The coefficients were determined by assuming that the first and second normal derivatives of the pressure at the wall are zero and that the remaining terms are dependent on the longitudinal curvature effects. The system of equations obtained were solved numerically. In the viscous region the x-momentum and the energyequations were expressed in finite difference form and solved simultaneously for u and T. The normal velocity distribution was obtained by integration of the continuity equation and the process repeated iteratively until convergence was obtained for u, v, T and p.

B. The Present Method

The present work is an extension of the idea of Ferri and Dash (reference 6) wherein the flow field is divided into two regions: a) an inner region which is highly viscous and mostly subsonic and

b) an outer region where the flow is supersonic and in which viscous effects are small but not negligible.

The inner region is treated by a system of equations of the boundary layer type. This system is obtained by reexamining the Navier-Stokes equations for steady compressible two-dimensional or axisymmetric flow in curvilinear coordinates and through an ordering procedure retaining terms of order unity and (δ/L). In addition to the classical boundary layer equations the system of equations so obtained includes in a consistent way the second order effects of longitudinal and transverse curvature as well as normal pressure gradient.

In this system the normal momentum equation is retained. The equations are a coupled parabolic set in the longitudinal velocity, u, the normal velocity component, v, and the static temperature, T. By incorporating a suitable effective viscosity hypothesis, the system can be used to calculate both laminar and turbulent boundary layers. The system of equations obtained is solved simultaneously in the physical coordinate plane using an implicit finite difference technique. This procedure provides an exact and stable numerical solution to the viscous flow equations in the inner region.

The numerical solutions for the outer region are obtained by applying the method of characteristics to a system of equations which includes viscous and conductive transport terms normal to streamlines. In this streamline-normal coordinate system, terms of order unity and (δ/L) are retained for the viscous and heat flux

terms added, whereas curvature effects are kept fully. By introducing the transport terms as corrections, the equations retain their hyperbolic character. These correction terms include additional second order terms, over and above those retained by Ferri and Dash (reference 6). The solution of the characteristic equations have been structured as an inverse grid scheme in a streamline-normal network. In this reverse scheme both characteristic Mach lines are extended back until they intersect the known data region on a normal to the streamlines. The streamline condition has been replaced by a streamfunction condition thereby preserving mass flow within a stream tube. This allows for a very equitable mesh distribution which always maintains itself in the downstream direction without redistribution of the grid points. The resulting system of equations in both the outer and the inner regions are consistent to order (δ/L).

In the interactive mode following the suggestion of Ferri and Dash (reference 6), the inner and the outer regions are matched along a line where the Mach number is approximately 1.2. The matching conditions are continuity of the flow variables u, v, T and p at the interface. The detailed algorithm of the interactive procedure for the interaction mode is given.

Each of the portions of this analysis will be discussed separately. The development of equations and numerical solution procedure for the outer region together with some illustrative examples is presented in Chapter II. This is followed in Chapter III by an equivalent presentation for the inner region. The interaction procedure between

the two regions is described in Chapter IV. Discussion and summary of the major portion of the present work is given in Chapter V.

CHAPTER II

OUTER REGION

A. Equations of Motion

The equations of motion for the outer region are written for steady viscous compressible two-dimensional or axisymmetric flow. These equations for the coordinate system shown in figure 1 are:

Continuity

$$\frac{\partial}{\partial x^*}(\rho^* u^* y^{*\sigma}) + \frac{\partial}{\partial y^*}(\rho^* v^* y^{*\sigma}) = 0 \tag{1}$$

Longitudinal momentum

$$\rho^* u^* \frac{\partial u^*}{\partial x^*} + \rho^* v^* \frac{\partial u^*}{\partial y^*} = -\frac{\partial p^*}{\partial x^*} + \frac{1}{y^{*\sigma}} \frac{\partial}{\partial y^*}(\mu^* y^{*\sigma} \frac{\partial u^*}{\partial y^*}) + \frac{\partial}{\partial x^*}(\mu^* \frac{\partial u^*}{\partial x^*}) \tag{2}$$

Normal-momentum

$$\rho^* u^* \frac{\partial v^*}{\partial x^*} + \rho^* v^* \frac{\partial v^*}{\partial y^*} = -\frac{\partial p^*}{\partial y^*} + \frac{1}{y^{*\sigma}} \frac{\partial}{\partial y^*}(\mu^* y^{*\sigma} \frac{\partial v^*}{\partial y^*}) + \frac{\partial}{\partial x^*}(\mu^* \frac{\partial v^*}{\partial x^*}) \tag{3}$$

Energy

$$\rho^* u^* C_p^* \frac{\partial T^*}{\partial x^*} + \rho^* v^* C_p^* \frac{\partial T^*}{\partial y^*} - (u^* \frac{\partial p^*}{\partial x^*} + v^* \frac{\partial p^*}{\partial y^*}) = \frac{1}{y^{*\sigma}} \frac{\partial}{\partial y^*}(y^{*\sigma} k^* \frac{\partial T^*}{\partial y^*}) + \frac{\partial}{\partial x^*}(k^* \frac{\partial T^*}{\partial x^*}) + \mu^*[\frac{\partial u^*}{\partial y^*} + \frac{\partial v^*}{\partial x^*}]^2 + 2\mu^*[(\frac{\partial u^*}{\partial x^*})^2 + (\frac{\partial v^*}{\partial y^*})^2] \tag{4}$$

Equation of State

$$p^* = \rho^* R^* T^* \tag{5}$$

In these equations

$\sigma = 1$ for axisymmetric flow

$\sigma = 0$ for two-dimensional flow.

The equations of motions (1) to (5) are made dimensionless in the following manner:

$$u = \frac{u^*}{u_{REF}};\ v = \frac{v^*}{u_{REF}};\ p = \frac{p^*}{p_{REF}};\ \rho = \frac{\rho^*}{\rho_{REF}};\ T = \frac{T^*}{T_{REF}};\ x = \frac{x^*}{L_{REF}}$$

$$y = \frac{y^*}{L_{REF}};\ \mu = \frac{\mu^*}{\mu_{REF}};\ C_p = \frac{C_p^*}{C_{p_{REF}}};\ k = \frac{k^*}{k_{REF}}. \tag{6}$$

The resulting dimensionless equations are:

Continuity

$$\frac{\partial}{\partial x}(\rho u y^\sigma) + \frac{\partial}{\partial y}(\rho v y^\sigma) = 0 \tag{7}$$

Longitudinal-momentum

$$\rho u \frac{\partial u}{\partial x} + \rho v \frac{\partial u}{y} = -\frac{1}{\gamma M^2_{REF}} \frac{\partial p}{\partial x} + \frac{1}{Re_{REF}} \left\{\frac{1}{y^\sigma}\frac{\partial}{\partial y}(\mu y^\sigma \frac{\partial u}{\partial y}) + \frac{\partial}{\partial x}(\mu \frac{\partial u}{\partial x})\right\} \tag{8}$$

Normal-momentum

$$\rho u \frac{\partial v}{\partial x} + \rho v \frac{\partial v}{\partial y} = -\frac{1}{\gamma M^2_{REF}} \frac{\partial p}{\partial y} + \frac{1}{Re_{REF}} \left\{\frac{1}{y^\sigma}\frac{\partial}{\partial y}(\mu y^\sigma \frac{\partial v}{\partial y}) + \frac{\partial}{\partial x}(\mu \frac{\partial v}{\partial x})\right\} \tag{9}$$

Energy

$$\rho u C_p \frac{\partial T}{\partial x} + \rho v C_p \frac{\partial T}{\partial y} - \frac{(\gamma-1)}{\gamma}\left(u \frac{\partial p}{\partial x} + v \frac{\partial p}{\partial y}\right)$$

$$= \frac{1}{Pr_{REF} Re_{REF}} \frac{1}{y^{\sigma}} \frac{\partial}{\partial y}\left(y^{\sigma} k \frac{\partial T}{\partial y}\right) + \frac{1}{Pr_{REF} Re_{REF}} \frac{\partial}{\partial x}\left(k \frac{\partial T}{\partial x}\right.$$

$$+ \frac{(\gamma-1)M_{REF}^2}{Re_{REF}} \mu\left[\left(\frac{\partial u}{\partial y} + \frac{\partial v}{\partial x}\right)^2 + 2\left(\left(\frac{\partial u}{\partial x}\right)^2 + \left(\frac{\partial v}{\partial y}\right)^2\right)\right] \qquad (10)$$

Equation of state

$$p = \rho T \qquad (11)$$

where:

$$M_{REF} \equiv \frac{u_{REF}}{(\gamma R T_{REF})^{1/2}} \quad - \quad \text{Reference Mach number}$$

$$Re_{REF} \equiv \frac{\rho_{REF} u_{REF} L_{REF}}{\mu_{REF}} \quad - \quad \text{Reference Reynolds number}$$

$$Pr_{REF} \equiv \frac{\mu_{REF} C_{p_{REF}}}{K_{REF}} \quad - \quad \text{Reference Prandtl number}$$

The equations of motions (7) to (11) are now transformed from cartesian coordinates (x,y) to curvilinear coordinates (s,n) where: s and n are respectively the distance along a streamline and the distance normal to a streamline. Transport effects such as viscous shear and heat flux are retained only normal to the streamline. This is because from an ordering procedure, terms such as $\frac{\partial^2}{\partial s^2}/\frac{\partial^2}{\partial n^2}$ are of order of $(\delta/L)^2$ that can be neglected in the present analysis.

The governing equations (7) to (11) when transformed and simplified (details given in Appendix A) are:

Continuity

$$\frac{\partial}{\partial s}(\rho q) + \rho q \frac{\partial \theta}{\partial n} = -\sigma \frac{\rho q}{y} \sin\theta \tag{12}$$

s-momentum

$$\rho q \frac{\partial q}{\partial s} + \frac{1}{\gamma M_{REF}^2} \frac{\partial p}{\partial s} = Q_1 \tag{13}$$

n-momentum

$$\rho q^2 \frac{\partial \theta}{\partial s} + \frac{1}{\gamma M_{REF}^2} \frac{\partial p}{\partial n} = Q_2 \tag{14}$$

Energy equation

$$\rho q \frac{\partial T}{\partial s} - \frac{(\gamma-1)}{\gamma} q \frac{\partial p}{\partial s} = (\gamma-1) M_{REF}^2 Q_3 \tag{15}$$

Equation of state

$$p = \rho T \tag{16}$$

where q is the velocity in the streamline direction, θ is the streamline direction and Q_1, Q_2, Q_3 are correction terms due to viscous shear and heat flux. The detailed expressions for the correction terms are rewritten here:

$$Q_1 = \frac{1}{Re_{REF}} \{\frac{\partial}{\partial n}(\mu \frac{\partial q}{\partial n}) + \sigma \frac{\mu \cos\theta}{y} \frac{\partial q}{\partial n} - \mu q (\frac{\partial \theta}{\partial n})^2 - \frac{\sigma \mu}{y} \sin^2\theta \frac{\partial q}{\partial n}\} \tag{17}$$

$$Q_2 = \frac{1}{Re_{REF}} \{\mu \frac{\partial q}{\partial n} \frac{\partial \theta}{\partial n} + \frac{\sigma \mu}{y} q \cos^3\theta \frac{\partial \theta}{\partial n} + \frac{\partial}{\partial n}(\mu q \frac{\partial \theta}{\partial n})\} \tag{18}$$

$$Q_3 = \frac{1}{Re_{REF}} \{\mu (\frac{\partial q}{\partial n})^2 + 2\mu q^2 (\frac{\partial \theta}{\partial n})^2 + \frac{1}{Pr_{REF}(\gamma-1)M_{REF}^2} [\frac{\partial}{\partial n}(\mu \frac{\partial T}{\partial n}) + \frac{\sigma \mu}{y} \cos^3\theta \frac{\partial T}{\partial n}]\} \tag{19}$$

By considering these terms as known source terms the systems of equations (12) to (16) retains its hyperbolic character.

B. Method of Characteristics

The characteristics derived from the system of equations (12) to (16) are defined by two ordinary first order differential equations where the independent variables are the static pressure, p and the streamline direction, θ. The detailed derivation of the characteristics relations is given in Appendix B.

The characteristics equation is:

$$\frac{dn}{ds} = \pm\tan\lambda \tag{20}$$

where $\lambda = \sin^{-1}\frac{1}{M}$ is the Mach angle. These characteristic directions are the same as for inviscid flow. The compatability relation is given by:

$$\frac{dp}{\gamma p} \pm \frac{d\theta}{\sin\lambda\cos\lambda} + \left[\frac{\sigma\sin\theta}{y} + \frac{Q_1}{\rho q^2} - \frac{(\gamma-1)M_{REF}^2}{pq}Q_3 \pm \frac{Q_2 M_{REF}^2 \sin\lambda}{p}\right]\frac{dx}{\cos\lambda\cos(\theta\pm\lambda)} = 0 \tag{21}$$

The + and - signs correspond to C^+ and C^- characteristic lines respectively. The quantities Q_1, Q_2, Q_3 are functions of the local normal gradients of velocity and temperature and have the same role as the entropy terms in equivalent equations for inviscid rotational flows.

The variations of entropy, S, and stagnation temperature along the streamline as derived in Appendix B are:

$$\frac{dS}{ds} = \frac{\gamma M_{REF}^2}{pq} Q_3 \tag{22}$$

$$\frac{dT_s}{ds} = \frac{(\gamma-1)M_{REF}^2}{\rho q} Q_3 + \frac{Q_1(\gamma-1)M_{REF}^2}{\rho} \qquad (23)$$

The oblique shock wave relation required in dealing with shock points in the characteristic net is obtained from Reference (7) and is given by:

$$\sin^6\beta_{SH} + b\sin^4\beta_{SH} + c\sin^2\beta_{SH} + d = 0 \qquad (24)$$

where

β_{SH} is the shock angle

$$b = -\frac{M^2+2}{M^2} - \gamma\sin^2\delta$$

$$c = \frac{2M^2+1}{M^4} + \left[\left(\frac{\gamma+1}{2}\right)^2 + \frac{(\gamma-1)}{M^2}\right]\sin^2\delta$$

$$d = -\frac{\cos^2\delta}{M^4}$$

In these equations, M is the Mach number upstream of shock wave and δ is the local streamline deflection angle.

In order to establish a well-posed problem, the following boundary conditions must be given:

(a) data for all quantities must be prescribed along an initial datum line. In the absence of the correction terms Q_1, Q_2 and Q_3, only p, θ and M need be specified to allow the characteristics calculation to proceed. However, upon including Q_1, Q_2 and Q_3 the velocity and temperature information is needed as well.

(b) the shape of the boundary surface or bounding streamline, $y = y_B(x)$.

C. Numerical Procedure

The conditions at each grid point (x,y) in the physical plane

are determined by the characteristic equation (20) and the compatibility condition (21). A non-uniform grid point distribution on the normal to the streamline is chosen to allow a fine mesh spacing in the inner portion of the outer region and coarse spacing at the outer portion of the outer region. The computational procedure divides itself into the following four basic elements:

1. Conical flow field calculation (for axisymmetric flow)
2. Boundary point calculation
3. Field point calculation
4. Shock point calculation

Conical Flow Field Calculation - The flow past an infinite cone with attached shock front is described by the Taylor-Maccoll equations which are solved numerically by means of Runge-Kutta integration (see Appendix C). The conical shock angle, β_{SH} is calculated by an iterative procedure beginning with a first guess of the shock angle for the given freestream conditions. The integration is continued to the cone surface and the resultant cone angle compared with the specified cone angle. A new estimate of the shock angle β_{SH} is made based on the error and the process is repeated until convergence is obtained. The converged solution gives complete information on the conical flow field.

Boundary Point Calculation - Calculation of a boundary point (Fig. 2) requires that the normal velocity at the boundary point be zero. The boundary point A can be either on a solid boundary or a point on a prescribed streamline whose deflection is known. The pressure at the boundary point A is calculated in an iterative way. Using a reverse scheme the C- characteristic is extended from point A in the upstream direction until it intersects the normal to the

streamlines at point B. The flow variables at point B are determined by interpolation. Using average values of points A and B the compatibility condition for the C- characteristic curve will give new flow variables for point A in terms of the known values at point B. Iteration is continued until convergence is obtained for point A.

Field Point Calculation - Calculation of point D (Fig. 3) is done using the reverse scheme, that is both the C+ characteristic and the C- characteristic lines are extended from point D in the upstream direction where they intersect the upstream datum line at points A and B respectively. Point D is located on the normal to the streamline through point E [x(2,J-1), y(2,J-1)].

The compatibility equations at point D determine the flow variables and the streamline slope for point D in terms of the flow variables at points A and B. Integrating the mass flow between point D and the previously calculated point E [x(2,J-1), y(2,J-1)] the stream function at point D is:

$$\psi_D = \psi_E + \Delta\psi \tag{25}$$

In order to preserve mass, the new location of point D on the normal to the streamline, is corrected with respect to the difference defined by:

$$\delta\psi = \psi_D - \psi(J) \tag{26}$$

Normally convergence is obtained in a few iterations.

Shock-Point Calculation - Shock point calculations are basically different than the field point calculations. Since conditions upstream of the shock wave are known, the oblique shock relations must be incorporated into the calculation procedure.

Point B (Fig. 4) is located just downstream of the shock wave and on the normal to the streamline from point C[x(2,J-1), y(2,J-1)]. An initial guess is required for the flow variables and streamline deflection at point B. Then point A can be determined by the intersection of the C+ characteristic through point B and the upstream normal to the streamlines. The shock wave angle is calculated using equation (24). This determines the flow variables at point B from oblique shock wave relations. The coefficients of the compatibility equation are updated using averages of the flow variables at points A and B. The streamline deflection is recalculated and thus a new shock wave angle is calculated. Again in an iterative way, convergence is obtained.

D. Numerical Results

To test and illustrate the procedure developed for the outer region, two sets of calculations were performed. The first of these is for the waisted body tested by Winter, Smith and Rotta (reference 8) while the second set is for a Mach number 3.5 mixed compression inlet for which characteristics calculations were performed by Syberg and Hickcox (reference 9) using a different scheme than developed herein.

The geometry of the waisted body of revolution is described (figure 5) by a set of five polynomial functions each pertaining to only a section of the body. Calculations were performed for a series of supersonic Mach numbers for which experimental data are available. The correction terms Q_1, Q_2 and Q_3 have been excluded

in these calculations.

Figure 6 shows the oblique shock waves for M_∞ = 1.7, 2.0, 2.4 and 2.8. The wall Mach number distributions along the body are shown in figure 7 for the same free stream Mach numbers. A comparison of the calculated Mach number distribution on the surface and the measured Mach number distribution at the edge of the boundary layer (reference 8) shown in figure 7 shows very good agreement except perhaps at M_∞ = 2.8 in the vicinity of $\frac{x}{L_{REF}} \approx 0.4$. Examination of the experimental velocity profile at this Mach number and location (figure 9 of reference 8) shows that the velocity is still slowly increasing beyond the nominal "edge" of the boundary layer as chosen by Winter et al (reference 8).

The calculated wall static pressure distributions for the same free stream Mach numbers are shown in figure 8. It is seen that the pressure minimum occurs consistently in the vicinity of the inflection point of the body ($\frac{x}{L_{REF}} \approx 0.42$). Unfortunately, experimental wall pressure data are not available in reference 8 for comparison with these results.

The streamline patterns as calculated for the waisted body at M_∞ = 1.7 and M_∞ = 2.8 are shown in figures 9 and 10 respectively. Of particular interest is the appearance at M_∞ = 2.8 of a noticeable second shock wave in the flow field emanating from $x/L_{REF} \approx 0.75$. This wave for the same Mach 2.8 test of Winter, Smith and Rotta was also identified in the "smooth shock-capturing" calculation of reference 10.

Figure 11 shows the pressure distribution along normals to the streamlines emanating from a number of stations on the body. The presentation for $M_\infty = 1.7$ (figure 11a) is a composite of the pressures along the normals to the streamlines labeled A through N in figure 9. The ordinate in figure 11a is $(y-y_B)/(y_{SH}-y_B)$ for the points on the aforementioned normal lines. From the pressure distributions for $x_B/L_{REF} \geq 0.787$, a mild shock wave seems to appear in the pressure distribution although there is no apparent corresponding streamline deflection in figure 9.

Figure 11b gives a similar portrayal for $M_\infty = 2.8$. The shock wave appearing in the pressure distribution for $x_B/L_{REF} \geq 0.787$ is readily identified with the locus of streamline deflections in figure 10 and is coincident with the shock location as calculated in reference 10.

Numerical calculations were also done for the Mach number 3.5 mixed compression inlet sketched in figure 12. Geometrical data for this inlet are given in reference 9. The pressure distribution calculated with the inlet by both the present streamline-normal procedure excluding the correction terms Q_1, Q_2 and Q_3 and by the more conventional characteristics scheme of reference 9 are compared in figure 13 for the center body surface and in figure 14 for the cowl surface. The excellent agreement between the two computational schemes indicates that little if any accuracy is lost by neglecting Mach wave intersections between the datum planes that is characteristic of inverse scheme methods.

In order to investigate the effects of the correction terms in the outer region, a power law velocity profile (n=11) of suitable thickness has been imposed in the initial datum line where the wall Mach number was chosen as Mw = 1.9. The wave pattern for the mixed compression inlet is calculated both with and without the correction terms. For the purposes of this exercise, the correction terms are evaluated using Sutherland viscosity and Pr = 0.72. The numerical results shown in figure 15 indicate a shift of the wave location and curving of the wave reflection due to the viscous and conduction terms. This partial simulation of the presence of a boundary layer gives some indication of what might be expected in an interactive calculation.

CHAPTER III

INNER REGION

The various methods for dealing with the viscous region differ in the order of the terms kept in the system of governing equations. In past work on interactions the tendency has been to use classical boundary layer equations (with $\frac{\partial p}{\partial y} = 0$) or else such equations augmented by a centrifugal correction for normal pressure gradients. The present interaction procedure depends however on having accurate representations of the normal velocity distributions at the matching location in the boundary layer even in situations with longitudinal and transverse curvature. Hence it is desirable herein to employ a set of equations that are consistent to order (δ/L) relative to the leading or classical boundary layer equations. In that way the sets of equations for the inner and outer regions are consistent to order (δ/L). Within this second order approximation, the normal momentum equation appears as a coupled member of the set of inner layer equations. Before proceeding into the details, a brief review of pertinent second-order effects is appropriate.

The boundary-layer concept introduced by Prandtl has been successful in yielding solutions for viscous flows at high Reynolds numbers, as long as the boundary layer remains attached to the surface and remains thin enough so that it does not noticably affect the external flow. A general discussion of higher-order approximation

for boundary layers has been given by Van Dyke (reference 11). In that review article, Van Dyke classified the second-order corrections into two categories according to whether the additional terms appear in the differential equation through the curvatures or through interaction with the external flow. Van Dyke further subdivided each category giving some analytical details and physical interpertation for the described effects.

Maslen (reference 12) has presented a set of equations that is complete with respect to the inclusion of second order boundary-layer effects. This set of equations is the starting set for the developments in this chapter. Maslen himself in reference 12 went on to study some weak interaction questions by means of similarity solutions. Seginer (reference 13) solved a system of equations retaining terms to order $\left(\frac{1}{Re_{L_{REF}}}\right)^{1/2}$ where $Re_{L_{REF}}$ is the reference length Reynolds number. In his system the normal momentum equation is a coupled member of the parabolic set of governing equations. Seginer then went on using the Stewartson transformation and similarity arguments to obtain ordinary differential equations for the second order boundary layer system. He obtained solutions for a two-dimensional flat plate at Mach number 4 to illustrate the very slight effect even for that case of the normal pressure gradient.

The present system draws on both of the above works in its development of the second order system of equations but the solution procedure is developed in physical coordinates for later interactive matching with the outer solution. Similarity arguments are not invoked.

A. Equations of Motion for the Inner Region - Laminar Flow

The highly viscous flow in the inner region is assumed to be steady, compressible, laminar or turbulent, two dimensional or axisymmetric flow over an adiabatic or non-adiabatic surface. The appropriate system of equations in dimensional form is given in reference 11. Expressed in curvilinear coordinates (ξ,ζ) in which ξ is measured along the surface and ζ normal to the surface (figure 16) and where u, v are the corresponding velocities, these equations are:

Continuity

$$\frac{\partial}{\partial \xi^*}(\rho^* u^* r^{*\sigma}) + \frac{\partial}{\partial \zeta^*}[\rho^* v^* (1 + \frac{\zeta^*}{R^*})] = 0 \tag{27}$$

ξ^* - momentum

$$\rho^* u^* \frac{\partial u^*}{\partial \xi^*} + \rho^* v^* \frac{\partial u^*}{\partial \zeta^*}(1 + \frac{\zeta^*}{k^*}) + \frac{u^* v^*}{R^*} = - \frac{\partial p^*}{\partial \xi^*}$$

$$+ \frac{1}{r^{*\sigma} R^* (R^*+\zeta^*)} \frac{\partial}{\partial \zeta^*}[\mu^* r^{*\sigma} (R^*+\zeta^*)^2 (\frac{\partial u^*}{\partial \zeta^*} + \frac{R^* \frac{\partial v^*}{\partial \xi^*} - u^*}{R^* + \zeta^*})]$$

$$+ \frac{2}{r^{*\sigma}} \frac{\partial}{\partial \xi^*}[\mu^* r^{*\sigma} (\frac{R^* \frac{\partial u^*}{\partial \xi^*} + v^*)}{(R^* + \zeta^*)}$$

$$- \frac{2\mu^* \sigma}{r^{*2}} (\frac{R^* + \zeta^*}{R^*})(u^* \sin\theta_w + v^* \cos\theta_w) \sin\theta_w$$

$$- \frac{2}{3} \frac{\partial}{\partial \xi^*}\{\mu^* \frac{R^* \frac{\partial u^*}{\partial \xi^*} + v^*}{(R^* + \zeta^*)} + \frac{\partial v^*}{\partial \zeta^*} + \frac{\sigma}{r^*}(u^* \sin\theta_w + v^* \cos\theta_w)]\} \tag{28}$$

ζ*-momentum

$$\frac{R^*}{(R^*+\zeta^*)}\rho^*u^*\frac{\partial v^*}{\partial \xi^*}+\rho^*v^*\frac{\partial v^*}{\partial \zeta^*}-\frac{\rho^*u^{*2}}{R^*+\zeta^*}=-\frac{\partial p^*}{\partial \zeta^*}$$

$$+\frac{2}{r^{*\sigma}(R^*+\zeta^*)}\frac{\partial}{\partial \zeta^*}\left[\mu^*r^{*\sigma}(R^*+\zeta^*)\frac{\partial v^*}{\partial \zeta^*}\right]-\frac{2\mu^*}{(R^*+\zeta^*)}\left[\frac{R^*\frac{\partial u^*}{\partial \xi^*}+v^*}{R^*+\zeta^*}\right]$$

$$+\frac{R^*}{(R^*+\zeta^*)r^*}\frac{\partial}{\partial \xi^*}\left[\mu^*r^{*\sigma}\left(\frac{\partial u^*}{\partial \zeta^*}+\frac{R^*\frac{\partial v^*}{\partial \xi^*}-u^*}{R^*+\zeta^*}\right)\right]-\frac{2\mu^{*\sigma}\cos\theta_w}{r^{*2}}(u^*\sin\theta_w$$

$$+v^*\cos\theta_w)-\frac{2}{3}\frac{\partial}{\partial \zeta^*}\left[\mu^*\left(\frac{R^*\frac{\partial u^*}{\partial \xi^*}-u^*}{R^*+\zeta^*}\right)+\mu^*\frac{\partial v^*}{\partial \zeta^*}\right.$$

$$\left.+\mu^*\sigma\left(\frac{u^*\sin\theta_w+v^*\cos\theta_w}{r^*}\right)\right] \qquad (29)$$

energy

$$\frac{R^*}{(R^*+\zeta^*)}\rho^*u^*\frac{\partial h^*}{\partial \xi^*}+\rho^*v^*\frac{\partial h^*}{\partial \zeta^*}-\left[\frac{R^*}{(R^*+\zeta^*)}u^*\frac{\partial p^*}{\partial \xi^*}+v^*\frac{\partial p^*}{\partial \zeta^*}\right]$$

$$=\frac{1}{r^{*\sigma}}\cdot\left[\frac{\partial}{\partial \zeta}\left(\frac{r^{*\sigma}\mu^*}{Pr}\frac{\partial h^*}{\partial \zeta^*}\right)+\frac{R^*}{(R^*+\zeta^*)}\frac{\partial}{\partial \xi^*}\left(\frac{R^*r^{*\sigma}}{(R^*+\zeta^*)Pr}\mu^*\frac{\partial h^*}{\partial \xi^*}\right)\right]$$

$$+\mu^*\frac{\frac{\partial h^*}{\partial \zeta^*}}{Pr(R^*+\zeta^*)}+\mu^*\left\{2\left(\frac{\partial v^*}{\partial \zeta^*}\right)^2+2\left(\frac{R^*\frac{\partial u^*}{\partial \xi^*}+v^*}{R^*+\zeta^*}+\frac{2\sigma}{r^{*2}}(u^*\sin\theta_w+v^*\cos\theta_w)^2\right.\right.$$

$$\left.\left.+\left(\frac{\partial u^*}{\partial \zeta^*}+\frac{R^*\frac{\partial v^*}{\partial \xi^*}-u^*}{R^*+\zeta^*}\right)^2-\frac{2}{3}\left[\frac{R^*\frac{\partial u^*}{\partial \xi^*}+v^*}{R^*+\zeta^*}+\frac{\partial v^*}{\partial \zeta^*}+\frac{\sigma}{r^*}(u^*\sin\theta_w+v^*\cos\theta_w)\right]\right\} \qquad (30)$$

In these equations r* is the lateral radius of curvature of the point (ξ^*,ζ^*), R* is the longitudinal radius of curvature of the surface, and is positive for convex surfaces (reference 11) while

$\sigma = 0$ for two dimensional flow

and

$\sigma = 1$ for axisymmetric flow.

The angle θ_w is the local slope of the axisymmetric body relative to the normal to the axis. Thus

$$\cos\theta_w = \frac{dr^*}{d\xi^*}$$

Reexamining the equations of motion using dimensional analysis (see Appendix D), a set of equations is obtained constituting a higher approximation than the classical boundary layer for the inner region, since terms of order unity and of order (δ/L_{REF}) are retained. The non-dimensional equations of motion obtained to this order expressed in terms of reference Reynolds number Re_{REF} become:

<u>continuity</u>

$$\frac{\partial}{\partial\xi}[\rho u r^\sigma] + \frac{\partial}{\partial\zeta}[\rho v r^\sigma (1 + \frac{1}{Re_{REF}^{1/2}} \frac{\zeta}{R})] = 0 \tag{31}$$

<u>ξ-momentum</u>

$$\rho u \frac{\partial u}{\partial\xi} + \rho v(1 + \frac{1}{Re_{REF}^{1/2}} \frac{\zeta}{R}) \frac{\partial u}{\partial\zeta} + \frac{1}{Re_{REF}^{1/2}} \frac{\rho uv}{R} + \frac{\partial p}{\partial\xi}$$

$$= \frac{1}{r^\sigma} \frac{\partial}{\partial\zeta}[\mu r^\sigma (1 + \frac{1}{Re_{REF}^{1/2}} \frac{\zeta}{R}) \frac{\partial u}{\partial\zeta}] - \frac{1}{Re_{REF}^{1/2}} \frac{1}{r^\sigma} \frac{u}{R} \frac{\partial}{\partial\zeta}(\mu r^\sigma) \tag{32}$$

<u>ζ-momentum</u>

$$\frac{1}{Re_{REF}^{1/2}}[\rho u \frac{\partial v}{\partial\xi} + \rho v(1 + \frac{1}{Re_{REF}^{1/2}} \frac{\zeta}{R}) \frac{\partial v}{\partial\zeta}] - \frac{\rho u^2}{R} + Re_{REF}^{1/2}(1 + \frac{1}{Re_{REF}^{1/2}} \frac{\zeta}{R}) \frac{\partial p}{\partial\zeta}$$

$$= \frac{2}{Re_{REF}^{1/2}} \frac{1}{r^\sigma} \frac{\partial}{\partial\zeta}(\mu r^\sigma \frac{\partial v}{\partial\zeta}) + \frac{1}{Re_{REF}^{1/2}} \frac{1}{r^\sigma} \frac{\partial}{\partial\xi}(\mu r^\sigma \frac{\partial u}{\partial\zeta})$$

$$- \frac{2}{3} Re_{REF}^{1/2} \frac{\partial}{\partial\zeta}[\mu \frac{\partial u}{\partial\xi} + \frac{\partial v}{\partial\zeta} + \frac{\sigma\mu\sin\theta_w}{r}] \tag{33}$$

energy

$$\rho u \frac{\partial T}{\partial \xi} + \rho v(1 + \frac{1}{Re_{REF}^{1/2}} \frac{\zeta}{R}) \frac{\partial T}{\partial \zeta} - (\gamma-1) M_{REF}^2 [u \frac{\partial p}{\partial \xi} + (1 + \frac{1}{Re_{REF}^{1/2}} \frac{\zeta}{R}) v \frac{\partial p}{\partial \zeta}]$$

$$= (1 + \frac{1}{Re_{REF}^{1/2}} \frac{\zeta}{R}) \frac{1}{r^\sigma} \frac{\partial}{\partial \zeta} [\mu \frac{r^\sigma}{Pr_{REF}} \frac{\partial T}{\partial \zeta}] + \frac{1}{Re_{REF}^{1/2}} \frac{}{Pr_{REF}} \frac{\mu}{R} \frac{\partial T}{\partial \zeta}$$

$$+ \mu(\gamma-1) M_{REF}^2 [(1 + \frac{1}{Re_{REF}^{1/2}} \frac{\zeta}{R}) (\frac{\partial u}{\partial \zeta})^2 - \frac{2}{Re_{REF}^{1/2}} \frac{u}{R} \frac{\partial u}{\partial \zeta}] \qquad (34)$$

equation of state

$$p = \frac{\rho T}{\gamma M_{REF}^2} \qquad (35)$$

B. Equations of Motion for the Inner Region - Turbulent Flow

When the equations of motion are written in terms of mean quantities (velocities, pressure, density, temperature, etc.) and fluctuations about the mean, and then averaged with respect to time, the resulting set for turbulent flow (a detailed development is given in Appendix E) keeping only the leading correlations $\overline{u'v'}$ and $\overline{v'T'}$ is:

continuity:

$$\frac{\partial}{\partial \xi} [\rho u r^\sigma] + \frac{\partial}{\partial \zeta} [\rho v r^\sigma (1 + \frac{1}{Re_{REF}^{1/2}} \frac{\zeta}{R})] = 0 \qquad (36)$$

ξ-momentum

$$\bar{\rho} \bar{u} \frac{\partial \bar{u}}{\partial \xi} + \bar{\rho} \bar{v} (1 + \frac{1}{Re_{REF}^{1/2}} \frac{\zeta}{R}) \frac{\partial \bar{u}}{\partial \zeta} + \frac{1}{Re_{REF}^{1/2}} \frac{\overline{\rho u v}}{R} + \frac{\partial \bar{p}}{\partial \xi}$$

$$= \frac{1}{r^\sigma} \frac{\partial}{\partial \zeta} [\mu r^\sigma (1 + \frac{1}{Re_{REF}^{1/2}} \frac{\zeta}{R}) \frac{\partial \bar{u}}{\partial \zeta}] - \frac{1}{r^\sigma} \frac{\partial}{\partial \zeta} [r^\sigma (1 + \frac{1}{Re_{REF}^{1/2}} \frac{\zeta}{R}) \bar{\rho} \overline{u'v'}]$$

$$- \frac{1}{Re_{REF}^{1/2}} \frac{1}{r^\sigma} \frac{\bar{u}}{R} \frac{\partial}{\partial \zeta} (\mu r^\sigma) - \frac{1}{Re_{REF}^{1/2}} \bar{\rho} \frac{\overline{u'v'}}{R} \qquad (37)$$

ζ-momentum

$$\frac{1}{Re_{REF}^{1/2}}\{\bar{\rho}\bar{u}\frac{\partial\bar{v}}{\partial\xi} + \bar{\rho}\bar{v}(1 + \frac{1}{Re_{REF}^{1/2}}\frac{\zeta}{R})\frac{\partial\bar{v}}{\partial\zeta}\} - \frac{\bar{\rho}\bar{u}^2}{R} + Re_{REF}^{1/2}(1 + \frac{1}{Re_{REF}^{1/2}}\frac{\zeta}{R})\frac{\partial\bar{p}}{\partial\zeta}$$

$$= \frac{2}{Re_{REF}^{1/2}}\frac{1}{r^\sigma}\frac{\partial}{\partial\zeta}[\mu r^\sigma\frac{\partial\bar{v}}{\partial\zeta}] + \frac{1}{Re_{REF}^{1/2}}\frac{1}{r^\sigma}\frac{\partial}{\partial\xi}[\mu r^\sigma\frac{\partial\bar{u}}{\partial\zeta}]$$

$$- \frac{2}{3Re_{REF}^{1/2}}\frac{\partial}{\partial\zeta}[\mu\frac{\partial\bar{u}}{\partial\xi} + \mu\frac{\partial\bar{v}}{\partial\zeta} + \mu\frac{\sigma\sin\theta_w\bar{u}}{r}] - \frac{1}{Re_{REF}^{1/2}}\frac{1}{r^\sigma}\frac{\partial}{\partial\xi}[r^\sigma\overline{\rho u'v'}] \tag{38}$$

energy

$$\bar{\rho}\bar{u}\frac{\partial\bar{T}}{\partial\xi} + \bar{\rho}\bar{v}(1 + \frac{1}{Re_{REF}^{1/2}}\frac{\zeta}{R})\frac{\partial\bar{T}}{\partial\zeta} - (\gamma-1)M_{REF}^2[\bar{u}\frac{\partial\bar{p}}{\partial\xi} + \bar{v}(1 + \frac{1}{Re_{REF}^{1/2}}\frac{\zeta}{R})\frac{\partial\bar{p}}{\partial\zeta}]$$

$$= (1 + \frac{1}{Re_{REF}^{1/2}}\frac{\zeta}{R})\frac{1}{r^\sigma}\frac{\partial}{\partial\zeta}[\frac{\mu r^\sigma}{Pr_{REF}}\frac{\partial\bar{T}}{\partial\zeta}] + \frac{\mu}{Re_{REF}^{1/2}}\frac{1}{Pr_{REF}}\frac{1}{R}\frac{\partial\bar{T}}{\partial\zeta}$$

$$+ (\gamma-1)M_{REF}^2\mu\{(1 + \frac{1}{Re_{REF}^{1/2}}\frac{\zeta}{R})(\frac{\partial\bar{u}}{\partial\zeta})^2 - \frac{2}{Re_{REF}^{1/2}}\frac{\bar{u}}{R}\frac{\partial\bar{u}}{\partial\zeta}\}$$

$$- \frac{1}{r^\sigma}\frac{\partial}{\partial\zeta}[(1 + \frac{1}{Re_{REF}^{1/2}}\frac{\zeta}{R})r^\sigma\overline{\rho v'T'}] \tag{39}$$

equation of state

$$\bar{p} = \frac{\bar{\rho}\bar{T}}{\gamma M_{REF}^2} \tag{40}$$

C. Viscosity Laws

The equations are formulated to accommodate any variation of viscosity that may be required in properly implementing a boundary layer calculation. For the examples presented in the work the dynamic or absolute viscosity is represented by the Sutherland viscosity relation which in dimensionless form is

$$\mu = \left(\frac{1+\alpha}{T+\alpha}\right) T^{3/2} \tag{41}$$

where:

$$\alpha = \frac{198.6}{T_{REF}}$$

For turbulent boundary layers, the momentum and energy transfer correlations $\overline{u'v'}$ and $\overline{v'T'}$ are included in the equations of motion and are evaluated using Boussinesq scalar eddy viscosity and eddy conductivity coefficients through which these transport terms are in turn related to local mean velocity and temperature gradients. Thus the turbulent transport coefficients are defined:

$$-\overline{u'v'} = \varepsilon_u \frac{\partial \bar{u}}{\partial \zeta}$$

$$-\overline{v'T'} = \varepsilon_t \frac{\partial \bar{T}}{\partial \zeta} = \frac{\varepsilon_u}{Pr_t} \frac{\partial \bar{T}}{\partial \zeta} \tag{42}$$

where ε_u is the scalar eddy viscosity and Pr_t is the turbulent Prandtl number.

Eddy Viscosity Model: Experimental data with equilibrium turbulent boundary layers indicates that the scalar eddy viscosity function can be simulated by a two-layer model (reference 14). The inner layer in the vicinity of the wall is characterized by increasing turbulence with distance from the wall namely ε_u varies almost linearly* with distance from the wall. In the outer layer the scalar eddy viscosity function is nearly constant except for the intermittency factor. Cebeci and Smith (reference 15) have extended the Van-driest

*In the very near neighborhood of the wall $\varepsilon_u \sim y^2$.

formulation of the law-of-the-wall (reference 16) in order to include effects of pressure gradient and heat and mass transfer at the wall. The Cebeci-Smith model for effective eddy viscosity will be used in the present calculations for turbulent flow. While these are other suggested models for the eddy viscosity (reference 17 for example), the Cebeci-Smith formulation has been shown to be adequate for engineering calculations.

The Cebeci-Smith model (reference 15) written for axisymmetric flow* is as follows:

Inner Layer

$$[\varepsilon_u]_i = L^2 \frac{r}{r_w} \left| \frac{\partial u}{\partial \zeta} \right| \qquad 0 \leq \zeta \leq \zeta_c$$

Outer Layer

$$[\varepsilon_u]_o = \Gamma \cdot \alpha U_e \delta^* \qquad \zeta_c \leq \zeta \leq \delta \tag{43}$$

where:

$$L = 0.40 r_w \ln \frac{r}{r_w} \{1.0 - \exp[-\frac{r_w}{A} \ln (\frac{r}{r_w})]\}$$

A-is a function of pressure gradient, mass transfer at the wall and viscous shear stress at the wall and is given by:

$$A = A^+ \frac{\nu}{N} (\frac{\tau_w}{\rho_w})^{-1/2} (\frac{\rho}{\rho_w})^{1/2} \tag{44}$$

where

*The two-dimensional version can be extracted by setting $\frac{r}{r_w} = 1 + \frac{y}{r_w}$ and evaluating the expressions in the limit as $r_w \to \infty$.

$$A^+ = 26$$

$$N^2 = \frac{\mu}{\mu_e}\left(\frac{\rho_e}{\rho_w}\right)^2 \frac{p^+}{v_w^+}\{1 - \exp(11{\cdot}8 \cdot \frac{\mu_w}{\mu} v_w^+)\} + \exp(11{\cdot}8 \frac{\mu_w}{\mu} v_w^+)$$

$$p^+ = \frac{\nu_e u_e}{U_r^3} \frac{du_e}{d\xi}$$

$$v_w^+ = \frac{v_w}{u_\tau}$$

$$u_\tau = \left(\frac{\tau_w}{\rho_w}\right)^{1/2}$$

$$\alpha = \alpha_o\left(\frac{1+\pi_o}{1+\pi}\right)$$

$$\alpha_o = 0.0168$$

$$\pi_o = .55$$

$$\pi = 0.55\ \{1 - \exp[-0.243 z_1^{1/2} - 0.298 z_1]\}$$

$$z_1 = \frac{R_\theta}{425} - 1$$

R_θ = Reynolds number based on momentum thickness

The intermittency factor is given by:

$$\Gamma = \frac{1}{1+5{\cdot}5\left(\frac{\zeta}{\delta}\right)^6} \tag{45}$$

The condition of continuity of the eddy viscosity function determines the values of ζ_c, i.e.:

$$\varepsilon_{u_i}(\zeta_c) = \varepsilon_{u_o}(\zeta_c) \tag{46}$$

The two-layer representation of the eddy viscosity function is sketched in figure 17.

Substituting the expressions (42) for the turbulent transport terms into equations (37) to (39) the system of equations becomes:

continuity

$$\frac{\partial}{\partial\xi}[\bar{\bar{\rho}}\bar{u}r^{\sigma}] + \frac{\partial}{\partial\zeta}[\bar{\bar{\rho}}\bar{v}r^{\sigma}(1 + \frac{1}{Re_{REF}^{1/2}}\frac{\zeta}{R})] = 0 \tag{47}$$

ξ-momentum

$$\bar{\bar{\rho}}\bar{u}\frac{\partial\bar{u}}{\partial\xi} + \bar{\bar{\rho}}\bar{v}(1 + \frac{1}{Re_{REF}^{1/2}}\frac{\zeta}{R})\frac{\partial\bar{u}}{\partial\zeta} + \frac{1}{Re_{REF}^{1/2}}\frac{\bar{\bar{\rho}}\bar{u}\bar{v}}{R} + \frac{\partial\bar{p}}{\partial\xi}$$

$$= \frac{1}{r^{\sigma}}\frac{\partial}{\partial\zeta}[r^{\sigma}(1 + \frac{1}{Re_{REF}^{1/2}}\frac{\zeta}{R})(\mu + \rho\varepsilon_u)\frac{\partial\bar{u}}{\partial\zeta}] + \frac{1}{Re_{REF}^{1/2}}\frac{\rho\varepsilon_u}{R}\frac{\partial\bar{u}}{\partial\zeta}$$

$$- \frac{1}{Re_{REF}^{1/2}}\frac{1}{r^{\sigma}}\frac{\bar{u}}{R}\frac{\partial}{\partial\zeta}(\mu r^{\sigma}) \tag{48}$$

ζ-momentum

$$\frac{1}{Re_{REF}^{1/2}}\{\bar{\bar{\rho}}\bar{u}\frac{\partial\bar{v}}{\partial\xi} + \bar{\bar{\rho}}\bar{v}(1 + \frac{1}{Re_{REF}^{1/2}}\frac{\zeta}{R})\frac{\partial\bar{v}}{\partial\zeta}\} - \frac{\bar{\bar{\rho}}\bar{u}^2}{R} + Re_{REF}^{1/2}(1 + \frac{1}{Re_{REF}^{1/2}}\frac{\zeta}{R})\frac{\partial\bar{p}}{\partial\zeta}$$

$$= \frac{2}{Re_{REF}^{1/2}}\frac{1}{r^{\sigma}}\frac{\partial}{\partial\zeta}[\mu r^{\sigma}\frac{\partial\bar{v}}{\partial\zeta}] + \frac{1}{Re_{REF}^{1/2}}\frac{1}{r^{\sigma}}\frac{\partial}{\partial\xi}[r^{\sigma}(\mu + \rho\varepsilon_u)\frac{\partial\bar{u}}{\partial\zeta}]$$

$$- \frac{2}{3Re_{REF}^{1/2}}\frac{\partial}{\partial\zeta}[\mu\frac{\partial\bar{u}}{\partial\xi} + \mu\frac{\partial\bar{v}}{\partial\zeta} + \frac{\mu\sigma\sin\theta_w}{r}\bar{u}] \tag{49}$$

energy

$$\bar{\bar{\rho}}\bar{u}\frac{\partial\bar{T}}{\partial\zeta} + \bar{\bar{\rho}}\bar{v}(1 + \frac{1}{Re_{REF}^{1/2}}\frac{\zeta}{R})\frac{\partial\bar{T}}{\partial\zeta} - (\gamma-1)M_{REF}^2[\bar{u}\frac{\partial\bar{p}}{\partial\xi} + \bar{v}(1 + \frac{1}{Re_{REF}^{1/2}}\frac{\zeta}{R})\frac{\partial\bar{p}}{\partial\zeta}]$$

$$= \frac{1}{r^{\sigma}}\frac{\partial}{\partial\zeta}[\frac{r^{\sigma}}{Pr_{REF}}(1 + \frac{1}{Re_{REF}^{1/2}}\frac{\zeta}{R})(\mu + \bar{\rho}\frac{Pr_{REF}\varepsilon_u}{Pr_t}$$

$$+ (\gamma-1)M_{REF}^2\mu\{(1 + \frac{1}{Re_{REF}^{1/2}}\frac{\zeta}{R})(\frac{\partial\bar{u}}{\partial\zeta})^2 - \frac{2}{Re_{REF}^{1/2}}\frac{\bar{u}}{R}\frac{\partial\bar{u}}{\partial\zeta}\} \tag{50}$$

equation of state

$$\bar{p} = \frac{\bar{\rho}\bar{T}}{\gamma M_{REF}^2} \tag{51}$$

Equations (31) to (35) for the laminar case or equations (47) to (51) for the turbulent case are a coupled parabolic system in the variables u, v, and T, hence two point boundary conditions for u, v, and T and one boundary condition for the pressure are required. For convenience in computation the pressure is split as follows:

$$p(\xi,\zeta) = P_{EXT}(\xi) + p_I(\xi,\zeta) \tag{52}$$

where $p_{EXT}(\xi)$ is the external pressure (presumably known), and $p_I(\xi,\zeta)$ is an induced pressure due to normal momentum consideration.

D. Boundary Conditions

The boundary conditions at the wall ($\zeta = 0$) are:

$$u(\xi,0) = 0$$

$$v(\xi,0) = \begin{cases} 0 & \text{for impermeable walls} \\ v_w(\xi) & \text{for suction or blowing} \end{cases}$$

$$T(\xi,0) = T_w(\xi)$$

or

$$\left.\frac{\partial T}{\partial \zeta}\right|_{\zeta=0} = 0 \tag{53}$$

The outer boundary conditions depend on the use made of the inner-region equations. Those presented here are the outer conditions for boundary layer calculations. The outer boundary conditions employed in the interaction procedure are described in Chapter IV. For com-

putational purposes, the outer edge of the boundary layer is taken to be well outside the conventionally defined thicknesses. In practice this turns out to be three to four times δ^* for the laminar boundary layer and of the order $10\delta^*$ for the turbulent boundary layers. At this location: ($\zeta \approx \delta$)

$$p_I(\xi,\delta) = 0$$

$$\frac{\partial}{\partial\xi}(\rho u r^\sigma)\Big|_{\zeta=\delta} + \frac{\partial}{\partial\zeta}[\rho v r^\sigma (1 + \frac{1}{Re_{REF}^{1/2}} \frac{\zeta}{R})]\Big|_{\zeta=\delta} = 0$$

$$\rho_\delta u_\delta \frac{du_\delta}{d\xi} = - \frac{dp_{EXT}(\xi)}{d\xi}$$

$$\rho_\delta u_\delta \frac{dT_\delta}{d\xi} = (\gamma-1)M_{REF}^2 \, u_\delta \frac{dp_{EXT}(\xi)}{d\xi} \qquad (54)$$

Initial Profile: For starting the finite difference calculation, profiles for the unknowns, u, v, T and p at a specified initial station ξ_o are needed. For laminar boundary layers, similarity solutions have been incorporated to start the finite difference flow field calculation. For incompressible turbulent boundary layers the starting profile has been constructed from the law-of-the-wall.

E. Numerical Solution of the Inner-Region Equations

For solution of the non-linear partial differential system, equations (31) to (35) for laminar flow or equations (47) to (51) for turbulent flow are linearized and then replaced by a system of linear algebraic equations using a modified Crank-Nicolson implicit finite difference scheme. Since because of the nonlinearity of the basic system the flow variables in the coefficient matrix depend on the

solution vector, an iterative procedure is applied until the differences between the flow variables for successive iterations is as small as desired.

A primary objective in the development of a numerical procedure is to get it to yield a stable and convergent solution for the system of finite difference equations. Stability and convergence of numerical solutions of partial differential equations is discussed by Roache (reference 18). Basically, instability results from unavoidable small perturbations in the flow field due for example to round-off error,truncation error, etc. If in marching downstream the errors diminish then the method is stable; if the errors grow in marching downstream the method is unstable.

It was decided to apply an implicit difference scheme rather than an explicit one. A broad discussion of the two schemes is given in reference 18. Generally it is expected that implicit difference schemes are far more stable than explicit difference schemes. On the other hand implicit schemes involve a system of algebraic equations that must be solved simultaneously since the equations are coupled.

Other investigators have attempted solving the flow equations in the physical plane using implicit difference schemes. Reyhner and Flugge-Lotz (reference 4) solved the system of classical boundary layer equations simultaneously in the physical plane for u, v and T. Their numerical results indicated an oscillation in the normal velocity at the edge of the boundary layer. Such oscillations are

undesirable if the method is to be used as part of an interaction calculation. Since their system of equations includes only continuity, x-momentum and energy equations the normal pressure gradient is assumed to be zero.

Ferri and Dash (reference 6) have included an uncoupled normal momentum equation in their mathematical model. Their numerical solution was also done in the physical plane. Although they used an implicit difference scheme, their procedure is quite different than that of Reyhner and Flugge-Lotz (reference 4). They assumed the pressure distribution across the boundary layer to be a polynomial of fourth order uncoupled from the rest of the system. The coefficients were determined by assuming that first and second normal derivatives of the pressure at the wall are zero and that the remaining terms are dependent on the longitudinal curvature effects. The system of equations i.e., continuity, x-momentum and the energy equations were expressed in finite difference form. Solution of the finite difference equations was done successively; that is they first solved simultaneously for u and T using the x-momentum and energy equations, then the normal velocity distribution was obtained by integration of the continuity equation. The process was repeated iteratively until convergence was obtained for u, v and T. The converged solution was then used to determine the variation of p across the boundary layer.

The objective in the present work is to solve the second order system of equations for the viscous region in the physical plane and by extending the Reyhner-Flugge-Lotz method (reference 4) and solving the coupled parabolic system of equations simultaneously.

Difference Scheme and Quotients - The grid scheme on which the expressions for the difference quotients are based is shown in figure 18. A grid with variable mesh size in the normal ζ direction and a uniform mesh size in the longitudinal ξ direction has been chosen. In order to obtain a fine mesh near the surface where the gradients are large and a coarse mesh away from the surface, a geometric series has been chosen to locate the grid points in the ζ direction.

$$\zeta_n = DK \cdot \frac{(K^{n-1} - 1.0)}{K - 1.0} \qquad n=1,2...N-1,N \qquad (55)$$

where:

DK = first interval

K = ratio between two consecutive intervals

ζ_n = ζ coordinate of the n^{th} grid point

The truncation errors of the difference quotients are based on a Taylor series expansion of a function with two independent variables about a point where the function and its derivatives are known. The validity of the expansion depends on the existence and continuity of all derivatives of the function f(x,y) which here represents any of the unknown functions u, v, T and p. The value of $f(x+h,y+\ell)$

can be expressed as follows:

$$f(x+h,y+\ell) = f(x,y) + (h\frac{\partial}{\partial x} + \ell\frac{\partial}{\partial y})f(x,y) + \frac{1}{2!}(h\frac{\partial}{\partial x} + \ell\frac{\partial}{\partial y})^2 f(x,y)$$

$$+ \frac{1}{3!}(h\frac{\partial}{\partial x} + \ell\frac{\partial}{\partial y})^3 f(x,y) + \ldots$$

$$= f(x,y) + h\frac{\partial f}{\partial x} + \ell\frac{\partial f}{\partial y} + \frac{1}{2!}(h^2\frac{\partial^2 f}{\partial x^2} + 2h\ell\frac{\partial^2 f}{\partial x\partial y} + \ell^2\frac{\partial^2 f}{\partial y^2}) + \ldots \quad (56)$$

For any of the unknown functions u, v, T and p represented here either by f(x,y) or g(x,y) the expressions for first and second derivatives of the above mentioned functions at the point A (figure 18) located at $(\xi_{m+1/2}, \zeta_n)$ depend on the differencing scheme. The expressions for centered differences, backward differences and forward differences are given below:

Centered Differences

1) First derivative in ξ-direction:

$$f_{m+1,n} = f_{m+1/2,n} + \frac{\partial f}{\partial \xi}\Big|_A \frac{\Delta\xi}{2} + \frac{1}{2!}\frac{\partial^2 f}{\partial \xi^2}\Big|_A (\frac{\Delta\xi}{2})^2 + \frac{1}{3!}\frac{\partial^3 f}{\partial \xi^3}\Big|_A (\frac{\Delta\xi}{2})^3 + \ldots \quad (57)$$

$$f_{m,n} = f_{m+1/2,n} - \frac{\partial f}{\partial \xi}\Big|_A \frac{\Delta\xi}{2} + \frac{1}{2!}\frac{\partial^2 f}{\partial \xi^2}\Big|_A (\frac{\Delta\xi}{2})^2 - \frac{1}{3!}\frac{\partial^3 f}{\partial \xi^3}\Big|_A (\frac{\Delta\xi}{2})^3 + \ldots \quad (58)$$

subtracting (58) from (57) yields

$$\frac{\partial f}{\partial \xi}\Big|_A = \frac{(f_{m+1,n} - f_{m,n})}{\Delta\xi} + \mathcal{O}[(\Delta\xi)^2] \quad (59)$$

2) First derivative in ζ-direction:

The derivative in ζ-direction is obtained as a weighted average of the derivatives in the ζ-direction at station m and station m+1.

$$f_{m+1,n+1} = f_{m+1,n} + \frac{\partial f}{\partial \zeta}\Big|_{m+1,n} \Delta\zeta_{n+1} + \frac{1}{2!}\frac{\partial^2 f}{\partial \xi^2}\Big|_{m+1,n} (\Delta\zeta_{n+1})^2 + \ldots \tag{60}$$

$$f_{m+1,n-1} = f_{m+1,n} - \frac{\partial f}{\partial \zeta}\Big|_{m+1,n} \Delta\zeta_{n} + \frac{1}{2!}\frac{\partial^2 f}{\partial \zeta^2}\Big|_{m+1,n} (\Delta\zeta_{n})^2 + \ldots \tag{61}$$

Since $\Delta\zeta_{n+1} = \Delta\zeta_n K$, the resulting expression is

$$\frac{\partial f}{\partial \zeta}\Big|_{m+1,n} = \frac{f_{m+1,n+1} - f_{m+1,n-1}}{\Delta\zeta_n (1+K)} + \mathcal{O}[(\Delta\zeta_n{}^2)] \tag{62}$$

Similarly for station m

$$\frac{\partial f}{\partial \zeta}\Big|_{m,n} = \frac{f_{m,n+1} - f_{m,n-1})}{\Delta\zeta_n (1+K)} \tag{63}$$

Finally we obtain:

$$\frac{\partial f}{\partial \zeta}\Big|_{m+1/2,n} = \lambda_1 \left(\frac{\partial f}{\partial \zeta}\right)\Big|_{m+1,n} + (1-\lambda_1)\left(\frac{\partial f}{\partial \zeta}\right)\Big|_{m,n} \tag{64}$$

For $\lambda_1 = 1/2$, the Crank-Nicolson centered difference expression is obtained.

Second Derivative - Second derivatives appear in the flow equations only in the ζ-direction. For centered differences:

$$f_{m+1,n+1} = f_{m+1,n} + \frac{\partial f}{\partial \zeta}\Big|_{m+1,n} \Delta\zeta_{n+1} + \frac{1}{2!}\frac{\partial^2 f}{\partial \zeta^2}\Big|_{m+1,n} (\Delta\zeta_{n+1})^2 + \ldots \tag{65}$$

$$f_{m+1,n-1} = f_{m+1,n} - \frac{\partial f}{\partial \zeta}\Big|_{m+1,n} \Delta\zeta_{n} + \frac{1}{2!}\frac{\partial^2 f}{\partial \zeta^2}\Big|_{m+1,n} (\Delta\zeta_{n})^2 - \ldots \tag{66}$$

Multiplying equation (65) by $(\Delta\zeta_n)$ and equation (66) by $(\Delta\zeta_{n+1})$ and adding the resulting equations yields

$$\left.\frac{\partial^2 f}{\partial \zeta^2}\right|_{m+1,n} = 2\,\frac{(f_{m+1,n+1} + K\,f_{m+1,n-1} - (1+K)f_{m+1,n})}{K(1+K)(\Delta\zeta_n)^2} \tag{67}$$

For flexibility a weighted average has been used to obtain the second derivative at point A:

$$\left.\frac{\partial^2 f}{\partial \zeta^2}\right|_{m+1/2,n} = \lambda_2 \left.\frac{\partial^2 f}{\partial \zeta^2}\right|_{m+1,n} + (1-\lambda_2) \left.\frac{\partial^2 f}{\partial \zeta^2}\right|_{m,n} \tag{68}$$

Again for $\lambda_2 = \frac{1}{2}$ the equal-weighted Crank-Nicolson result is obtained.

Other Derivatives

$$\left.\left(\frac{\partial f}{\partial \zeta}\right)^2\right|_{m+1/2,n} = \frac{(f_{m+1,n+1} - f_{m+1,n+1})(f_{m,n+1} - f_{m,n-1})}{(1+K)^2(\Delta\zeta_n)^2} \tag{69}$$

$$\left.\frac{\partial f}{\partial \zeta}\frac{\partial g}{\partial \zeta}\right|_{m+1/2,n} = \frac{(f_{m+1,n+1} - f_{m+1,n-1})(g_{m,n+1} - g_{m,n-1})}{2(\Delta\zeta_n)^2(1+K)^2} + \frac{(g_{m+1,n+1} - g_{m+1,n-1})(f_{m,n+1} - f_{m,n-1})}{2(\Delta\zeta_n)^2(1+K)^2} \tag{70}$$

To be noted is the linearity of these expressions in the quantities evaluated at station m+1.

Backward Differences

First Derivative

$$f_{m+1,n-1} = f_{m+1,n} - \left.\frac{\partial f}{\partial \zeta}\right|_{m+1,n} \Delta\zeta_n + \frac{1}{2!}\left.\frac{\partial^2 f}{\partial \zeta^2}\right|_{m+1,n} (\Delta\zeta_n)^2 \ldots \tag{71}$$

$$f_{m+1,n-2} = f_{m+1,n} - \frac{\partial f}{\partial \zeta}\Big|_{m+1,n} (\Delta\zeta_{n-1} + \Delta\zeta_n) + \frac{1}{2!} \frac{\partial^2 f}{\partial \zeta^2}\Big|_{m+1,n} [(\Delta\zeta_{n-1})+(\Delta\zeta_n)]^2$$

(72)

Multiply equation (71) by $(\Delta\zeta_n + \Delta\zeta_{n-1})^2$ and equation (72) by $(\Delta\zeta_n)^2$. Then subtraction of (72) from (71) yields:

$$\frac{\partial f}{\partial \zeta}\Big|_{m+1,n} = f_{m+1,n} \frac{(1+2K)}{(1+K)\Delta\zeta_n} - f_{m+1,n-1} \frac{(1+K)}{\Delta\zeta_n} + f_{m+1,n-2} \frac{K^2}{(1+K)\Delta\zeta_n} + \mathcal{O}[(\Delta\zeta_n)^2]$$

(73)

Hence the first derivative for point A (figure 18) using backward differencing and weighted averaging becomes:

$$\frac{\partial f}{\partial \zeta}\Big|_{m+1/2,n} = \lambda_3 \frac{\partial f}{\partial \zeta}\Big|_{m+1,n} + (1-\lambda_3) \frac{\partial f}{\partial \zeta}\Big|_{m,n} \qquad (74)$$

Forward Differences

First Derivative

$$f_{m+1,n+1} = f_{m+1,n} + \frac{\partial f}{\partial \zeta}\Big|_{m+1,n} \Delta\zeta_{n+1} + \frac{1}{2!} \frac{\partial^2 f}{\partial \zeta^2}\Big|_{m+1,n} (\Delta\zeta_{n+1})^2 + \ldots$$

(75)

$$f_{m+1,n+2} = f_{m+1,n} + \frac{\partial f}{\partial \zeta}\Big|_{m+1,n} (\Delta\zeta_{n+2} + \Delta\zeta_{n+1}) + \frac{1}{2!} \frac{\partial^2 f}{\partial \zeta^2}\Big|_{m+1,n} (\Delta\zeta_{n+1}+\Delta\zeta_{n+2})^2 + \ldots$$

(76)

Multiplying equation (75) by $(\Delta\zeta_{n+1} + \Delta\zeta_{n+2})^2$ and equation (76) by $(\Delta\zeta_{n+1})^2$ then subtracting equation (76) from equation (75) and expressing in terms of $\Delta\zeta_n$ we obtain:

$$\left.\frac{\partial f}{\partial \zeta}\right|_{m+1,n} = - f_{m+1,n} \frac{(2+K)}{(1+K)K\Delta\zeta_n} + \frac{(1+K)}{K^2\Delta\zeta_n} f_{m+1,n+1} - f_{m+1,n+2} \frac{1}{K^2(1+K)\Delta\zeta_n} \tag{77}$$

Then as for backward differencing, the expression for the first derivative at point A is:

$$\left.\frac{\partial f}{\partial \zeta}\right|_{m+1/2,n} = \lambda_3 \left.\frac{\partial f}{\partial \xi}\right|_{m+1,n} + (1-\lambda_3) \left.\frac{\partial f}{\partial \zeta}\right|_{m,n} \tag{78}$$

Difference Equations

Following the suggestion of Reyhner and Flugge-Lotz(reference 4) the system of non linear partial differential equations has been linearized in the following way:

continuity

$$\frac{\partial}{\partial \xi}[r^\sigma \rho u] + \frac{\partial}{\partial \zeta}[r^\sigma \rho v(1 + \frac{1}{Re_{REF}^{1/2}} \frac{\zeta}{R})] = 0 \tag{79}$$

ξ-momentum

$$\begin{aligned}(\rho u)^{(i)} \frac{\partial u}{\partial \xi} + (\rho \frac{\partial u}{\partial \zeta})^{(i)} (1 + \frac{1}{Re_{REF}^{1/2}} \frac{\zeta}{R})v \\ = - \frac{\partial p}{\partial \xi} + [(1 + \frac{1}{Re_{REF}^{1/2}} \frac{\zeta}{R})\mu(1 + \frac{\rho\varepsilon}{\mu})]^{(i)} \frac{\partial^2 u}{\partial \zeta^2} \\ + [\frac{1}{r^\sigma} \frac{\partial}{\partial \zeta}(r^\sigma(1 + \frac{1}{Re_{REF}^{1/2}} \frac{\zeta}{R})\mu(1 + \frac{\rho\varepsilon}{\mu}))]^{(i)} \frac{\partial u}{\partial \zeta} \\ - \frac{1}{Re_{REF}^{1/2}} (\frac{u}{Rr^\sigma})^{(i)} \frac{\partial}{\partial \zeta}(\mu r^\sigma) \\ - \frac{(\rho\varepsilon)^{(i)}}{Re_{REF}^{1/2} R} \frac{\partial u}{\partial \zeta} - \frac{\rho^{(i)}}{Re_{REF}^{1/2}} \frac{uv}{R}\end{aligned} \tag{80}$$

ζ-momentum

$$\frac{(\rho u)^{(i)}}{Re_{REF}^{1/2}}\frac{\partial v}{\partial \xi} + \left[\left(1 + \frac{1}{Re_{REF}^{1/2}}\frac{\zeta}{R}\right)\rho v\right]^{(i)}\frac{1}{Re_{REF}^{1/2}}\frac{\partial v}{\partial \zeta} = -Re_{REF}^{1/2}\left(1 + \frac{1}{Re_{REF}^{1/2}}\frac{\zeta}{R}\right)\frac{\partial p}{\partial \zeta}$$

$$+ \frac{2}{Re_{REF}^{1/2}}\left[\mu^{(i)}\frac{\partial^2 v}{\partial \zeta^2} + \frac{1}{r^{\sigma}}\frac{\partial v}{\partial \zeta}\cdot\frac{\partial}{\partial \zeta}(\mu r^{\sigma})\right]$$

$$+ \frac{1}{Re_{REF}^{1/2}}\left\{\left[\mu\left(1 + \frac{\rho\varepsilon}{\mu}\right)\right]^{(i)}\frac{\partial^2 u}{\partial \xi \partial \zeta}\right.$$

$$\left. + \left[\frac{\partial u}{\partial \zeta}\left(1 + \frac{\rho\varepsilon}{\mu}\right)\right]^{(i)}\left(\frac{\partial \mu}{\partial T}\right)^{(i)}\frac{\partial T}{\partial \xi} + \left(\frac{\mu}{r^{\sigma}}\frac{\partial u}{\partial \zeta}\right)^{(i)}\frac{\partial}{\partial \xi}\left[\left(1 + \frac{\rho\varepsilon}{\mu}\right)r^{\sigma}\right]\right\}$$

$$- \frac{2}{3Re_{REF}^{1/2}}\left\{\left(\frac{\partial \mu}{\partial T}\right)^{(i)}\left(\frac{\partial u}{\partial \xi}\right)^{(i)}\frac{\partial T}{\partial \zeta} + \mu^{(i)}\frac{\partial^2 u}{\partial \zeta \partial \xi} + \left(\frac{\partial \mu}{\partial T}\right)^{(i)}\left(\frac{\partial v}{\partial \zeta}\right)^{(i)}\frac{\partial T}{\partial \zeta}\right.$$

$$\left. + \mu^{(i)}\frac{\partial^2 v}{\partial \zeta^2} + \sigma\left(\frac{\partial \mu}{\partial T}\right)^{(i)}\left(\frac{u\sin\theta}{r} - w\right)^{(i)}\frac{\partial T}{\partial \zeta} + \sigma\mu^{(i)}\left(\frac{\sin\theta}{r} - w\right)^{(i)}\frac{\partial u}{\partial \zeta}\right\}$$

$$+ \frac{(\rho u)^{(i)}}{R}u - \frac{2}{3}\frac{\sigma\mu^{(i)}}{Re_{REF}^{1/2}r^2}\left(\frac{\partial r}{\partial \zeta}\right)^{(i)}u \qquad (81)$$

energy

$$(\rho u)^{(i)}\frac{\partial T}{\partial \xi} + \left(1 + \frac{1}{Re_{REF}^{1/2}}\frac{\zeta}{R}\right)v\left(\rho\frac{\partial T}{\partial \zeta}\right)^{(i)} = (\gamma-1)M_{REF}^2\left[u^{(i)}\frac{\partial p}{\partial \xi}\right.$$

$$\left. + \left(1 + \frac{1}{Re_{REF}^{1/2}}\frac{\zeta}{R}\right)^{(i)}v^{(i)}\frac{\partial p}{\partial \zeta}\right] + (\gamma-1)M_{REF}^2\,\mu^{(i)}$$

$$\left[\left(1 + \frac{\zeta}{Re_{REF}^{1/2}R}\right)^{(i)}\left(\frac{\partial u}{\partial \zeta}\right)^{(i)}\frac{\partial u}{\partial \zeta} - \frac{2u^{(i)}}{Re_{REF}^{1/2}R}\frac{\partial u}{\partial \zeta}\right]$$

$$+ \left[\left(1 + \frac{\zeta}{Re_{REF}^{1/2}R}\right)\frac{\mu}{Pr_{REF}}\left(1 + \frac{\rho\varepsilon}{\mu}\frac{Pr_{REF}}{Pr_t}\right)^{(i)}\right]\frac{\partial^2 T}{\partial \zeta^2}$$

$$+ \frac{1}{r^{\sigma}}\left[\frac{\partial}{\partial \zeta}\left(r^{\sigma}\left(1 + \frac{1}{Re_{REF}^{1/2}}\frac{\zeta}{R}\right)\frac{\mu}{Pr_{REF}}\left(1 + \frac{\rho\varepsilon}{\mu}\frac{Pr_{REF}}{Pr_t}\right)\right)\right]^{(i)}\frac{\partial T}{\partial \zeta} \qquad (82)$$

Terms with superscript (i) are linearized terms and are updated after each iteration.

Following reference 4, to enhance stability, the continuity equation is written for point B (figure 18) and the two momentum equations and the energy equation are written for point A. The resulting system of algebraic linear finite difference equations which is derived in detail in Appendix F is:

$$A_{in}u_{m+1,n-1} + B_{in}u_{m+1,n} + G_{in}u_{m+1,n+1} + D_{in}v_{m+1,n-1} + E_{in}v_{m+1,n}$$
$$+ F_{in}v_{m+1,n+1} + G_{in}T_{m+1,n-1} + H_{in}T_{m+1,n} + I_{in}T_{m+1,n+1}$$
$$+ J_{in}p_{m+1,n-1} + K_{in}p_{m+1,n} + L_{in}p_{m+1,n+1} = S_{in} \qquad (83)$$

where:

$i = 1, 2, 3, 4$

$2 \leq n \leq N-1$

A centered differencing has been used for the variables u, v, and T in which the truncation error is of order $[(\Delta\zeta)^2]$, while for the pressure a forward two-point differencing has been applied. Though it is accurate only up to $(\Delta\zeta)$ it gives a more stable solution than a centered differencing which is accurate up to $(\Delta\zeta)^2$. This numerical instability associated with including the normal pressure gradient has been noted also by other investigators (reference 19).

In matrix notation the system of equations (83) can be written in a more compact form:

$$\bar{\bar{M}}\bar{\bar{X}} = \bar{g} \tag{84}$$

where $\bar{\bar{M}}$ is a block tridiagonal matrix defined:

$$\bar{\bar{M}} = \begin{vmatrix} \bar{M}_2 & \bar{E}_2 & 0 & & & 0 & 0 \\ \bar{D}_3 & \bar{M}_3 & \bar{E}_3 & & & & 0 \\ 0 & \bar{D}_4 & \bar{M}_4 & \bar{E}_4 & & & \\ & & & & & & \\ & & & \bar{D}_{N-2} & \bar{M}_{N-2} & \bar{E}_{N-2} & \\ 0 & 0 & & 0 & \bar{D}_{N-1} & \bar{M}_{N-1} & \end{vmatrix} \tag{85}$$

Each element in $\bar{\bar{M}}$ is a 4x4 matrix incorporating the coefficients of the system of the finite difference equations:

$$\bar{\bar{M}}_k = \begin{vmatrix} B_{1k} & E_{1k} & H_{1k} & K_{1k} \\ B_{2k} & E_{2k} & H_{2k} & K_{2k} \\ B_{3k} & E_{3k} & H_{3k} & K_{3k} \\ B_{4k} & E_{4k} & H_{4k} & K_{4k} \end{vmatrix} \qquad \bar{\bar{E}}_k = \begin{vmatrix} C_{1k} & F_{1k} & I_{1k} & L_{1k} \\ C_{2k} & F_{2k} & I_{2k} & L_{2k} \\ C_{3k} & F_{3k} & I_{3k} & L_{3k} \\ C_{4k} & F_{4k} & I_{4k} & L_{4k} \end{vmatrix}$$

and

$$\bar{D}_k = \begin{vmatrix} A_{1k} & D_{1k} & G_{1k} & J_{1k} \\ A_{2k} & D_{2k} & G_{2k} & J_{2k} \\ A_{3k} & D_{3k} & G_{3k} & J_{3k} \\ A_{4k} & D_{4k} & G_{4k} & J_{4k} \end{vmatrix} \tag{86}$$

in equations (84) $\bar{X}$ is the unknown column vector. Each element of $\bar{X}$ is itself a 4-element column vector defined:

$$\bar{X}_k = \begin{vmatrix} u_{m+1,k} \\ v_{m+1,k} \\ T_{m+1,k} \\ p_{m+1,k} \end{vmatrix} \tag{87}$$

$\bar{g}$ in equation (84) is a known column vector whose elements are defined by:

$$\bar{g}_k = \begin{vmatrix} S_{1k} \\ S_{2k} \\ S_{3k} \\ S_{4k} \end{vmatrix} \tag{88}$$

Writing the equations for $2 \leq n \leq N-1$ (see Appendix G) 4N-8 equations in 4N-1 unknowns are obtained, i.e., $u_{m+1,n}$, $v_{m+1,n}$, $T_{m+1,n}$ for

$1 \leq n \leq N$ and $p_{m+1,n}$ for $2 \leq n \leq N$. After applying the three boundary conditions at the wall (n=1) and the four conditions at the edge of the boundary layer (n=N), an additional calculation for the pressure at the wall is needed in order to obtain the density at the wall through the equation of state. The induced pressure at the wall is calculated by applying the ζ-momentum equation at the wall to obtain the pressure gradient and using a two-point differencing scheme the wall pressure can be determined and hence also the density at the wall. A detailed derivation of the expressions for calculating the pressure at the wall is given in Appendix H.

Method of Solution

Using the technique for block tridiagonal systems the block tridiagonal matrix $\bar{M}$ in equation (84) is decomposed into:

$$\bar{M} = \bar{L}\bar{U} \tag{89}$$

where $\bar{L}$ is the lower block diagonal matrix, and $\bar{U}$ is the upper block diagonal matrix. $\bar{L}$ and $\bar{U}$ are defined by:

$$\bar{L} = \begin{vmatrix} \bar{A}_2 & 0 & 0 & & & 0 \\ \bar{D}_3 & \bar{A}_3 & 0 & & & \\ 0 & \bar{D}_4 & \bar{A}_4 & & & \\ & & & & & 0 \\ & & & \bar{D}_{N-2} & \bar{A}_{N-2} & 0 \\ 0 & & & & \bar{D}_{N-1} & \bar{A}_{N-1} \end{vmatrix} \tag{90}$$

and

$$\bar{U} = \begin{vmatrix} \bar{I}_2 & \bar{N}_2 & 0 & 0 & & 0 \\ 0 & \bar{I}_3 & \bar{N}_3 & & & \\ & & & & & \\ & & & & & \\ & & & \bar{I}_{N-3} & \bar{N}_{N-3} & 0 \\ & & & & \bar{I}_{N-2} & \bar{N}_{N-2} \\ 0 & & & & 0 & \bar{I}_{N-1} \end{vmatrix} \tag{91}$$

By comparison of the corresponding elements from both sides of equation (89) the following relationships are obtained:

$$\bar{A}_2 = \bar{M}_2$$

$$\bar{N}_2 = A_2^{-1} \bar{E}_2 \tag{92}$$

and:

$$\bar{A}_n = \bar{M}_n - \bar{D}_n \bar{N}_{n-1} \qquad 3 \leq n \leq N-1$$

$$\bar{N}_n = \bar{A}_n^{-1} \bar{E}_n \qquad 2 \leq n \leq N-2$$

The method for solving equation (84) is then to write it as

$$\bar{L}\bar{U}\bar{X} = \bar{g} \tag{93}$$

or letting $\bar{U}\bar{X} = \bar{W}$ (94)

Equation (93) becomes:

$$\bar{L}\bar{W} = \bar{g} \tag{95}$$

The unknown vectors $\bar{W}_n$ are solved as follows:

$$\bar{W}_2 = \bar{A}_2^{-1}\bar{g}_2$$

$$\bar{W}_n = \bar{A}_n^{-1}(\bar{g}_n - \bar{D}_n\bar{W}_{n-1}) \quad \text{for } 3 \leq n \leq N-1 \tag{96}$$

After solving for $\bar{W}_n$, the required unknown $\bar{X}_n$ vectors can be obtained using the following procedure:

$$\bar{X}_{N-1} = \bar{W}_{N-1}$$

$$\bar{X}_n = \bar{W}_n - \bar{N}_n\bar{X}_{n+1} \qquad N-2 \geq n \geq 2 \tag{97}$$

By underrelaxing the solution vectors the coefficients of the linear difference equations are updated and thus the iteration procedure is continued until convergence of the solution vector is obtained. The equation for the underrelaxation procedure is:

$$\bar{X}_n = \bar{X}_{n_{OLD}} + \Omega\,(\bar{X}_{n_{NEW}} - \bar{X}_{n_{OLD}}) \tag{98}$$

where Ω is a positive number that is less than one. Most calculations were performed with $\Omega \approx 0.75$.

F. Numerical Results

Numerical solutions using the second-order inner region procedure have been obtained for a) the compressible laminar boundary layer on a flat plate over the Mach number range from 0 to 4, b) the compressible laminar boundary layer on a 20 degree half-angle cone at a free steam Mach number of 2.8, c) the compressible laminar boundary layer over the waisted body of reference 8 also at $M_\infty = 2.8$, and d) the turbulent boundary layer on a flat plate at $M_\infty = 0$. The laminar cases were computed for Pr = 0.72 and Sutherland viscosity.

To get the inner region solution started on its march downstream, data are required along an initial station in addition to the specification of boundary conditions. In the present system of equations, profiles for u, v, T and p must be given. For the presented laminar cases which all begin with nearly zero pressure gradient, the Blasius solution corrected for compressibility through the Howarth-Dorodintsyn transformation and adjusted when necessary for axial symmetry by the Mangler transformation has been used. The temperature profile has been obtained from the velocity profile using the Crocco integral and the induced pressure had been assumed to be zero across the boundary layer. Once the u, T and p profiles are known, the initial v profile is obtained by integration of the continuity equation. Sometimes, particularly at high Mach number, iteration of these approximate initial profiles is required in order to proceed downstream in a stable and convergent manner.

a) Laminar Flat Plate: The results obtained for the flat plate are in excellent agreement with classical boundary layer solutions. This is quite understandable since curvature effects are unimportant in this case. Nonetheless the present program is in physical coordinates and also gives direct calculation of the normal velocity distribution. In figures 19 and 20 the longitudinal and normal velocity distributions at $M = 0$ are seen to be essentially indistinguishable from their Blasius counterparts. Similarly for the variation of the normal velocity at the edge of the boundary layer at $M = 0$ (figure 21), except for a small blip at the beginning

indicating an initial datum line defect which however is damped out immediately. With increase in Mach number the calculation procedure yields convergent, smooth normal velocity distributions. The variation of their edge values with distance along the plate at different Mach numbers is shown in figure 22. The induced pressure distribution is very small in this case as expected.

The skin friction coefficient, form factor and displacement thickness distributions along the plate are shown in figure 23 for $M_\infty = 0$ for a range of unit Reynolds numbers and are seen to be indistinguishable from the similarity solutions. The very very slight differences are attributable to the different viscosity laws used, i.e. a linear viscosity temperature assumption in the Howarth-Dorodnitsyn stretching of the similarity solution as compared to the Sutherland viscosity relation in the finite difference solution. The same information at a Reynolds number of 1.5×10^6 but at Mach numbers up to 4 is shown in figure 24. These results again show good agreement with the similarity solutions.

b) Cone: As a first axisymmetric example, numerical solutions for the compressible laminar boundary layer over a 20 degree half-angle cone, were obtained for a free stream Mach number of 2.8. The normal velocity at the edge of the boundary layer is given in figure 25 which indicates that a stable and convergent solution has been achieved. As shown in the normal velocity has a negative sign for this cone angle indicating that the streamlines are directed into the surface whereas in the case of the flat plate or more slender cones

the edge streamlines are directed away from the surface. The skin friction coefficient along the surface is given in figure 26 indicating that a stable and convergent solution has been achieved.

c) Laminar Flow over Waisted Body: The compressible laminar boundary layer over the waisted body of revolution of Winter, Smith and Rotta (reference 8) has been calculated for $M_\infty = 2.799$. Curvature effects, lateral as well as longitudinal are pronounced in this case.

Variation of displacement thickness along the surface of $M_\infty = 2.799$ is shown in figure 27. The relatively large increase of the displacement thickness is mainly due to longitudinal curvature effect. In figure 28 the wall skin friction distribution is given and is seen to drop quite rapidly after $X/L_{REF} \approx 0.30$. The normal velocity distribution at the edge of the boundary layer is shown in figure 29. On the conical part of the waisted body the normal velocity is negative while further downstream the normal velocity at the edge changes sign due to curvature effects.

The pressure distribution across the boundary layer is shown in figure 30 at three stations: $X/L_{REF} = 0.1125$ on the conical part, $X/L_{REF} = 0.325$ near the maximum diameter and at $X/L_{REF} = 0.450$ after the inflection point of the surface. As shown the normal pressure gradient in the conical part is quite small whereas near the peak where curvature is pronounced the difference in wall pressure can be of the order of 5% of the inviscid wall pressure. Downstream at $X/L_{REF} = 0.450$ the pressure distribution across the boundary

layer changes due to curvature and differs noticeably from the inviscid value.

d. Incompressible Turbulent Flow Over Flat Plate

Numerical solutions have been obtained for the incompressible turbulent boundary layer over a flat plate using the two layer model for eddy viscosity. Initial profiles were generated using the law of the wall as formulated by Walz (reference 20) in terms of the following three algebraic relations corresponding respectively to the laminar sublayer for $y+ \leq 4$, a transition region for $4 < y+ < 26$, and the logarithmic law for $y+ \geq 26$.

$$u+ = y+ \qquad y+ \leq 4 \tag{99}$$

$$u+ = c_1 \cdot \ln(1 + y+) + c_2 + [(1 - c_1 - c_2 \cdot \alpha)y+ - c_2]\, e^{-ay+} \qquad 4 < y+ < 26 \tag{100}$$

$$u+ = c_1 \ell n\ y+ + c_2 \qquad y+ \geq 26 \tag{101}$$

In these expressions

$$u+ = \frac{u^*}{u_\tau}$$

$$y+ = y^* u_\tau / \nu$$

$$u_\tau = \sqrt{\tau_w / \rho}$$

The constants c_1, c_2 and α in equation (100) are taken as 2.50, 5.10 and 0.3 respectively.

All the following results are for a reference Reynolds number of 1.588×10^5. In figure 31 are shown distributions of skin friction coefficient, displacement and momentum thicknesses as well as edge normal velocity. The skin friction coefficience compare well with the Karman-Schoenherr relation as given in reference 21. Some oscillations are seen in the beginning of the edge normal velocity distribution but these rapidly die out. Obviously the initial datum line has some inconsistencies with the difference equations. Any such deviations in the initial data show up immediately in the normal velocity and induced pressure profiles. The displacement and momentum thickness distributions generally behave as expected. Figure 32 displays the u and v velocity profiles along the plate. The u-profiles that were calculated are as expected while for the normal velocity profiles a slight oscillatory character can be seen in the first three stations.

G. Convergence and Stability

The objective of this section is to list some of the major difficulties that have been met while trying to solve the non-linear partial differential equations that were replaced for solution by a system of linear algebraic equations using an implicit finite difference scheme.

It seems that in a complex system of non-linear partial differential equations such as developed herein for the inner layer, it is quite difficult to estimate stability criteria in closed form

by applying the VonNeumann method or some equivalent numerical stability analysis. Also when the solution becomes unstable it is difficult to trace the cause for that instability. Therefore only by trying different grid sizing and different weighting coefficients λ_c, λ_u, λ_v, λ_T and λ_p, have regions of stable calculation been found. The accuracy of the numerical solution has been checked with cases for which exact solutions exist.

Continuity Equation: It has been recognized that the continuity equation written as a central differencing in the ζ direction may lead to strong oscillations or even to divergence because of the boundary condition at the wall for the density or pressure (reference 22). One way to overcome this oscillatory behavior is to add an artificial eddy viscosity term into the continuity equation. In the present analysis however, a weighting factor of $\lambda_c = 0.85$ gives well behaved results (see Appendix F). Figures 33, 34, and 35 shows the normal velocity at the edge of the incompressible laminar boundary layer along a flat plate for $\lambda_c = 0.50$; $\lambda_c = 0.85$ and $\lambda_c = 1.20$ respectively. For $\lambda_c = 0.5$, the solution is clearly oscillatory and with increasing amplitude of oscillation. The solution for $\lambda_c = 1.20$ (figure 35) is overdamped. A value of $\lambda_c = 0.85$ is nearly optimal since only slight overdamping is seen for the first two stations and further downstream the results are the same as for the exact solution. The oscillatory behavior for $\lambda_c = 0.5$ is also maintained for the compressible boundary layers. A representative result at $M_\infty = 0.5$ is seen in figure 36. All inner

layer calculations other than these stability and convergence tests were performed with $\lambda_c = 0.85$.

The solutions of Reyhner and Flugge-Lotz (reference 4) which utilize central differencing ($\lambda_c = 0.5$) display the same oscillatory behavior as seen in figures 33 and 36. For the purposes of interactive calculation their edge normal velocity distribution was taken as the average of the peak-to-peak oscillations. They did not succeed in obtaining a smooth longitudinal variation of edge normal velocity.

Pressure

It has been recognized and reported (references 19 and 23) that departures from the proper solution can occur as a result of the $(\partial p/\partial \xi)$ terms in the ξ momentum and the energy equations. Besides in the present system there is an additional pressure gradient term $(\partial p/\partial \zeta)$ in the ζ-momentum equations and in the energy equation. It is found that these departures can be controlled by splitting the pressure as follows:

$$p(\xi,\zeta) = p_{EXT}(\xi) + p_I(\xi,\zeta) \tag{102}$$

where $p_{EXT}(\xi)$ is the external pressure imposed on the viscous layer by some outer region solution and $p_I(\xi,\zeta)$ is the induced pressure which is generally small compared to $p_{EXT}(\xi)$.

Basically two options are used for calculating the pressure gradient in the ξ direction. They are:

a) a centered difference for point A (see figure 18)

$$\frac{\partial p}{\partial \xi}(\xi,\zeta) = \frac{\partial p_{EXT}(\xi)}{\partial \xi} + (p_{I_{m+1,n}} - p_{I_{m,n}})/\Delta\xi_{m+1}$$

where: $\frac{\partial p_{EXT}(\xi)}{\partial \xi}$ is a presumably known function and $p_{I,m+1,n}$ is the unknown induced pressure.

b) The induced pressure gradient is taken as the gradient of average induced pressure across the boundary layer as follows:

$$\frac{\partial p_I}{\partial \xi} = \frac{\partial}{\partial \xi}\left[\frac{1}{\delta}\int_o^{\delta} p_{I_{m+1,n}}(\xi,\zeta)d\zeta\right]$$

In this option the induced pressure gradient is a known function which depends on the updated induced pressure distribution across the boundary layer. Both of these options have been used successfully in the present calculations. There is no clear preference among them at this time.

For each of the above-mentioned options for $\frac{\partial p_I}{\partial \zeta}$, the ζ-derivative of induced pressure was treated in several ways:

a) a centered-difference scheme accurate to order of $(\Delta\zeta_n^2)$ and for which a stable solution could not be achieved. In marching downstream a growing oscillatory behavior developed that could not be controlled.

b) a backward difference scheme which includes two-point differencing accurate to order of $(\Delta\zeta_n)$. With this option stable solutions have been obtained.

c) a forward difference-scheme which includes two-point differencing accurate to order of $(\Delta\zeta_n)$. Also here stable solutions have been obtained. The forward differencing is preferred since it is most convenient for matching when the inner region solution procedure is used in interactive calculations.

Grid Size: From experience with the program, it has been realized that careful selection of $\Delta\xi_{m+1}$ and $\Delta\zeta_n$ must be made in order to obtain stable and convergent solutions. The choice has an upper bound as well as a lower bound. Roughly speaking taking $\Delta\xi_{m+1}$ of the order of 4 to 5 times $\Delta\zeta_N$ will give stable solutions.

CHAPTER IV

INTERACTION PROCEDURE

In the interactive mode, following the suggestion of Ferri and Dash (reference 6), the inner and outer regions are matched at grid points where the Mach number is approximately 1.2 (figure 37). The matching procedure is however differently structured.

In order that the computer programs for each region interact properly, the two programs have been restructured and written in an overlay mode. Namely the computer program is divided into segments, a main segment and other segments of lesser heirarchy connected to the main segment like branches of a tree. Thus when the main segment calls for a program in a particular segment of lesser hierarchy all other segments of equivalent lesser hierarchy are ignored and only this segment is in the operating mode for use. Overlay operation is needed mainly for three reasons: a) to reduce the need for storage capacity b) to eliminate the rewriting of the program because of the similar name variables in the two programs, and c) for convenience, while calculating one of the regions, the computer program for the other region is not needed, and therefore can be stored in a scratch file.

A general flow diagram for the interactive mode is given in figure 38. Flow diagrams for the component outer region and inner region programs are shown in figures 39 and 40 respectively.

A. Initial Datum Line

In order to start the numerical calculation in the interactive mode, an initial datum line is required which must be consistent in an interactive sense between the inner and outer regions. For convenience the initial datum line has been fixed in a region where the cone flow solution is still valid. Accordingly the procedure for creating the initial datum line for axisymmetric flow is as follows:

1. Calculate the "inviscid" flow field using the outer region program.

2. Solve the inner region flow field using edge boundary conditions taken from the outer region solution of step 1.

3. At a station sufficiently downstream of the apex such that the inner region solution is well behaved, the Mach number 1.2 location is determined within the inner region and the slope of the local streamline ($\tan\theta = \frac{v}{u}$) is obtained.

4. At the station chosen in step 3, the outer region is recalculated using the Taylor-Maccoll equations with the slope of the streamline at the interface of the two regions (from step 3) taken as a boundary condition in place of the usual surface slope. Thus the shock angle and the flow field variables are changed slightly doe to the interaction.

5. The portion of the outer region profile from Mach number 1.2 to the edge of the boundary layer was scaled in order to get continuous profiles of the flow variables for this portion of the outer region. This was done simply by multiplying the outer region profile by a dimensionless form of the inner profile.

The procedure then gives complete information at the initial datum station.

B. Matching Procedure

The matching between the inner and outer regions requires an iterative procedure. The matching conditions are continuity of the flow variables u, v, T and p. Discontinuities in the derivatives with respect fo ζ of the flow variables about the matching grid points are due to the use of different numerical procedures on either side of the match points and to inconsistencies of order $(\delta/L_{REF})^2$ or higher in the systems of equations describing the two regions. The numerical results indicate that these discontinuities are very minor. Referring to figure 37, the matching grid points A and B are in the transonic regime where the Mach number is of the order of 1.2.

Point B is chosen at the intersection of an extended streamline through point A and a normal to the wall at station (m+1). The slope θ_B of the streamline at point B (station m+1) is assumed initially to be equal to the streamline slope θ_A at point A (station m), where the flow variables are all known. The flow variables u_B, v_B, T_B and p_B can be determined from information at point C (station m) using the boundary point procedure of the outer region program.

The inner region can now be calculated for station m+1 using the following converged data for point B as "edge condition":

$u_{(m+1,N)}$

$T_{(m+1,N)}$

$P_{(m+1,N)}$

Using the normal velocity gradient at the edge of the inner region as determined through the continuity equation, a new normal velocity v_{BI} for point B is obtained from the inner region solution. The new normal velocity is used to correct the slope at B to:

$$\theta_{B_{NEW}} = \tan^{-1} \frac{v_{BI}}{u_B} \tag{103}$$

with the new stream slope for point B the entire process is repeated until convergence is obtained for the flow variables at point B. Following this, the flow field in the outer region at station m+1 can be solved using the outer region system thus completing the calculation for station m+1.

C. Numerical Results

The interactive program has been applied to two examples: a) a supersonic flow over a 20 degree half angle cone at $M_\infty = 2.80$ and b) supersonic flow over the waisted body described in reference 8 also at $M_\infty = 2.80$. Both cases were for compressible laminar flow.

a. Cone: Numerical results for the wall static pressure are very slightly different than the inviscid flow field results as expected for this weakly interactive case. The difference of the shock angle between the interactive solution and the outer region solution is shown in figure 41. A slight oscillation is noticed at about $x/L_{REF} \sim 0.3$.

b. Waisted Body: Variation of static pressure difference relative to the inviscid static pressure is shown in figure 42 for the interactive and inner region solutions. The inner region solution

shows the reduction in surface pressure due to longitudinal curvature effects. This reduction is restored by the displacement effects in the interaction solution.

In Figure 43 the Mach number profile from the interactive calculation is compared with the separately calculated inviscid and boundary layer profiles. The interactive profile is reasonably continuous in slope at the matching line between the inner and outer regions. The interactive calculation indicates a larger skin friction than the boundary layer calculation and the approach to the inviscid Mach number distribution is slower than one would expect from comparison with the non-interactive boundary layer profile. It is suspected that this solution is not fully converged to the weak interaction solution.

Nevertheless, the interactive program does work and the indication from these results is that more experience is required in starting procedure, choice of matching location and convergence criteria to make the program fully useful as a design tool.

CHAPTER V

SUMMARY

A method has been developed for analysis of viscous-inviscid interactions in supersonic flows. The outer supersonic region of the flow field is represented by a two-family method of characteristics. In the present scheme, inclusion of viscous and conductive terms in the formulation allows calculation of the supersonic portion of boundary layers and the tracing of wave reflection within those supersonic regions. It has been shown that shock wave patterns can be altered by inclusion of the correction terms. The inner region is handled by a second order boundary layer system that includes longitudinal and transverse curvature effects and a normal momentum equation. This nonlinear partial differential system of equations of parabolic type have been solved numerically in the physical plane by replacing them by a system of linear algebraic equations using a modified Crank-Nicolson implicit finite difference scheme. The nonlinearity of inner region equations was taken into account by an iterative procedure until the difference between the flow variables for successive iterations is as small as desired. Generally 4 to 10 iterations are needed to get a convergent solution. This depends however on the accuracy of information on the initial datum line.

An interesting and useful byproduct of the present work is the experience gained in overcoming the difficulties of obtaining a stable and convergent solution for the coupled parabolic non-linear partial differential set in the inner region. Other investigators have encountered these difficulties even for less complicated systems of equations. They overcame the difficulties either by decoupling the equations, i.e., solving the equations successively or by arbitrarily smoothing the oscillatory results. It has been recognized by other investigators that the terms involving the pressure gradient $(\partial p/\partial \xi)$ lead to instabilities in the numerical results. Besides in the present procedure an additional pressure gradient $(\partial p/\partial \zeta)$ appearing in the ζ-momentum equation and energy equation is another source for causing numerical instabilities. It is found in the present work that the numerical instabilities can be controlled by splitting the pressure into $P_{EXT}(\xi)$ and an induced pressure $P_I(\xi,\zeta)$, where $P_{EXT}(\xi)$, the "external" pressure is obtained from the outer layer solution procedure. The ζ derivative of the induced pressure was treated by a two-point backward or forward difference scheme that leads to a stable and convergent solution. A centered difference scheme would lead to an unstable solution. Also it has been recognized here that the continuity equation which is a first order differential equation when written as a central differencing in the ζ direction leads to strong oscillation and divergence of the numerical solution. In the present work a weighted differencing scheme has been used. The oscillatory behavior that was particularly pronounced in the normal

velocity has been damped out by choosing a proper weighting factor.

Numerical results obtained herein for compressible laminar boundary layers agree very well with exact solutions. Numerical results for the waisted body where longitudinal curvature is important leads to pressure variation in the normal direction across the boundary layer. The wall static pressures differ by as much as 5% from P_{EXT}.

In the interactive mode the matching between the inner and the outer regions requires an iterative procedure. The normal velocity is the key parameter for matching the two solutions in the transonic region where the Mach number is of the order of 1.2. Thus it is important to get a stable and convergent inner solution for the normal velocity. It is interesting to note that the inner region solution converges at a faster rate in an interactive mode compared to the solution of the inner region in the non-interactive mode. The matching procedure works satisfactorily and numerical results for a 20 degree half angle cone and for the waisted body of Winter, Smith and Rotta at $M_\infty = 2.8$ have been obtained.

Supersonic viscous-inviscid interactive analysis is an important area that has received only limited attention to date. The interactive procedure developed herein should be quite useful in dealing with supersonic flow fields where separation and strong-shock interaction effects are absent. Further work is required in order to make interaction procedures such as the present one more encompassing and versatile.

REFERENCES

1. Crocco, L., and L. Lees, "A Mixing Theory for the Interaction Between Dissipative Flows and Nearly Isentropic Streams", J. Aerospace Sci., 19, 649-676 (1952).

2. Lees, L. and Reeves, B. L., "Supersonic Separated and Reattaching Laminar Flows: I. General Theory and Application to Adiabatic Boundary Layer/Shock Wave Interaction", AIAA Journal, Vol. 2, No. 11, Nov. 1964, pp. 1907-1920.

3. Klineberg, J. M. and Lees, L., "Theory of Laminar Viscous-Inviscid Interaction in Supersonic Flow", AIAA J., 7, 1969, pp. 2211-2221.

4. Reyhner, T.A., and Flugge-Lotz, I., "The Interaction of a Shock Wave with Laminar Boundary Layer", Tech. Rep. 163, Div. Engin. Mech., Stanford University, Nov. 1966.

5. Miller, G., "Mathematical Formulation of Viscous-Inviscid Interaction Problems in Supersonic Flow", AIAA J., Nov. 1973, pp. 938-942.

6. Ferri, A. and Dash, S., "Viscous Flow at High Mach Numbers with Pressure Gradients", Viscous-Interaction Phenomena in Super Sonic and Hypersonic Flow, University of Dayton, Ohio, 1969.

7. Ames Research Staff: Equations, Tables and Charts for Compressible Flow, NACA Rep. 1135 (1953).

8. Winter, R.G., Smith, K.G., and Rotta, J.C., "Turbulent Boundary Layer Studies on a Waisted Body of Revolution in Subsonic and Supersonic Flow", AGARDograph 97, 993-962, 1962.

9. Syberg, J. and Hickcox, T.E., "Design of Bleed System for a Mach 3.5 Inlet", NASA CR-2187, January 1973.

10. Walkden, F., Laws, G.T., and Caine, P., "Shock Capturing Numerical Method for Calculating Supersonic Flows", AIAA J. Vol. 12, No. 5, pp. 642-647, May 1964.

11. Van-Dyke, M.D., "Higher Order Boundary Layer Theory", Annual Review of Fluid Mechanics Vol. 1, Annual Reviews, Inc., Palo-Alto, Calif., 1969, pp. 265-292.

12. Maslen, H.S., "Second Order Effects in Laminar Boundary Layers", AIAA Journal, Vol. 1, No. 1, January 1963, pp. 33-40.

13. Seginer, A., "Compressible Boundary Layer with Normal Pressure Gradients. Quasi-Similarity Equations - Their Properties at the Wall and at Sharp and Blunt Leading Edges", AIAA paper No. 72-696 (June 1972).

14. Clauser, F.H., "The Turbulent Boundary Layer", Advances in Applied Mechanics, Vol. IV, Academic Press, New York, 1956, pp. 1-51.

15. Cebeci, T. and Smith, A.M.O., "Analysis of Turbulent Boundary Layers", Applied Mathematics and Mechanics, Academic Press, New York, 1974, pp. 215-217.

16. Van Driest, E.R., "On Turbulent Flow Near a Wall", Jour. Aero. Sci., Vol. 23, No. 11, Nov. 1956, pp. 1007-1011, 1036.

17. Bradshaw, P., Ferris, D. H., and Atwell, N.P., "Calculation of Boundary Layer Development Using the Turbulent Energy Equation", Journal of Fluid Mechanics, Vol. 28, Part 3, May 1967, pp. 593-616.

18. Roache, Patrick, J., "Computational Fluid Dynamics", Hermosa Publishers, 1972.

19. Lin, T.C. and Rubin, S.G., "Viscous Flow Over a Cone at Incidence I-Hypersonic Tip Region", Computers and Fluids, 1, 1, pp. 37-57, 1972.

20. Walz, A., "Boundary Layers of Flow and Temperature", MIT Press, 1969, pp. 115.

21. Schlichting, H., "Boundary Layer Theory", Sixth Edition, McGraw-Hill, 1968.

22. Peyret, R. and Viviand, H., "Computation of Viscous Compress Flows Based on the Navier-Stokes Equations", AGARD-AG-212, Sept. 1975.

23. Lubard, S.C., and Helliwell, W.S., "Calculation of Flow on a Cone at High Angle of Attach", AIAA Journal, July 1974.

24. Courant, R., and Friedrichs, K.O., "Supersonic Flow and Shock Waves", Interscience Publishers, Inc., New York, 1948.

APPENDIX A

TRANSFORMATION TO STREAMLINE-NORMAL COORDINATES

The non-dimensional system of equations (7) to (11) written in cartesian coordinates (x,y) is transformed to a curvilinear coordinate system (s,n) where s and n are respectively the distance along a streamline and the distance normal to the streamline. In this form it is easy and straightforward to identify and retain the transport effects such as viscous shear and heat flux only normal to the streamlines.

Transformation Relation: The transformation relations from cartesian coordinates (x,y) to the curvilinear coordinates (s,n) are (see figure 1):

$$\frac{\partial}{\partial x} = \cos\theta \frac{\partial}{\partial s} - \sin\theta \frac{\partial}{\partial n}$$

$$\frac{\partial}{\partial y} = \sin\theta \frac{\partial}{\partial s} + \cos\theta \frac{\partial}{\partial n} \qquad \text{(A-1)}$$

Also the velocity components (u,v) in cartesian coordinates expressed in terms of the velocity vector magnitude q, and flow direction, θ, are:

$$u = q \cos\theta$$

$$v = q \sin\theta \qquad \text{(A-2)}$$

After substitution of relations (A-1) and (A-2), the governing equations (7) to (11) when simplified and expressed in curvilinear system (s,n) are:

Continuity

$$\cos\theta \frac{\partial}{\partial s}(\rho q \cos\theta\, y^{\sigma}) - \sin\theta \frac{\partial}{\partial n}(\rho q \cos\theta y^{\sigma}) + \sin\theta \frac{\partial}{\partial s}(\rho q \sin\theta y^{\sigma}) + \cos\theta \frac{\partial}{\partial n}(\rho q \sin\theta y^{\sigma}) = 0 \qquad \text{(A-3)}$$

Expanding and rearranging the terms, the resulting equation is:

$$\frac{\partial}{\partial s}(\rho q) + \rho q \frac{\partial \theta}{\partial n} = - \frac{\sigma \rho q \sin\theta}{y} \qquad \text{(A-4)}$$

Longitudinal momentum

$$\rho q \cos\theta[\cos\theta \frac{\partial}{\partial s}(q\cos\theta) - \sin\theta \frac{\partial}{\partial n}(q\cos\theta)] + \rho q \sin\theta[\sin\theta \frac{\partial}{\partial s}(q\cos\theta) + \cos\theta \frac{\partial}{\partial n}(q\cos\theta)] = - \frac{1}{\gamma M_{REF}^2}[\cos\theta \frac{\partial p}{\partial s} - \sin\theta \frac{\partial p}{\partial n}] + \overline{AQ}_1 \qquad \text{(A-5)}$$

Considering an ordering procedure, $\frac{\partial^2}{\partial s^2}/\frac{\partial^2}{\partial n^2}$ is of the order of $(\delta/L)^2$, therefore terms of this order are neglected in the present analysis. The resulting expression is:

$$\overline{AQ}_1 = \frac{1}{Re_{REF}}\{\frac{1}{y^{\sigma}} \cos\theta \frac{\partial}{\partial n}[\mu y^{\sigma} \cos\theta \frac{\partial}{\partial n}(q\cos\theta)] + \sin\theta \frac{\partial}{\partial n}[\mu \sin\theta \frac{\partial}{\partial n}(q\cos\theta)]\} \qquad \text{(A-6)}$$

Expanding equation (A-5) and rearranging terms yields:

$$\rho q \frac{\partial}{\partial s}(q\cos\theta) = - \frac{1}{\gamma M_{REF}^2} \cos\theta \frac{\partial p}{\partial s} + \frac{1}{\gamma M_{REF}^2} \sin\theta \frac{\partial p}{\partial n} + \overline{AQ}_1 \qquad \text{(A-7)}$$

Normal momentum

$$\rho q \cos\theta[\cos\theta \frac{\partial}{\partial s}(q\sin\theta) - \sin\theta \frac{\partial}{\partial n}(q\sin\theta)]$$
$$+ \rho q\sin\theta[\sin\theta \frac{\partial}{\partial s}(q\sin\theta) + \cos\theta \frac{\partial}{\partial n}(q\sin\theta)]$$
$$= - \frac{1}{\gamma M^2_{REF}}[\sin\theta \frac{\partial p}{\partial s} + \cos\theta \frac{\partial p}{\partial n}] + \overline{AQ}_2 \qquad \text{(A-8)}$$

where:

$$\overline{AQ}_2 = \frac{1}{Re_{REF}}\{\frac{1}{y^\sigma} \cos\theta \frac{\partial}{\partial n}[\mu y^\sigma \cos\theta \frac{\partial}{\partial n}(q\sin\theta)]$$
$$+ \sin\theta \frac{\partial}{\partial n}[\mu \sin\theta \frac{\partial}{\partial n}(q\sin\theta)]\} \qquad \text{(A-9)}$$

Expanding and rearranging yields:

$$\rho q \frac{\partial}{\partial s}(q\sin\theta) = - \frac{1}{\gamma M^2_{REF}} \sin\theta \frac{\partial p}{\partial s} - \frac{1}{\gamma M^2_{REF}} \cos\theta \frac{\partial p}{\partial n} + \overline{AQ}_2 \qquad \text{(A-10)}$$

Energy

For the simplified thermodynamic assumptions used herein, namely

$$\frac{Pr_{REF}}{Pr_\infty} = 1 = \mu \frac{C_p}{k}$$

$$\frac{C_{p_{REF}}}{C_{p_\infty}} = 1 \qquad \text{,,} \quad \mu = k$$

the energy equation becomes:

$$\rho q\cos\theta(\cos\theta \frac{\partial T}{\partial s} - \sin\theta \frac{\partial T}{\partial n}) + \rho q\sin\theta(\sin\theta \frac{\partial T}{\partial s} + \cos\theta \frac{\partial T}{\partial n})$$
$$- \frac{(\gamma-1)}{\gamma}[q\cos\theta(\cos\theta \frac{\partial p}{\partial s} - \sin\theta \frac{\partial p}{\partial n}) + q\sin\theta(\sin\theta \frac{\partial p}{\partial s} + \cos\theta \frac{\partial p}{\partial n})]$$
$$= \overline{AQ}_3 \qquad \text{(A-11)}$$

where:

$$\overline{AQ}_3 = \frac{1}{Pr_{REF}Re_{REF}}\{\frac{1}{y^\sigma}\cos\theta\,\frac{\partial}{\partial n}[y^\sigma\mu\cos\theta\,\frac{\partial T}{\partial n}] + \sin\theta\,\frac{\partial}{\partial n}[\mu\sin\theta\,\frac{\partial T}{\partial n}]\}$$
$$+ \frac{(\gamma-1)M^2_{REF}}{Re_{REF}}\{\mu[\cos\theta\,\frac{\partial}{\partial n}(q\cos\theta) - \sin\theta\,\frac{\partial}{\partial n}(q\sin\theta)]^2$$
$$+ 2\mu[\sin^2\theta(\frac{\partial}{\partial n}(q\cos\theta))^2 + \cos^2\theta(\frac{\partial}{\partial n}(q\sin\theta))^2]\} \qquad \text{(A-12)}$$

Expansion and rearrangement yields:

$$\rho q\,\frac{\partial T}{\partial s} = \frac{(\gamma-1)}{\gamma}\,q\,\frac{\partial p}{\partial s} + \overline{AQ}_3 \qquad \text{(A-13)}$$

Upon multiplication of equation (A-7) by $\cos\theta$ and (A-10) by $\sin\theta$ and then adding the equations, the following is obtained:

$$\rho q\,\frac{\partial q}{\partial s} + \frac{1}{\gamma M^2_{REF}}\,\frac{\partial p}{\partial s} = Q_1 \qquad \text{(A-14)}$$

where:

$$Q_1 = \overline{AQ}_1\cos\theta + \overline{AQ}_2\sin\theta \qquad \text{(A-15)}$$

Multiplication of equation (A-7) by $(-\sin\theta)$ and (A-10) by $\cos\theta$ and then adding the equations yields the following:

$$\rho q^2\,\frac{\partial\theta}{\partial s} + \frac{1}{\gamma M^2_{REF}}\,\frac{\partial p}{\partial n} = -Q_2 \qquad \text{(A-16)}$$

where:

$$Q_2 = \sin\theta\,\overline{AQ}_1 - \cos\theta\,\overline{AQ}_2 \qquad \text{(A-17)}$$

The energy equation becomes:

$$\rho q\,\frac{\partial T}{\partial s} - \frac{(\gamma-1)}{\gamma}\,q\,\frac{\partial p}{\partial s} = (\gamma-1)M^2_{REF}Q_3 \qquad \text{(A-18)}$$

where:

$$Q_3 = \overline{AQ}_3/(\gamma-1)M^2_{REF}$$

Transport terms

The correction terms Q_1, Q_2 and Q_3 due to viscous shear and heat flux which are considered as source terms in the method of characteristics solution of the system of equations (A-4), (A-7), (A-10) and (A-13) can be simplified in the following way:

Q_1 - term

$$Q_1 = \cos\theta\ \overline{AQ}_1 + \sin\theta\ \overline{AQ}_2$$

$$= \frac{\cos\theta}{Re_{REF}}\{\frac{1}{y^\sigma}\cos\theta\ \frac{\partial}{\partial n}[\mu y^\sigma \cos\theta\ \frac{\partial}{\partial n}(q\cos\theta)]$$

$$+ \sin\theta\ \frac{\partial}{\partial n}[\mu\sin\theta\ \frac{\partial}{\partial n}(q\cos\theta)]\}$$

$$+ \frac{\sin\theta}{Re_{REF}}\{\frac{\cos\theta}{y^\sigma}\ \frac{\partial}{\partial n}[\mu y^\sigma \cos\theta\ \frac{\partial}{\partial n}(q\sin\theta)] + \sin\theta\ \frac{\partial}{\partial n}[\mu\sin\theta\ \frac{\partial}{\partial n}(q\sin\theta)]\} \quad \text{(A-19)}$$

Expansion and cancellation of terms reduces the expression for Q_1 to:

$$Q_1 = \frac{1}{Re_{REF}}\{\frac{\partial}{\partial n}(\mu\ \frac{\partial q}{\partial n}) + \frac{\sigma\cos\theta\mu}{y}\ \frac{\partial q}{\partial n} - \mu q(\frac{\partial\theta}{\partial n})^2 - \frac{\sigma\mu}{y}\ \frac{\partial q}{\partial n}\sin^2\theta\} \quad \text{(A-20)}$$

Q_2 - term

$$Q_2 = \sin\theta\cdot\overline{AQ}_1 - \cos\theta\cdot\overline{AQ}_2$$

$$= \frac{\sin\theta}{Re_{REF}}\{\frac{1}{y^\sigma}\cos\theta\ \frac{\partial}{\partial n}[\mu y^\sigma \cos\theta\ \frac{\partial}{\partial n}(q\cos\theta)]$$

$$+ \sin\theta\ \frac{\partial}{\partial n}[\mu\sin\theta\ \frac{\partial}{\partial n}(q\cos\theta)\} - \frac{\cos\theta}{Re_{REF}}\{\frac{\cos\theta}{y^\sigma}\ \frac{\partial}{\partial n}[\mu y^\sigma \cos\theta\ \frac{\partial}{\partial n}(q\sin\theta)]$$

$$+ \sin\theta\ \frac{\partial}{\partial n}[\mu\sin\theta\ \frac{\partial}{\partial n}(q\sin\theta)]\} \quad \text{(A-21)}$$

Expanding and rearranging the terms yields:

$$Q_2 = -\frac{1}{Re_{REF}}\{\mu \frac{\partial q}{\partial n}\frac{\partial \theta}{\partial n} + \frac{\partial}{\partial n}(\mu q \frac{\partial \theta}{\partial n}) + \frac{\sigma \mu q \cos^3\theta}{y}\frac{\partial \theta}{\partial n}\} \qquad (A\text{-}22)$$

Q_3 - term

$$E_{REF}Q_3 = \frac{1}{Pr_{REF}Re_{REF}}\{\frac{\cos\theta}{y^\sigma}\frac{\partial}{\partial n}[\mu y^\sigma \cos\theta \frac{\partial T}{\partial n}] + \sin\theta \frac{\partial}{\partial n}[\mu \sin\theta \frac{\partial T}{\partial n}]\}$$
$$+ \frac{(\gamma-1)M^2_{REF}\mu}{Re_{REF}}\{[\cos\theta \frac{\partial}{\partial n}(q\cos\theta) - \sin\theta \frac{\partial}{\partial n}(q\sin\theta)]^2$$
$$+ 2[\sin^2\theta(\frac{\partial}{\partial n}(q\cos\theta))^2 + \cos^2\theta(\frac{\partial}{\partial n}(q\sin\theta))^2]\} \qquad (A\text{-}23)$$

Expansion and rearrangement yields:

$$(\gamma-1)M^2_{REF}Q_3 = \frac{1}{Pr_{REF}Re_{REF}}\{\frac{\partial}{\partial n}(\mu \frac{\partial T}{\partial n}) + \frac{\sigma \mu \cos^3\theta}{y}\frac{\partial T}{\partial n}\}$$
$$+ \frac{(\gamma-1)M^2_{REF}}{Re_{REF}}\{\mu(\frac{\partial q}{\partial n})^2 + 2\mu q^2(\frac{\partial \theta}{\partial n})^2\} \qquad (A\text{-}24)$$

The Q_1, Q_2 and Q_3 are correct to order (δ/L).

APPENDIX B

METHOD OF CHARACTERISTICS

The characteristic equations are derived here for steady viscous compressible rotational two-dimensional or axisymmetric configurations in supersonic flow. The independent variables chosen are the static pressure, p and the streamline direction, θ.

For convenience equations (12) to (16) are repeated here as (B-1) through (B-5).

Continuity

$$\frac{\partial}{\partial s}(\rho q) + \rho q \frac{\partial \theta}{\partial n} = - \frac{\sigma \rho q}{y} \sin\theta \qquad \text{(B-1)}$$

s-momentum

$$\rho q \frac{\partial q}{\partial s} + \frac{1}{\gamma M_{REF}^2} \frac{\partial p}{\partial s} = Q_1 \qquad \text{(B-2)}$$

n-momentum

$$\rho q^2 \frac{\partial \theta}{\partial s} + \frac{1}{\gamma M_{REF}^2} \frac{\partial p}{\partial n} = -Q_2 \qquad \text{(B-3)}$$

Energy

$$\rho q \frac{\partial T}{\partial s} - \frac{(\gamma-1)}{\gamma} q \frac{\partial p}{\partial s} = (\gamma-1) M_{REF}^2 Q_3 \qquad \text{(B-4)}$$

Equation of state

$$p = \rho T \qquad \text{(B-5)}$$

Equation (B-1) can be written as follows:

$$\frac{1}{\rho}\frac{\partial \rho}{\partial s} + \frac{1}{q}\frac{\partial q}{\partial s} + \frac{\partial \theta}{\partial n} = -\frac{\sigma \sin\theta}{y} \tag{B-6}$$

Equation (B-2) upon dividing through by ρq^2 becomes:

$$\frac{1}{q}\frac{\partial q}{\partial s} = \frac{Q_1}{\rho q^2} - \frac{1}{\gamma M_{REF}^2}\frac{1}{\rho q^2}\frac{\partial p}{\partial s} \tag{B-7}$$

The equation of state in differential form is:

$$\frac{1}{\rho}\frac{\partial \rho}{\partial s} = \frac{1}{p}\frac{\partial p}{\partial s} - \frac{1}{T}\frac{\partial T}{\partial s} \tag{B-8}$$

and upon dividing through by ρqT the energy equation becomes:

$$\frac{1}{T}\frac{\partial T}{\partial s} = \frac{(\gamma-1)M_{REF}^2}{\rho qT} Q_3 + \frac{(\gamma-1)}{\gamma}\frac{1}{\rho T}\frac{\partial p}{\partial s} \tag{B-9}$$

Substitution of (B-7), (B-8) and (B-9) into (B-6) yields:

$$\frac{1}{p}\frac{\partial p}{\partial s} - \left\{\frac{(\gamma-1)M_{REF}^2}{\rho qT} Q_3 + \frac{(\gamma-1)}{\gamma}\frac{1}{\rho T}\frac{\partial p}{\partial s}\right\} + \frac{Q_1}{\rho q^2} - \frac{1}{M_{REF}^2}\frac{1}{\rho q^2}\frac{\partial p}{\partial s}$$

$$+ \frac{\partial \theta}{\partial n} = -\frac{\sigma \sin\theta}{y}$$

or

$$\frac{1}{\gamma M_{REF}^2 \rho q^2}\frac{\partial p}{\partial s}(M^2-1) + \frac{\partial \theta}{\partial n} = -\frac{\sigma \sin\theta}{y} + \frac{(\gamma-1)M_{REF}^2}{\rho qT} Q_3 - \frac{Q_1}{\rho q^2} \tag{B-10}$$

In order to obtain the characteristics the following system consisting of equations (B-10), (B-3) and identities for the differentials dp and $d\theta$ must be solved:

$$\frac{(M^2-1)}{\gamma M_{REF}^2 q^2}\frac{\partial p}{\partial s} + \frac{\partial \theta}{\partial n} = -\frac{\sigma \sin\theta}{y} + \frac{(\gamma-1)M_{REF}^2}{\rho q T}Q_3 - \frac{Q_1}{\rho q^2}$$

$$\frac{1}{\gamma M_{REF}^2}\frac{\partial p}{\partial n} + \rho q^2 \frac{\partial \theta}{\partial s} = -Q_2$$

$$\frac{\partial p}{\partial s}\,ds + \frac{\partial p}{\partial n}\,dn = dp$$

$$\frac{\partial \theta}{\partial s}\,ds + \frac{\partial \theta}{\partial n}\,dn = d\theta$$

(B-11)

The characteristic curves must satisfy the following relations:

$$\begin{vmatrix} \frac{(M^2-1)}{\gamma M_{REF}^2 \rho q^2} & 0 & 0 & 1 \\ 0 & \frac{1}{\gamma M_{REF}^2} & \rho q^2 & 0 \\ ds & dn & 0 & 0 \\ 0 & 0 & ds & dn \end{vmatrix} = 0 \qquad \text{(B-12)}$$

$$\begin{vmatrix} \frac{(M^2-1)}{M_{REF}^2 q^2} & 0 & 0 & \left[\frac{\sigma \sin\theta}{y} + \frac{(\gamma-1)M_{REF}^2 Q_3}{\rho q T} - \frac{Q_1}{\rho q^2}\right] \\ 0 & \frac{1}{\gamma M_{REF}^2} & \rho q^2 & -Q_2 \\ ds & dn & 0 & dp \\ 0 & 0 & ds & d\theta \end{vmatrix} = 0$$

(B-13)

Upon expanding equation (B-12) the equation of characteristics is obtained:

$$\frac{dn}{ds} = \pm\tan\lambda \tag{B-14}$$

where:

$\lambda = \sin^{-1}\frac{1}{M}$ is the Mach angle.

The compatibility condition is obtained by solving equation (B-13):

$$\frac{dp}{\gamma p} \mp \frac{d\theta}{\sin\lambda\cos\lambda} + \left[\frac{\sigma\sin\theta}{y} + \frac{Q_1}{\rho q^2} - \frac{(\gamma-1)M_{REF}^2}{\rho q T} Q_3 \pm Q_2 \frac{M_{REF}^2 \sin\lambda}{p}\right] \frac{dx}{\cos\lambda\cos(\theta\pm\lambda)} = 0 \tag{B-15}$$

The + and - signs correspond to C+ and C- characteristic lines respectively.

The non-dimensional form of the entropy relation in terms of temperature, T and the pressure, p is:

$$dS = \frac{\gamma}{(\gamma-1)}\frac{dT}{T} - \frac{dp}{p} \tag{B-16}$$

where:

$$S = \frac{S^*}{R}$$

The viscous shear and heat flux lead to entropy changes along a streamline. Using the energy equation (B-4):

$$\frac{\partial T}{\partial s} = \frac{(\gamma-1)M_{REF}^2}{\rho q} Q_3 + \frac{(\gamma-1)}{\gamma}\frac{1}{\rho}\frac{\partial p}{\partial s}$$

Thus:

$$\frac{dS}{ds} = \frac{\gamma}{(\gamma-1)}\frac{1}{T}\frac{\partial T}{\partial s} - \frac{1}{p}\frac{\partial p}{\partial s} = \frac{\gamma}{(\gamma-1)}\left[\frac{(\gamma-1)M_{REF}^2}{\rho T q} Q_3 + \frac{(\gamma-1)}{\gamma}\frac{1}{\rho T}\frac{\partial p}{\partial s}\right] - \frac{1}{p}\frac{\partial p}{\partial s}$$

or upon further reduction

$$\frac{dS}{ds} = \frac{(\gamma-1)M^2_{REF}}{pq} Q_3 = \frac{\gamma M^2_{REF}}{pq} Q_3 \qquad \text{(B-17)}$$

The variation of stagnation temperature, T_s along a streamline as derived from the energy equation (B-4) and s-momentum (B-2) is:

$$\frac{dT_s}{ds} = \frac{(\gamma-1)M^2_{REF}}{\rho q} Q_3 + Q_1 \frac{(\gamma-1)M^2_{REF}}{\rho} \qquad \text{(B-18)}$$

APPENDIX C

CONICAL FLOWFIELD

The conical flowfield is derived for steady, isentropic, and irrotational flow with cylindrical symmetry about the x-axis (reference 24). For the mathematical construction of the conical flow pattern, since there is no length scale, all flow variables depend only on the ray angle from the apex or on the ratio:

$$\omega = \frac{x}{y} \tag{C-1}$$

The differential equations used for this potential flow are:

$$\frac{\partial v}{\partial x} = \frac{\partial u}{\partial y} \qquad \text{(irrotational flow)} \tag{C-2}$$

$$\left(1 - \frac{u^2}{c^2}\right) \frac{\partial u}{\partial x} - 2 \frac{uv}{c^2} \frac{\partial v}{\partial x} + \left(1 - \frac{v^2}{c^2}\right) \frac{\partial v}{\partial y} + \frac{v}{y} = 0 \tag{C-3}$$

and

$$\left(\frac{\gamma-1}{\gamma+1}\right)(u^2+v^2) + \frac{2}{(\gamma+1)} c^2 = c_*^2 \tag{C-4}$$

where u is the velocity component in the x-direction, v is the velocity component in the y-direction, c is the local speed of sound and c_* is the critical sound speed.

Expressing the equation in terms of ω equations (C-2) and (C-3) become respectively:

$$\frac{\partial v}{\partial \omega} + \omega \frac{\partial u}{\partial \omega} = 0 \tag{C-5}$$

and

$$(c^2 - u^2)\frac{\partial u}{\partial \omega} - 2uv\frac{\partial v}{\partial \omega} - (c^2 - v^2)\,\omega\frac{\partial v}{\partial \omega} + c^2 v = 0 \qquad \text{(C-6)}$$

Clearly this pair is equivalent to one equation of second order for one function only. Equation (C-6) assumes a particularly useful form when v is introduced as a function of u. Thus from (C-5):

$$\omega = -\frac{\frac{\partial v}{\partial \omega}}{\frac{\partial u}{\partial \omega}} = -\frac{\partial v}{\partial u} \qquad \text{(C-7)}$$

Differentiating (C-7) with respect to ω

$$1 = -\frac{\partial}{\partial \omega}\left(\frac{\partial v}{\partial u}\right) = -\frac{\partial}{\partial u}\left(\frac{\partial v}{\partial u}\right)\frac{\partial u}{\partial \omega}$$

or

$$\frac{\partial u}{\partial \omega} = -\frac{1}{\frac{\partial^2 v}{\partial u^2}} \qquad \text{(C-8)}$$

Substituting (C-8) into (C-5) yields the relation:

$$\frac{\partial v}{\partial \omega} = -\frac{\frac{\partial v}{\partial u}}{\frac{\partial^2 v}{\partial u^2}} \qquad \text{(C-9)}$$

Introducing (C-7), (C-8) and (C-9) into equation (C-6) leads to the following particularly simple form of the Taylor-Maccoll equation:

$$v\frac{\partial v}{\partial u} = 1 + \left(\frac{\partial v}{\partial u}\right)^2 - \frac{(u+v\frac{\partial v}{\partial u})}{c^2}\frac{\partial v}{\partial u}^2 \qquad \text{(C-10)}$$

Eliminating c^2 by means of equation (C-4) yields:

$$v\frac{\partial u}{\partial v} = 1 + \left(\frac{\partial v}{\partial u}\right)^2 - \frac{\left(\frac{\gamma+1}{2}\right)(u+v\frac{\partial v}{\partial u})^2}{c_*^2 - \left(\frac{\gamma-1}{\gamma+1}\right)(u^2+v^2)} \qquad \text{(C-11)}$$

Along the cone surface the flow has the direction of tne ray $\omega = \frac{x}{y}$ traced by the cone in the x,y plane and thus:

$$\omega = \frac{u}{v}$$

$$\frac{\partial v}{\partial u} = - \frac{u}{v} \tag{C-12}$$

The conditions to be satisfied along the conical shock (reference 24) are given by:

$$u = (1 - \frac{\gamma-1}{\gamma+1})\ q_o \cos^2\beta_{SH} + \frac{c_*^2}{q_o} \tag{C-13}$$

and

$$v = (q_o - u)\ \mathrm{cotg}\beta_{SH} \tag{C-14}$$

where q_o is the dimensionless free stream velocity and β_{SH} is the conical shock-angle. In addition the initial slope along the shock is given by:

$$\frac{\partial v}{\partial u} = \frac{v}{u-q_o} \tag{C-15}$$

APPENDIX D

DIMENSIONAL ANALYSIS OF INNER REGION EQUATIONS

The highly viscous flow in the inner region is assumed to be steady, compressible, laminar or turbulent, two-dimensional or axisymmetric flow over an adiabatic or non-adiabatic surface. The gas is assumed to be perfect. The system of equations is that presented by Maslen (reference 12) consisting of continuity, compressible Navier-Stokes and energy equations. The equations are put into curvilinear coordinates (ξ^*,ζ^*) in which ξ^* measured along the surface and ζ^* is measured normal to the surface. The equations in dimensional form are:

continuity

$$\frac{\partial}{\partial \xi^*}(\rho^* u^* r^{*\sigma}) + \frac{\partial}{\partial \zeta^*}[\rho^* v^* r^{*\sigma}(1 + \frac{\zeta^*}{R^*})] = 0 \qquad \text{(D-1)}$$

ξ-momentum

$$\rho^* u^* \frac{\partial u^*}{\partial \xi} + \rho^* v^*(1 + \frac{\zeta^*}{R^*}) \frac{\partial u^*}{\partial \zeta^*} + \frac{\rho^* u^* v^*}{R^*} + \frac{\partial p^*}{\partial \xi^*}$$

$$= \frac{1}{r^{*\sigma}} \frac{}{R^*(R^*+\zeta^*)} \frac{\partial}{\partial \zeta^*}[\mu^* r^{*\sigma}(R^*+ \zeta^*)^2(\frac{\partial u^*}{\partial \zeta^*} + \frac{R^* \frac{\partial v^*}{\partial \xi^*} - u^*}{R^*+\zeta^*})]$$

$$+ \frac{2}{r^{*\sigma}} \frac{\partial}{\partial \xi^*}[\mu^* r^{*\sigma}(\frac{R^* \frac{\partial u^*}{\partial \xi^*} + v^*}{R^*+\zeta^*})] - \frac{2\mu^*\sigma}{r^{*2}}(\frac{R^*+\zeta^*}{R^*})(u^*\sin\theta_w + v^*\cos\theta_w)\sin\theta_w$$

$$- \frac{2}{3} \frac{\partial}{\partial \xi^*}[\mu^*(\frac{R^* \frac{\partial u^*}{\partial \xi^*} + v^*}{R^*+\zeta^*}) + \mu^* \frac{\partial v^*}{\partial \zeta^*} + \frac{\sigma\mu^*}{r^{*\sigma}}(u^*\sin\theta_w + v^*\cos\theta_w)] \qquad \text{(D-2)}$$

ζ^*-momentum

$$\rho^* u^* \frac{R^*}{R^*+\zeta^*} \frac{\partial v^*}{\partial \xi^*} + \rho^* v^* \frac{\partial v^*}{\partial \zeta^*} - \frac{\rho^* u^{*2}}{R^*+\zeta^*} + \frac{\partial p^*}{\partial \zeta^*} = \frac{2}{r^{*\sigma}(R^*+\zeta^*)} \frac{\partial}{\partial \zeta^*}[\mu^* r^{*\sigma}(R^*+\zeta^*)\frac{\partial v^*}{\partial \zeta^*}]$$

$$- \frac{2\mu^*}{R^*+\zeta^*}\left(\frac{R^* \frac{\partial u^*}{\partial \xi^*} + v^*}{R^*+\zeta^*}\right) + \frac{R^*}{(R^*+\zeta^*)} \frac{}{r^{*\sigma}} \frac{\partial}{\partial \xi^*}[\mu^* r^{*\sigma}\left(\frac{\partial u^*}{\partial \zeta^*} + \frac{R^* \frac{\partial v^*}{\partial \xi^*} - u^*}{R^*+\zeta^*}\right)]$$

$$- \frac{2\mu^*\sigma}{r^{*2}} \cos\theta_w(u^*\sin\theta_w + v^*\cos\theta_w) - \frac{2}{3} \frac{\partial}{\partial \zeta^*}[\mu^*\left(\frac{R^* \frac{\partial u^*}{\partial \xi^*} + v^*}{R^*+\zeta^*}\right) + \mu^* \frac{\partial v^*}{\partial \zeta^*}$$

$$+ \mu^*\sigma \frac{(u^*\sin\theta_w + v^*\cos\theta_w)}{r^*}] \qquad \text{(D-3)}$$

energy

$$\frac{\rho^* u^* R^*}{(R^*+\zeta^*)} \frac{\partial h^*}{\partial \xi^*} + \rho^* v^* \frac{\partial h^*}{\partial \zeta^*} - \left(\frac{R^* u^*}{(R^*+\zeta^*)} \frac{\partial p^*}{\partial \xi^*} + v^* \frac{\partial p^*}{\partial \zeta^*}\right)$$

$$= \frac{1}{r^{*\sigma}} \frac{\partial}{\partial \zeta^*}\left(\frac{r^{*\sigma}\mu^* \frac{\partial h^*}{\partial \zeta^*}}{Pr^*}\right) + \frac{1}{r^{*\sigma}} \frac{R^*}{(R^*+\zeta^*)} \frac{\partial}{\partial \xi^*}\left(\frac{R^* r^{*\sigma}\mu^* \frac{\partial h^*}{\partial \xi^*}}{Pr^*(R^*+\zeta^*)}\right)$$

$$+ \frac{\mu^* \frac{\partial h^*}{\partial \xi^*}}{Pr^*(R^*+\zeta^*)} + \mu^*[2\left(\frac{\partial v^*}{\partial \zeta^*}\right)^2 + 2\left(\frac{R^* \frac{\partial u^*}{\partial \xi^*} + v^*}{R^*+\zeta^*}\right)^2$$

$$+ \frac{2\sigma}{r^{*2}}(u^*\sin\theta_w + v^*\cos\theta_w)^2 + \left(\frac{\partial u^*}{\partial \zeta^*} + \frac{R^* \frac{\partial v^*}{\partial \xi^*} - u^*}{R^*+\zeta^*}\right)^2$$

$$- \frac{2}{3}\left(\frac{R^* \frac{\partial u^*}{\partial \xi^*} + v^*}{R^*+\zeta^*} + \frac{\partial v^*}{\partial \zeta^*} + \frac{\sigma}{r^*}(u^*\sin\theta_w + v^*\cos\theta_w)\right)^2] \qquad \text{(D-4)}$$

Equation of state

$$p^* = \rho^* R T^* \qquad \text{(D-5)}$$

In these equations, the angle θ_w is the local slope of the axisymmetric body relative to the normal to the axis $\cos\theta_w = \frac{dr^*}{d\xi^*}$, and R^* is the longitudinal radius of curvature taken as positive for convex surfaces (ref. 11).

Dimensionless Equations

Reexamining the equations of motion using dimensional analysis, a set of equations is obtained constituting a higher approximation

than the classical boundary layer for the inner region, since terms of order unity and of order (δ/L_{REF}) are retained.

The non-dimensional variables are defined as follows:

$$\xi = \frac{\xi^*}{L_{REF}};\ \zeta = \frac{\zeta^*}{\delta};\quad R = \frac{R^*}{L_{REF}};\quad r = \frac{r^*}{L_{REF}};\ u = \frac{u^*}{u_{REF}};\quad v = \frac{v^*}{v_{REF}}$$

$$p = \frac{p^*}{\rho_{REF} u^2_{REF}};\quad \rho = \frac{\rho^*}{\rho_{REF}};\quad T = \frac{T^*}{T_{REF}};\quad h = \frac{h^*}{h_{REF}};\quad \mu = \frac{\mu^*}{\mu_{REF}} \tag{D-6}$$

The transformation relations are:

$$\frac{\partial}{\partial \xi^*} = \frac{\partial}{\partial \xi}\frac{\partial \xi}{\partial \xi^*} = \frac{1}{L_{REF}}\frac{\partial}{\partial \xi}$$

$$\frac{\partial}{\partial \zeta^*} = \frac{\partial}{\partial \zeta}\frac{\partial \zeta}{\partial \zeta^*} = \frac{1}{\delta}\frac{\partial}{\partial \zeta} \tag{D-7}$$

using the non-dimensional variables and the transformation relation, the dimensionless equations are then obtained.

<u>continuity</u>

$$\frac{\partial}{\partial \xi}[\rho u r^{\sigma}] + \frac{v_{REF}}{u_{REF}}\frac{L_{REF}}{\delta}\frac{\partial}{\partial \zeta}[\rho v r^{\sigma}(1 + \frac{\delta}{L_{REF}}\frac{\zeta}{R})] = 0 \tag{D-8}$$

By setting

$$\frac{v_{REF} L_{REF}}{u_{REF}\delta} = 1$$

it is established that in conserving mass, the normal velocity is of the following mangitude compared to the longitudinal velocity:

$$v_{REF} = u_{REF}(\frac{\delta}{L_{REF}}) \tag{D-9}$$

Thus equation (D-8) becomes:

$$\frac{\partial}{\partial \xi}[\rho u r^{\sigma}] + \frac{\partial}{\partial \zeta}[\rho v r^{\sigma}(1 + \frac{\delta}{L_{REF}}\frac{\zeta}{R}] = 0 \tag{D-10}$$

The remaining equations are:

ξ-momentum

$$\rho u \frac{\partial u}{\partial \xi} + \rho v\left(1 + \frac{\delta}{L_{REF}} \frac{\zeta}{R}\right) \frac{\partial u}{\partial \zeta} + \left(\frac{\delta}{L_{REF}}\right) \frac{\rho uv}{R} + \frac{\partial p}{\partial \xi}$$

$$= \frac{1}{\left(\frac{\delta}{L_{REF}}\right)^2} \frac{1}{Re_{REF}} \frac{1}{\left(1 + \frac{\delta}{L_{REF}} \frac{\zeta}{R}\right)} \frac{1}{r^\sigma R^2} \frac{\partial}{\partial \zeta}\left[\mu r^\sigma R^2 \left(1 + \frac{\delta}{L_{REF}} \frac{\zeta}{R}\right)^2 \left(\frac{\partial u}{\partial \zeta}\right.\right.$$

$$\left.\left. + \frac{\frac{\delta}{L_{REF}}\left(\frac{\delta}{L_{REF}} \frac{\partial v}{\partial \xi} - \frac{u}{R}\right)}{\left(1 + \frac{\delta}{L_{REF}} \frac{\zeta}{R}\right)}\right)\right] + \frac{2}{Re_{REF}} \frac{1}{r^\sigma} \frac{\partial}{\partial \xi}\left[\mu r^\sigma \left(\frac{\frac{\partial u}{\partial \xi} + \frac{\delta}{L_{REF}} \frac{v}{R}}{\left(1 + \frac{\delta}{L_{REF}} \frac{\zeta}{R}\right)}\right)\right]$$

$$- \frac{2}{Re_{REF}} \frac{\sigma \mu}{r^2}\left(1 + \frac{\delta}{L_{REF}} \frac{\zeta}{R}\right)\left(u \sin\theta_w + \frac{\delta}{L_{REF}} v \cos\theta_w\right) \sin\theta_w$$

$$- \frac{2}{3Re_{REF}} \frac{\partial}{\partial \xi}\left[\mu \frac{\left(\frac{\partial u}{\partial \xi} + \frac{\delta}{L_{REF}} \frac{v}{R}\right)}{\left(1 + \frac{\delta}{L_{REF}} \frac{\zeta}{R}\right)}\right.$$

$$\left. + \mu \frac{\partial v}{\partial \zeta} + \frac{\mu \sigma}{r}\left(u \sin\theta_w + \frac{\delta}{L_{REF}} v \cos\theta_w\right)\right] \qquad \text{(D-11)}$$

ζ-momentum

$$\left[\rho u \frac{\partial v}{\partial \xi} + \rho v\left(1 + \frac{\delta}{L_{REF}} \frac{\zeta}{R}\right) \frac{\partial v}{\partial \zeta}\right] \frac{\delta}{L_{REF}} - \frac{\rho u^2}{R} + \frac{\partial p}{\partial \zeta} \frac{\left(1 + \frac{\delta}{L_{REF}} \frac{\zeta}{R}\right)}{(\delta / L_{REF})}$$

$$= \frac{2}{\frac{\delta}{L_{REF}}} \frac{1}{Re_{REF} \cdot r^\sigma R} \frac{\partial}{\partial \zeta}\left[\mu r^\sigma R \left(1 + \frac{\delta}{L_{REF}} \frac{\zeta}{R}\right) \frac{\partial v}{\partial \zeta}\right]$$

$$- \frac{2}{Re_{REF}} \frac{\mu}{R} \frac{(\frac{\partial u}{\partial \xi} + \frac{\delta}{L_{REF}} \frac{v}{R})}{(1 + \frac{\delta}{L_{REF}} \frac{\zeta}{R})} + \frac{1}{(\frac{\delta}{L_{REF}})} \frac{}{Re_{REF} r^{\sigma}} \frac{\partial}{\partial \xi}[\mu r^{\sigma} \frac{\partial u}{\partial \zeta}$$

$$+ \frac{\mu(\frac{\delta}{L_{REF}})^2 \frac{\partial v}{\partial \xi} - \frac{\delta}{L_{REF}} \mu \frac{u}{R}}{(1 + \frac{\delta}{L_{REF}} \frac{\zeta}{R})}] - \frac{2}{Re_{REF}} \frac{\mu\sigma}{r^2} \cos\theta_w (u\sin\theta_w$$

$$+ \frac{\delta}{L_{REF}} v\cos\theta_w)(1 + \frac{\delta}{L_{REF}} \frac{\zeta}{R})$$

$$- \frac{2}{3} \frac{(1 + \frac{\delta}{L_{REF}} \frac{\zeta}{R})}{(\frac{\delta}{L_{REF}}) Re_{REF}} \frac{\partial}{\partial \zeta}[\mu \frac{(\frac{\partial u}{\partial \xi} + \frac{\delta}{L_{REF}} \frac{v}{R})}{(1 + \frac{\delta}{L_{REF}} \frac{\zeta}{R})} + \mu \frac{\partial v}{\partial \zeta}$$

$$+ \frac{\mu\sigma}{r}(u\sin\theta_w + \frac{\delta}{L_{REF}} v\cos\theta_w)] \qquad \text{(D-12)}$$

energy

$$\rho u \frac{\partial h}{\partial \xi} + \rho v(1 + \frac{\delta}{L_{REF}} \frac{\zeta}{R}) \frac{\partial h}{\partial \zeta} - \frac{u_{REF}^2}{h_{REF}}[u \frac{\partial p}{\partial \xi} + v(1 + \frac{\delta}{L_{REF}} \frac{\zeta}{R}) \frac{\partial p}{\partial \zeta}]$$

$$= \frac{(1 + \frac{\delta}{L_{REF}} \frac{\zeta}{R})}{(\frac{\delta}{L_{REF}})^2 Re_{REF}} \frac{1}{r^{\sigma}} \frac{\partial}{\partial \zeta}(\frac{\mu r^{\sigma}}{Pr_{REF}} \frac{\partial h}{\partial \zeta}) + \frac{1}{Re_{REF} r^{\sigma}} \frac{\partial}{\partial \xi}[\frac{r^{\sigma}}{Pr_{REF}} \frac{\frac{\partial h}{\partial \xi}}{(1 + \frac{\delta}{L_{REF}} \frac{\zeta}{R})}]$$

$$+ \frac{\mu}{(\frac{\delta}{L_{REF}}) Re_{REF} Pr_{REF} R} \frac{1}{} \frac{\partial h}{\partial \zeta} + \frac{(1 + \frac{\delta}{L_{REF}} \frac{\zeta}{R})}{Re_{REF}} \frac{u_{REF}^2}{h_{REF}} \mu\{2(\frac{\partial v}{\partial \zeta})^2$$

$$+ 2 \frac{(\frac{\partial u}{\partial \xi} + \frac{\delta}{L_{REF}} \frac{v}{R})^2}{(1 + \frac{\delta}{L_{REF}} \frac{\zeta}{R})^2} + \frac{2\sigma}{r^2}(u\sin\theta_w + \frac{\delta}{L_{REF}} v\sin\theta_w)^2$$

$$+ (\frac{1}{\frac{\delta}{L_{REF}}} \frac{\partial u}{\partial \zeta} + \frac{\frac{\delta}{L_{REF}} \frac{\partial v}{\partial \xi} - \frac{u}{R}}{(1 + \frac{\delta}{L_{REF}} \frac{\zeta}{R})})^2 - \frac{2}{3}(\frac{\frac{\partial u}{\partial \xi} + \frac{\delta}{L_{REF}} \frac{v}{R}}{(1 + \frac{\zeta}{R} \frac{\delta}{L_{REF}})} + \frac{\partial v}{\partial \zeta}$$

$$+ \frac{\sigma}{r}(u\sin\theta_w + \frac{\delta}{L_{REF}} v\cos\theta_w))^2\} \qquad \text{(D-13)}$$

where:

$Re_{REF} = \frac{\rho_{REF} u_{REF} L_{REF}}{\mu_{REF}}$ is the reference Reynolds number

and

$Pr_{REF} = \frac{\mu_{REF} c_{p_{REF}}}{K_{REF}}$ is the reference Prandtl number.

In order that viscous forces be of same order as inertia forces;

$$\frac{1}{Re_{REF}} = (\frac{\delta}{L_{REF}})^2 \qquad \text{(D-14)}$$

The non-dimensional equations of motion obtained by retaining terms of order unity and terms of order (δ/L_{REF}) are now presented. By using the Taylor series expansion for:

$$\frac{1}{1 + \frac{\delta}{L_{REF}} \frac{\zeta}{R}} = 1 - \frac{\delta}{L_{REF}} \cdot \frac{\zeta}{R} + \mathcal{O}[(\frac{\delta}{L_{REF}})^2] \qquad \text{(D-15)}$$

equations (D-10) to (D-13) become:

<u>continuity</u>

$$\frac{\partial}{\partial \xi}[\rho u r^\sigma] + \frac{\partial}{\partial \zeta}[\rho u r^\sigma (1 + \frac{\delta}{L_{REF}} \frac{\zeta}{R})] = 0 \qquad \text{(D-16)}$$

<u>ξ-momentum</u>

$$\rho u \frac{\partial u}{\partial \xi} + \rho v(1 + \frac{\delta}{L_{REF}} \frac{\zeta}{R}) \frac{\partial u}{\partial \zeta} + \frac{\delta}{L_{REF}} \frac{\rho uv}{R} + \frac{\partial p}{\partial \xi}$$

$$= \frac{1}{(1 + \frac{\delta}{L_{REF}} \frac{\zeta}{R}) r^\sigma R^2} \frac{\partial}{\partial \zeta}[\mu r^\sigma R^2 ((1 + \frac{\delta}{L_{REF}} \frac{\zeta}{R})^2 \frac{\partial u}{\partial \zeta}$$

$$- (1 + \frac{\delta}{L_{REF}} \frac{\zeta}{R}) \frac{\delta}{L_{REF}} \frac{u}{R})] \qquad \text{(D-17)}$$

ζ-momentum

$$[\rho u \frac{\partial v}{\partial \xi} + \rho v(1 + \frac{\delta}{L_{REF}} \frac{\zeta}{R}) \frac{\partial v}{\partial \zeta}] \frac{\delta}{L_{REF}} - \frac{\rho u^2}{R} + \frac{(1 + \frac{\delta}{L_{REF}} \frac{\zeta}{R})}{\frac{\delta}{L_{REF}}} \frac{\partial p}{\partial \zeta}$$

$$= \frac{2}{r^\sigma R} \frac{\delta}{L_{REF}} \frac{\partial}{\partial \zeta}[\mu r^\sigma R(1 + \frac{\delta}{L_{REF}} \frac{\zeta}{R}) \frac{\partial v}{\partial \zeta}] + \frac{\delta}{L_{REF}} \frac{1}{r^\sigma} \frac{\partial}{\partial \xi}[\mu r^\sigma \frac{\partial u}{\partial \zeta}]$$

$$- \frac{2}{3}(\frac{\delta}{L_{REF}}) \frac{\partial}{\partial \zeta}[\mu \frac{\partial u}{\partial \xi} + \mu \frac{\partial v}{\partial \zeta} + \frac{\mu\sigma}{r} u \sin\theta_w] \qquad \text{(D-18)}$$

energy

$$\rho u \frac{\partial h}{\partial \xi} + \rho v(1 + \frac{\delta}{L_{REF}} \frac{\zeta}{R}) \frac{\partial h}{\partial \zeta} - \frac{u_{REF}^2}{h_{REF}}[u \frac{\partial p}{\partial \xi} + v(1 + \frac{\delta}{L_{REF}} \frac{\zeta}{R}) \frac{\partial p}{\partial \zeta}]$$

$$= (1 + \frac{\delta}{L_{REF}} \frac{\zeta}{R}) \frac{1}{r^\sigma} \frac{\partial}{\partial \zeta}(\frac{\mu r^\sigma}{Pr_{REF}} \frac{\partial h}{\partial \zeta}) + \frac{\delta}{L_{REF}} \frac{1}{Pr_{REF}} \frac{\mu}{R} \frac{\partial h}{\partial \zeta}$$

$$+ (1 + \frac{\delta}{L_{REF}} \frac{\zeta}{R}) \frac{u_{REF}^2}{h_{REF}} \mu\{(\frac{\partial u}{\partial \zeta})^2 - 2 \frac{\delta}{L_{REF}} \frac{u}{R} \frac{\partial u}{\partial \zeta} \frac{1}{(1 + \frac{\delta}{L_{REF}} \frac{\zeta}{R})}\}$$

(D-19)

The energy equation in terms of temperature using perfect gas relation:

$$dh = c_p dT \qquad \text{(D-20)}$$

becomes:

$$\rho u \frac{\partial T}{\partial \xi} + \rho v(1 + \frac{\delta}{L_{REF}} \frac{\zeta}{R}) \frac{\partial T}{\partial \zeta} - (\gamma-1)M_{REF}^2[u \frac{\partial p}{\partial \xi} + v(1 + \frac{\delta}{L_{REF}} \frac{\zeta}{R}) \frac{\partial p}{\partial \zeta}]$$

$$= (1 + \frac{\delta}{L_{REF}} \frac{\zeta}{R}) \frac{1}{r^\sigma} \frac{\partial}{\partial \zeta}(\frac{\mu r^\sigma}{Pr_{REF}} \frac{\partial T}{\partial \zeta}) + \frac{\delta}{L_{REF}} \frac{1}{Pr_{REF}} \frac{\mu}{R} \frac{\partial T}{\partial \zeta}$$

$$+ (\gamma-1)M_{REF}^2 \mu\{(1 + \frac{\delta}{L_{REF}} \frac{\zeta}{R})(\frac{\partial u}{\partial \zeta})^2 - 2 \frac{\delta}{L_{REF}} \frac{u}{R} \frac{\partial u}{\partial \zeta}\} \qquad \text{(D-21)}$$

Rewriting equations (D-16) to (D-21) in terms of Re_{REF} using relation (D-14) yields:

continuity

$$\frac{\partial}{\partial \xi}[\rho u r^{\sigma}] + \frac{\partial}{\partial \zeta}[\rho v r^{\sigma}(1 + \frac{1}{Re_{REF}^{1/2}} \frac{\zeta}{R})] = 0 \qquad \text{(D-22)}$$

ξ-momentum

$$\rho u \frac{\partial u}{\partial \xi} + \rho v(1 + \frac{1}{Re_{REF}^{1/2}} \frac{\zeta}{R}) \frac{\partial u}{\partial \zeta} + \frac{1}{Re_{REF}^{1/2}} \frac{\rho u v}{R} + \frac{\partial p}{\partial \xi}$$

$$= \frac{1}{r^{\sigma}} \frac{\partial}{\partial \zeta}[\mu r^{\sigma}(1 + \frac{1}{Re_{REF}^{1/2}} \frac{\zeta}{R}) \frac{\partial u}{\partial \zeta}] - \frac{1}{Re_{REF}^{1/2}} \frac{1}{r^{\sigma}} \frac{u}{R} \frac{\partial}{\partial \zeta}(\mu r^{\sigma}) \qquad \text{(D-23)}$$

ζ-momentum

$$\frac{1}{Re_{REF}^{1/2}}[\rho u \frac{\partial v}{\partial \xi} + \rho v(1 + \frac{1}{Re_{REF}^{1/2}} \frac{\zeta}{R}) \frac{\partial v}{\partial \zeta}] - \frac{\rho u^2}{R} + Re_{REF}^{1/2}(1 + \frac{1}{Re_{REF}^{1/2}} \frac{\zeta}{R}) \frac{\partial p}{\partial \zeta}$$

$$= \frac{2}{Re_{REF}^{1/2}} \frac{1}{r^{\sigma}} \frac{\partial}{\partial \zeta}[\mu r^{\sigma} \frac{\partial v}{\partial \zeta}] + \frac{1}{Re_{REF}^{1/2}} \frac{1}{r^{\sigma}} \frac{\partial}{\partial \xi}[\mu r^{\sigma} \frac{\partial u}{\partial \zeta}]$$

$$- \frac{2}{3Re_{REF}^{1/2}} \frac{\partial}{\partial \zeta}[\mu \frac{\partial u}{\partial \xi} + \mu \frac{\partial v}{\partial \zeta} + \mu \frac{\sigma u \sin\theta}{r} w] \qquad \text{(D-24)}$$

energy

$$\rho u \frac{\partial T}{\partial \xi} + \rho v(1 + \frac{1}{Re_{REF}^{1/2}} \frac{\zeta}{R}) \frac{\partial T}{\partial \zeta} - (\gamma-1)M_{REF}^2[u \frac{\partial p}{\partial \xi} + (1 + \frac{1}{Re_{REF}^{1/2}} \frac{\zeta}{R}) v \frac{\partial p}{\partial \zeta}]$$

$$= (1 + \frac{1}{Re_{REF}^{1/2}} \frac{\zeta}{R}) \frac{1}{r^{\sigma}} \frac{\partial}{\partial \zeta}[\frac{\mu r^{\sigma}}{Pr_{REF}} \frac{\partial T}{\partial \zeta}] + \frac{1}{Re_{REF}^{1/2} Pr_{REF}} \frac{\mu}{R} \frac{\partial T}{\partial \zeta}$$

$$+ (\gamma-1)M_{REF}^2 \mu\{(1 + \frac{1}{Re_{REF}^{1/2}} \frac{\zeta}{R})(\frac{\partial u}{\partial \zeta})^2 - \frac{2}{Re_{REF}^{1/2}} \frac{u}{R} \frac{\partial u}{\partial \zeta}\} \qquad \text{(D-25)}$$

equation of state

$$p = \frac{\rho T}{\gamma M_{REF}^2} \qquad \text{(D-26)}$$

APPENDIX E

TURBULENT INNER LAYER

The dimensionless time-dependent second-order boundary layer equations are:

continuity

$$r^{\sigma}\frac{\partial \rho}{\partial t} + \frac{\partial}{\partial \xi}(\rho u r^{\sigma}) + \frac{\partial}{\partial \zeta}\left[\rho v r^{\sigma}\left(1 + \frac{1}{Re_{REF}^{1/2}}\frac{\zeta}{R}\right)\right] = 0 \qquad (E\text{-}1)$$

ξ-momentum

$$\rho\frac{\partial u}{\partial t} + \rho u\frac{\partial u}{\partial \xi} + \rho v\left(1 + \frac{1}{Re_{REF}^{1/2}}\frac{\zeta}{R}\right)\frac{\partial u}{\partial \zeta} + \frac{1}{Re_{REF}^{1/2}}\frac{\rho u v}{R} + \frac{\partial p}{\partial \xi}$$

$$= \frac{1}{r^{\sigma}}\frac{\partial}{\partial \zeta}\left[\mu r^{\sigma}\left(1 + \frac{1}{Re_{REF}^{1/2}}\frac{\zeta}{R}\right)\frac{\partial u}{\partial \zeta}\right] - \frac{1}{Re_{REF}^{1/2}}\frac{1}{r^{\sigma}}\frac{u}{R}\frac{\partial}{\partial \zeta}(\mu r^{\sigma}) \qquad (E\text{-}2)$$

ζ-momentum

$$\frac{1}{Re_{REF}^{1/2}}\left[\rho\frac{\partial v}{\partial t} + \rho u\frac{\partial v}{\partial \xi} + \rho v\left(1 + \frac{1}{Re_{REF}^{1/2}}\frac{\zeta}{R}\right)\frac{\partial v}{\partial \zeta}\right]$$

$$- \frac{\rho u^2}{R} + Re_{REF}^{1/2}\left(1 + \frac{1}{Re_{REF}^{1/2}}\frac{\zeta}{R}\right)\frac{\partial p}{\partial \zeta} = \frac{2}{Re_{REF}^{1/2}}\frac{1}{r^{\sigma}}\frac{\partial}{\partial \zeta}\left[\mu r^{\sigma}\frac{\partial v}{\partial \zeta}\right]$$

$$+ \frac{1}{Re_{REF}^{1/2}}\frac{1}{r^{\sigma}}\frac{\partial}{\partial \xi}\left[\mu r^{\sigma}\frac{\partial u}{\partial \zeta}\right]$$

$$- \frac{2}{3Re_{REF}^{1/2}}\frac{\partial}{\partial \zeta}\left(\mu\frac{\partial u}{\partial \xi} + \mu\frac{\partial v}{\partial \zeta} + \mu^{\sigma}\frac{u\sin\theta_w}{r}\right) \qquad (E\text{-}3)$$

energy

$$\rho \frac{\partial T}{\partial t} + \rho u \frac{\partial T}{\partial \xi} + \rho v\left(1 + \frac{1}{Re_{REF}^{1/2}} \frac{\zeta}{R}\right)\frac{\partial T}{\partial \zeta} - (\gamma-1)M_{REF}^2\left[u \frac{\partial p}{\partial \xi} + v\left(1 + \frac{1}{Re_{REF}^{1/2}} \frac{\zeta}{R}\right)\frac{\partial p}{\partial \zeta}\right]$$

$$= \left(1 + \frac{1}{Re_{REF}^{1/2}} \frac{\zeta}{R}\right) \frac{1}{r^{\sigma}} \frac{\partial}{\partial \zeta}\left[\frac{\mu r^{\sigma}}{Pr_{REF}} \frac{\partial T}{\partial \zeta}\right] + \frac{1}{Re_{REF}^{1/2}} \frac{1}{Pr_{REF}} \frac{\mu}{R} \frac{\partial T}{\partial \zeta}$$

$$+ (\gamma-1)M_{REF}^2 \mu\left\{\left(1 + \frac{1}{Re_{REF}^{1/2}} \frac{\zeta}{R}\right)\left(\frac{\partial u}{\partial \zeta}\right)^2 - \frac{2}{Re_{REF}^{1/2}} \frac{u}{R} \frac{\partial u}{\partial \zeta}\right\} \qquad \text{(E-4)}$$

Derivation of the second-order turbulent boundary layer equations follows by using the Reynolds procedure of representing each quantity by the sum of its time average and its departure or fluctuation from the time average; namely

$$u = \bar{u} + u'$$

$$v = \bar{v} + v'$$

$$T = \bar{T} + T'$$

$$p = \bar{p} + p'$$

$$\rho = \bar{\rho} + \rho' \qquad \text{(E-5)}$$

where the barred quantities are time-averaged and the primed quantities are the fluctuations. Viscosity fluctuations are neglected herein as they do not contribute to the leading turbulent transport effects. The time average of any of the quantities in equation (E-5) is defined by:

$$\bar{f} = \frac{1}{\tau}\int_{t_o}^{t_o + \tau} f(t + \tau')d\tau' \qquad \text{(E-6)}$$

C 2

Also by definition:

$$\bar{f}' = \frac{1}{\tau}\int_{t_o}^{t_o+\tau} f'(t+\tau')d\tau' = 0 \qquad \text{(E-7)}$$

where τ is a time period large enough to give a stationary characterization to the turbulence.

The indicated time averaging is best carried out on transport forms of equations (E-2), (E-3) and (E-4) obtained by using the continuity equation (E-1).

ξ-momentum

Multiplying equation (E-2) by r^σ and equation (E-1) by u and adding the resulting equations yields:

$$\frac{\partial}{\partial t}(\rho u r^\sigma) + \frac{\partial}{\partial \xi}[\rho u^2 r^\sigma] + \frac{\partial}{\partial \zeta}[\rho u v r^\sigma (1 + \frac{1}{Re_{REF}^{1/2}} \frac{\zeta}{R})]$$

$$+ \frac{\rho u v r^\sigma}{Re_{REF}^{1/2} R} + r^\sigma \frac{\partial p}{\partial \xi} = \frac{\partial}{\partial \zeta}[\mu r^\sigma (1 + \frac{1}{Re_{REF}^{1/2}} \frac{\zeta}{R}) \frac{\partial u}{\partial \zeta}]$$

$$- \frac{1}{Re_{REF}^{1/2}} \frac{1}{R} \frac{\partial}{\partial \zeta}(\mu r^\sigma) \qquad \text{(E-8)}$$

ζ-momentum

Multiplying equation (E-1) by $\frac{v}{Re_{REF}^{1/2}}$ and equation (E-3) by r^σ and adding the equations yields:

$$\frac{1}{Re_{REF}^{1/2}} \{ \frac{\partial}{\partial t}(\rho v r^\sigma) + \frac{\partial}{\partial \xi}[\rho u v r^\sigma] + \frac{\partial}{\partial \zeta}[\rho v^2 r^\sigma (1 + \frac{1}{Re_{REF}^{1/2}} \frac{\zeta}{R})]\}$$

$$- \frac{\rho u^2 r^\sigma}{Re_{REF}^{1/2}} + r^\sigma Re_{REF}^{1/2} (1 + \frac{1}{Re_{REF}^{1/2}} \frac{\zeta}{R}) \frac{\partial p}{\partial \zeta}$$

$$= \frac{2}{Re_{REF}^{1/2}} \frac{\partial}{\partial \zeta}[\mu r^{\sigma} \frac{\partial v}{\partial \zeta}] + \frac{1}{Re_{REF}^{1/2}} \frac{\partial}{\partial \xi}[\mu r^{\sigma} \frac{\partial u}{\partial \zeta}]$$

$$- \frac{2}{3Re_{REF}^{1/2}} r^{\sigma} \frac{\partial}{\partial \zeta}[\mu \frac{\partial u}{\partial \xi} + \mu \frac{\partial v}{\partial \zeta} + \mu \frac{\sigma u \sin\theta}{r} w] \qquad \text{(E-9)}$$

energy

Similarly following the same procedure multiply equation (E-4) by T and add them to obtain:

$$\frac{\partial}{\partial t}(\rho T r^{\sigma}) + \frac{\partial}{\partial \xi}[\rho u r^{\sigma} T] + \frac{\partial}{\partial \zeta}[\rho v r^{\sigma}(1 + \frac{1}{Re_{REF}^{1/2}} \frac{\zeta}{R})T]$$

$$- (\gamma-1)M_{REF}^2 r^{\sigma}[u \frac{\partial p}{\partial \xi} + v(1 + \frac{1}{Re_{REF}^{1/2}} \frac{\zeta}{R}) \frac{\partial p}{\partial \zeta}]$$

$$= (1 + \frac{1}{Re_{REF}^{1/2}} \frac{\zeta}{R}) \frac{\partial}{\partial \zeta}[\frac{\mu r^{\sigma}}{Pr_{REF}} \frac{\partial T}{\partial \zeta}] + \frac{r^{\sigma}}{Re_{REF}^{1/2} Pr_{REF}} \frac{\mu}{R} \frac{\partial T}{\partial \zeta}$$

$$+ r^{\sigma}(\gamma-1)M_{REF}^2 \mu\{(1 + \frac{1}{Re_{REF}^{1/2}} \frac{\zeta}{R})(\frac{\partial u}{\partial \zeta})^2 - \frac{2}{Re_{REF}^{1/2}} \frac{u}{R} \frac{\partial u}{\partial \zeta}\} \qquad \text{(E-10)}$$

The following substitutions are introduced into equations (E-1), (E-8), (E-9) and (E-10):

$$\rho u = \bar{\rho}\bar{u} + (\rho u)'$$

$$\rho v = \bar{\rho}\bar{v} + (\rho v)' \qquad \text{(E-11)}$$

The time average of the above mentioned equations yields:

continuity

$$\frac{\partial}{\partial \xi}[(\bar{\rho}\bar{u} + \overline{\rho' u'}) r^{\sigma}] + \frac{\partial}{\partial \zeta}[\bar{\rho}\bar{v} + \overline{\rho' v'})(1 + \frac{1}{Re_{REF}^{1/2}} \frac{\zeta}{R}) r^{\sigma}] = 0 \qquad \text{(E-12)}$$

ξ-momentum

$$(\bar{\rho}\bar{u} + \overline{\rho'u'})\frac{\partial \bar{u}}{\partial \xi} + (\bar{\rho}\bar{v} + \overline{\rho'v'})\left(1 + \frac{1}{Re_{REF}^{1/2}}\frac{\zeta}{R}\right)\frac{\partial \bar{u}}{\partial \zeta}$$

$$+ \frac{1}{Re_{REF}^{1/2}}\frac{1}{R}(\bar{\rho}\bar{u}\bar{v} + \bar{\rho}\,\overline{u'v'} + \bar{v}\,\overline{\rho'u'} + \bar{u}\,\overline{\rho'v'}) = -\frac{\partial \bar{p}}{\partial \xi}$$

$$+ \frac{1}{r^{\sigma}}\frac{\partial}{\partial \zeta}\left[\mu r^{\sigma}\left(1 + \frac{1}{Re_{REF}^{1/2}}\frac{\zeta}{R}\right)\frac{\partial \bar{u}}{\partial \zeta}\right] - \frac{1}{Re_{REF}^{1/2}}\frac{\bar{u}}{Rr^{\sigma}}\frac{\partial}{\partial \zeta}(\mu r^{\sigma})$$

$$- \frac{1}{r^{\sigma}}\frac{\partial}{\partial \zeta}\left[r^{\sigma}\left(1 + \frac{1}{Re_{REF}^{1/2}}\frac{\zeta}{R}\right)\bar{\rho}\,\overline{u'v'}\right] \qquad \text{(E-13)}$$

ζ-momentum

$$\frac{1}{Re_{REF}^{1/2}}\{(\bar{\rho}\bar{u} + \overline{\rho'u'})\frac{\partial \bar{v}}{\partial \xi} + (\bar{\rho}\bar{v} + \overline{\rho'v'})\left(1 + \frac{1}{Re_{REF}^{1/2}}\frac{\zeta}{R}\right)\frac{\partial \bar{v}}{\partial \zeta}$$

$$- \frac{(\bar{\rho}\bar{u}^2 + 2\bar{u}\,\overline{\rho'u'})}{R} + Re_{REF}^{1/2}\left(1 + \frac{1}{Re_{REF}^{1/2}}\frac{\zeta}{R}\right)\frac{\partial \bar{p}}{\partial \zeta}$$

$$= \frac{2}{Re_{REF}^{1/2}}\frac{1}{r^{\sigma}}\frac{\partial}{\partial \zeta}\left[\mu r^{\sigma}\frac{\partial \bar{v}}{\partial \zeta}\right] + \frac{1}{Re_{REF}^{1/2}r^{\sigma}}\frac{\partial}{\partial \xi}\left[\mu r^{\sigma}\frac{\partial \bar{u}}{\partial \zeta}\right]$$

$$- \frac{2}{3Re_{REF}^{1/2}}\frac{\partial}{\partial \zeta}\left[\mu\frac{\partial \bar{u}}{\partial \xi} + \mu\frac{\partial \bar{v}}{\partial \zeta} + \frac{\mu\sigma\sin\theta_w\bar{u}}{r}\right] - \frac{1}{Re_{REF}^{1/2}}\frac{1}{r^{\sigma}}\frac{\partial}{\partial \xi}\left[r^{\sigma}\,\bar{\rho}\,\overline{u'v'}\right]$$

(E-14)

energy

$$(\bar{\rho}\bar{u} + \overline{\rho'u'})\frac{\partial \bar{T}}{\partial \xi} + (\bar{\rho}\bar{v} + \overline{\rho'v'})\left(1 + \frac{1}{Re_{REF}^{1/2}}\frac{\zeta}{R}\right)\frac{\partial \bar{T}}{\partial \zeta} - (\gamma-1)M_{REF}^2\left[\bar{u}\frac{\partial \bar{p}}{\partial \xi}\right.$$

$$\left. + \left(1 + \frac{1}{Re_{REF}^{1/2}}\frac{\zeta}{R}\right)\bar{v}\frac{\partial \bar{p}}{\partial \zeta}\right] = \left(1 + \frac{1}{Re_{REF}^{1/2}}\frac{\zeta}{R}\right)\frac{1}{r^{\sigma}}\frac{\partial}{\partial \zeta}\left[\frac{\mu r^{\sigma}}{Pr_{REF}}\frac{\partial \bar{T}}{\partial \zeta}\right]$$

$$+ \frac{\mu}{Re_{REF}^{1/2}} \frac{}{Pr_{REF}R} \frac{\partial \bar{T}}{\partial \zeta} + (\gamma-1)M_{REF}^2 \mu[(1 + \frac{1}{Re_{REF}^{1/2}} \frac{\zeta}{R})(\frac{\partial \bar{u}}{\partial \zeta})^2$$

$$- \frac{2}{Re_{REF}^{1/2}} \frac{\bar{u}}{R} \frac{\partial \bar{u}}{\partial \zeta}] - \frac{1}{r^\sigma} \frac{\partial}{\partial \zeta}[(1 + \frac{1}{Re_{REF}^{1/2}} \frac{\zeta}{R}) r^\sigma \bar{\rho}\, \overline{v'T'}] \qquad \text{(E-15)}$$

An ordering procedure shows that the leading apparent transport terms are the correlations $\overline{u'v'}$ and $\overline{v'T'}$. Within this ordering the equations reduce to:

continuity

$$\frac{\partial}{\partial \xi}[\bar{\bar{\rho}} \bar{u} r^\sigma] + \frac{\partial}{\partial \zeta}[\bar{\bar{\rho}} \bar{v}(1 + \frac{1}{Re_{REF}^{1/2}} \frac{\zeta}{R}) r^\sigma] = 0 \qquad \text{(E-16)}$$

ξ-momentum

$$\bar{\bar{\rho}} \bar{u} \frac{\partial \bar{u}}{\partial \zeta} + \bar{\bar{\rho}} \bar{v}(1 + \frac{1}{Re_{REF}^{1/2}} \frac{\zeta}{R}) \frac{\partial \bar{u}}{\partial \zeta} + \frac{1}{Re_{REF}^{1/2}} \frac{\bar{\bar{\rho}} \bar{\bar{u}} \bar{v}}{R} + \frac{\partial \bar{p}}{\partial \xi}$$

$$= \frac{1}{r^\sigma} \frac{\partial}{\partial \zeta}[\mu r^\sigma (1 + \frac{1}{Re_{REF}^{1/2}} \frac{\zeta}{R}) \frac{\partial \bar{u}}{\partial \zeta} - \frac{1}{r^\sigma} \frac{\partial}{\partial \zeta}[r^\sigma (1 + \frac{1}{Re_{REF}^{1/2}} \frac{\zeta}{R}) - \overline{\rho u'v'}]$$

$$- \frac{1}{r^\sigma Re_{REF}^{1/2}} \frac{\bar{u}}{R} \frac{\partial}{\partial \zeta}(\mu r^\sigma) - \frac{1}{Re_{REF}^{1/2}} \frac{\bar{\rho}\, \overline{u'v'}}{R} \qquad \text{(E-17)}$$

ζ-momentum

$$\frac{1}{Re_{REF}^{1/2}} \{\bar{\bar{\rho}} \bar{u} \frac{\partial \bar{v}}{\partial \xi} + \bar{\bar{\rho}} \bar{v}(1 + \frac{1}{Re_{REF}^{1/2}} \frac{\zeta}{R}) \frac{\partial \bar{v}}{\partial \zeta}\} - \frac{\bar{\bar{\rho}} \bar{u}^2}{R} + Re_{REF}^{1/2}(1 + \frac{1}{Re_{REF}^{1/2}} \frac{\zeta}{R}) \frac{\partial \bar{p}}{\partial \zeta}$$

$$= \frac{2}{Re_{REF}^{1/2}} \frac{1}{r^\sigma} \frac{\partial}{\partial \zeta}[\mu r^\sigma \frac{\partial \bar{v}}{\partial \zeta}] + \frac{1}{Re_{REF}^{1/2}} \frac{}{r^\sigma} \frac{\partial}{\partial \xi}[\mu r^\sigma \frac{\partial \bar{u}}{\partial \zeta}]$$

$$- \frac{2}{3Re_{REF}^{1/2}} \frac{\partial}{\partial \zeta}[\mu \frac{\partial \bar{u}}{\partial \xi} + \mu \frac{\partial \bar{v}}{\partial \zeta} + \mu \frac{\sigma \sin\theta_w}{r} \bar{u}]$$

$$- \frac{1}{Re_{REF}^{1/2}} \frac{1}{r^{\sigma}} \frac{\partial}{\partial \xi}[r^{\sigma} \bar{\rho}\, \overline{u'v'}] \qquad \text{(E-18)}$$

energy

$$\bar{\rho}\bar{u} \frac{\partial \bar{T}}{\partial \xi} + \bar{\rho}\bar{v}\left(1 + \frac{1}{Re_{REF}^{1/2}} \frac{\zeta}{R}\right) \frac{\partial \bar{T}}{\partial \zeta} - (\gamma-1)M_{REF}^2 \left[\bar{u} \frac{\partial \bar{p}}{\partial \xi} + \bar{v}\left(1 + \frac{1}{Re_{REF}^{1/2}} \frac{\zeta}{R}\right) \frac{\partial \bar{p}}{\partial \zeta}\right]$$

$$= \left(1 + \frac{1}{Re_{REF}^{1/2}} \frac{\zeta}{R}\right) \frac{1}{r^{\sigma}} \frac{\partial}{\partial \zeta}\left[\frac{\mu r^{\sigma}}{Pr_{REF}} \frac{\partial \bar{T}}{\partial \zeta}\right] + \frac{\mu}{Re_{REF}^{1/2} Pr_{REF}} \frac{1}{R} \frac{\partial \bar{T}}{\partial \zeta}$$

$$+ (\gamma-1)M_{REF}^2\, \mu\left[\left(1 + \frac{1}{Re_{REF}^{1/2}} \frac{\zeta}{R}\right)\left(\frac{\partial \bar{u}}{\partial \zeta}\right)^2 - \frac{2}{Re_{REF}^{1/2}} \frac{\bar{u}}{R} \frac{\partial \bar{u}}{\partial \zeta}\right]$$

$$- \frac{1}{r^{\sigma}} \frac{\partial}{\partial \zeta}\left[\left(1 + \frac{1}{Re_{REF}^{1/2}} \frac{\zeta}{R}\right) r^{\sigma}\, \bar{\rho}\, \overline{v'T'}\right] \qquad \text{(E-19)}$$

These are the equations used for the finite difference solution of the turbulent inner region consistent to second order in effects of curvature.

APPENDIX F

COEFFICIENTS OF THE FINITE DIFFERENCE EQUATIONS

A detailed derivation of the coefficients for the finite difference equations is herein given. The linearized equations (79) to (82) are written in difference form and have been multiplied by $\Delta\xi_{m+1}$ in order that magnitude of the coefficients be less sensitive to step size.

continuity

The continuity equation is

$$\frac{\partial}{\partial\xi}[r^{\sigma}\rho u] + \frac{\partial}{\partial\zeta}[\rho v r^{\sigma}(1 + \frac{1}{Re_{REF}^{1/2}}\frac{\zeta}{R}] = 0 \qquad \text{(F-1)}$$

Following the suggestion of Reyhner and Flugge-Lotz (reference 4) the continuity equation is written for point B (figure 18) as follows:

$$\frac{(r^{\sigma}\rho u)_{m+1,n} - (r^{\sigma}\rho u)_{m,n} + (r^{\sigma}\rho u)_{m+1,n-1} - (r^{\sigma}\rho u)_{m,n-1}}{2\Delta\xi_{m+1}}$$

$$+ \frac{\lambda c\{[(1 + \frac{1}{Re_{REF}^{1/2}}\frac{\zeta}{R})\rho v r^{\sigma}]_{m+1,n} - [(1 + \frac{1}{Re_{REF}^{1/2}}\frac{\zeta}{R})\rho v r^{\sigma}]_{m+1,n-1}\}}{\Delta\zeta_n}$$

$$+ (1 - \lambda c)\frac{\{[(1 + \frac{1}{Re_{REF}^{1/2}}\frac{\zeta}{R})\ \rho v r^{\sigma}]_{m,n} - [(1 + \frac{1}{Re_{REF}^{1/2}}\frac{\zeta}{R})\rho v r^{\sigma}]_{m,n-1}\}}{\Delta\zeta_n} = 0$$

(F-2)

The ζ derivative has been taken as a weighted average with λc as the weighting factor. $\lambda c = \frac{1}{2}$ corresponds to a centered differencing scheme. Expanding equation (F-2) and multiplying by $\Delta\xi_{m+1}$ yields:

$$r^{\sigma}_{m+1,n}\rho^{(i)}_{m+1,n}u_{m+1,n} - (r^{\sigma}\rho u)_{m,n} + r^{\sigma}_{m+1,n-1}\rho^{(i)}_{m+1,n-1}u_{m+1,n-1} - (r^{\sigma}\rho u)_{m,n-1}$$

$$+ 2\frac{\Delta\xi_{m+1}}{\Delta\zeta_n}\lambda_c\left[\left(1 + \frac{1}{Re^{1/2}_{REF}}\frac{\zeta}{R}\right)_{m+1,n}\rho^{(i)}_{m+1,n}r^{\sigma}_{m+1,n}\right]v_{m+1,n}$$

$$- 2\frac{\Delta\xi_{m+1}}{\Delta\zeta_n}\lambda_c\cdot\left[\left(1 + \frac{1}{Re^{1/2}_{REF}}\frac{\zeta}{R}\right)_{m+1,n-1}\rho^{(i)}_{m+1,n-1}r^{\sigma}_{m+1,n-1}\right]v_{m+1,n-1}$$

$$+ 2\frac{\Delta\xi_{m+1}}{\Delta\zeta_n}(1-\lambda_c)\left\{\left[\left(1 + \frac{1}{Re^{1/2}_{REF}}\frac{\zeta}{R}\right)\rho v r^{\sigma}\right]_{m,n} - \left[\left(1 + \frac{1}{Re^{1/2}_{REF}}\frac{\zeta}{R}\right)\rho v r^{\sigma}\right]_{m,n-1}\right\}=0 \qquad \text{(F-3)}$$

Written in coefficient form:

$$A_{ln}u_{m+1,n-1} + B_{ln}u_{m+1,n} + C_{ln}u_{m+1,n+1} + D_{ln}v_{m+1,n-1} + E_{ln}v_{m+1,n}$$

$$+ F_{ln}v_{m+1,n+1,} + G_{ln}T_{m+1,n-1} + H_{ln}T_{m+1,n} + I_{ln}T_{m+1,n+1}$$

$$+ J_{ln}p_{m+1,n-1} + K_{ln}p_{m+1,n} + L_{ln}p_{m+1,n+1} = S_{ln} \qquad \text{(F-4)}$$

the coefficients for the continuity equation (F-3) are:

$$A_{ln} = r^{\sigma}_{m+1,n-1}\rho^{(i)}_{m+1,n-1}$$

$$B_{ln} = r^{\sigma}_{m+1,n}\rho^{(i)}_{m+1,n}$$

$$C_{ln} = 0$$

$$D_{ln} = -\frac{\Delta\xi_{m+1}}{\Delta\zeta_n}2\cdot\lambda_c\left[\left(1 + \frac{1}{Re^{1/2}_{REF}}\frac{\zeta}{R}\right)_{m+1,n-1}\rho^{(i)}_{m+1,n-1}r^{\sigma}_{m+1,n-1}\right]$$

$$E_{1n} = \frac{\Delta\xi_{m+1}}{\Delta\zeta_n} 2\cdot\lambda_c\left[\left(1 + \frac{1}{Re_{REF}^{1/2}}\frac{\zeta}{R}\right)_{m+1,n}\rho^{(i)}_{m+1,n} r^{\sigma}_{m+1,n}\right]$$

$$F_{1n} = 0$$

$$G_{1n} = 0$$

$$H_{1n} = 0$$

$$I_{1n} = 0$$

$$J_{1n} = 0$$

$$K_{1n} = 0$$

$$L_{1n} = 0$$

$$S_{1n} = (r^{\sigma}\rho u)_{m,n} + (r^{\sigma}\rho u)_{m,n-1} - \frac{2\Delta\xi_{m+1}}{\Delta\zeta_n}(1-\lambda_c)\left\{\left[1 + \frac{1}{Re_{REF}^{1/2}}\frac{\zeta}{R}\right)\rho v r^{\sigma}\right]_{m,n}$$

$$- \left[\left(1 + \frac{1}{Re_{REF}^{1/2}}\frac{\zeta}{R}\right)\rho v r^{\sigma}\right]_{m,n-1}\Big\} \qquad \text{(F-5)}$$

<u>ξ-momentum</u>

The linearized ξ-momentum is:

$$(\rho u)^{(i)}\frac{\partial u}{\partial \xi} + \left(\rho\frac{\partial u}{\partial \zeta}\right)^{(i)}\left(1 + \frac{1}{Re_{REF}^{1/2}}\frac{\zeta}{R}\right)v = -\frac{\partial p}{\partial \xi}$$

$$+ \left[\left(1 + \frac{1}{Re_{REF}^{1/2}}\frac{\zeta}{R}\right)\mu\left(1 + \frac{\rho\varepsilon}{\mu}\right)\right]^{(i)}\frac{\partial^2 u}{\partial \zeta^2}$$

$$+ \left[\frac{1}{r^{\sigma}}\frac{\partial}{\partial \zeta}\left(r^{\sigma}\left(1 + \frac{1}{Re_{REF}^{1/2}}\frac{\zeta}{R}\right)\mu\left(1 + \frac{\rho\varepsilon}{\mu}\right)\right)\right]^{(i)}\frac{\partial u}{\partial \zeta}$$

$$- \frac{1}{Re_{REF}^{1/2}}\left(\frac{u}{R}\right)^{(i)}\left(\frac{\partial u}{\partial T}\right)^{(i)}\frac{\partial T}{\partial \zeta} - \frac{1}{Re_{REF}^{1/2}}\left(\frac{}{Rr^{\sigma}}\frac{\partial r^{\sigma}}{\partial \zeta}\right)^{(i)}\mu^{(i)}u$$

$$+ \frac{(\rho\varepsilon)^{(i)}}{Re_{REF}^{1/2}}\frac{1}{R}\frac{\partial u}{\partial \zeta} - \frac{\rho^{(i)}}{Re_{REF}^{1/2}}\frac{uv}{R} \qquad \text{(F-6)}$$

The difference equation for point A is written (figure 18) as follows:

$$(\rho u)^{(i)} \frac{(u_{m+1,n} - u_{m,n})}{\Delta\xi_{m+1}}$$

$$+ (\rho \frac{\partial u}{\partial \zeta})^{(i)} \frac{[(1 + \frac{1}{Re_{REF}^{1/2}} \frac{\zeta}{R})_{m+1,n} v_{m+1,n} + (1 + \frac{1}{Re_{REF}^{1/2}} \frac{\zeta}{R})_{m,n} v_{m,n}]}{2}$$

$$= - \frac{dp_{EXT}(\xi)}{d\xi} - \frac{(p_{m+1,n} - p_{m,n})}{\Delta\xi_{m+1}}$$

$$+ [(1 + \frac{1}{Re_{REF}^{1/2}} \frac{\zeta}{R}) (1 + \frac{\rho\varepsilon}{\mu})]^{(i)} \{\lambda_u \frac{(u_{m+1,n+1} + Ku_{m+1,n-1}}{\frac{K(1+K)}{2}\Delta\zeta_n^2}$$

$$\frac{- (1+K)u_{m+1,n})}{} + (1-\lambda_u) \frac{(u_{m,n+1} + Ku_{m,n-1} - (1+K)u_{m,n})}{\frac{K(1+K)}{2}\Delta\zeta_n^2}\}$$

$$+ [(\frac{1}{r^\sigma} \frac{\partial}{\partial\zeta}(r^\sigma (1 + \frac{1}{Re_{REF}^{1/2}} \frac{\zeta}{R}) (1 + \frac{\rho\varepsilon}{\mu}))) + \frac{(\rho\varepsilon)^{(i)}}{Re_{REF}^{1/2} R}] \{\lambda_u \frac{(u_{m+1,n+1} - u_{m+1,n-1})}{(1+K)\Delta\zeta_n}$$

$$+ (1-\lambda_u) \frac{(u_{m,n+1} - u_{m,n-1})}{(1+K)\Delta\zeta_n}\} - \frac{\mu^{(i)}}{Re_{REF}^{1/2} Rr^\sigma} (\frac{\partial r^\sigma}{\partial\zeta})^{(i)} \frac{(u_{m+1,n} + u_{m,n})}{2}$$

$$- \frac{1}{Re_{REF}^{1/2}} (\frac{u}{R})^{(i)} (\frac{\partial\mu}{\partial T})^{(i)} \{\lambda_T \frac{(T_{m+1,n+1} - T_{m+1,n-1})}{(1+K)\Delta\zeta_n}$$

$$+ (1-\lambda_T) \frac{(T_{m,n+1} - T_{m,n-1})}{(1+K)\Delta\zeta_n}\}$$

$$- \frac{\rho^{(i)}}{4Re_{REF}^{1/2} R}[(u_{m+1,n} + u_{m,n})v_{m,n} + (v_{m+1,n} + v_{m,n})u_{m,n}] \qquad (F-7)$$

Rearranging terms and multiplying all the equation by $\Delta\xi_{m+1}$ yields:

$$u_{m+1,n-1}\{-[(1 + \frac{1}{Re_{REF}^{1/2}} \frac{\zeta}{R})\mu(1 + \frac{\rho\varepsilon}{\mu})]^{(i)} \frac{2\lambda_u \Delta\xi_{m+1}}{(1+K)\Delta\zeta_n^2}$$

$$+ \left[\left(\frac{1}{r^{\sigma}}\frac{\partial}{\partial\zeta}\left(r^{\sigma}\left(1+\frac{1}{Re_{REF}^{1/2}}\frac{\zeta}{R}\right)\mu\left(1+\frac{\rho\varepsilon}{\mu}\right)\right)\right)+\frac{(\rho\varepsilon)}{Re_{REF}^{1/2}R}\right]^{(i)}\lambda_u\frac{\Delta\xi_{m+1}}{(1+K)\Delta\zeta_n}\}$$

$$+ u_{m+1,n}\left\{(\rho u)^{(i)}+\left[\left(1+\frac{1}{Re_{REF}^{1/2}}\frac{\zeta}{R}\right)\mu\left(1+\frac{\rho\varepsilon}{\mu}\right)\right]^{(i)}\lambda_u\frac{2\Delta\xi_{m+1}}{K\Delta\zeta_n^2}\right.$$

$$\left.+\frac{\mu^{(i)}}{2Re_{REF}^{1/2}}\frac{\Delta\xi_{m+1}}{Rr^{\sigma}}\left(\frac{\partial r^{\sigma}}{\partial\zeta}\right)^{(i)}+\frac{\rho^{(i)}}{4Re_{REF}^{1/2}R}v_{m,n}\Delta\xi_{m+1}\right\}$$

$$+ u_{m+1,n+1}\left\{-\left[\left(1+\frac{1}{Re_{REF}^{1/2}}\frac{\zeta}{R}\right)\mu\left(1+\frac{\rho\varepsilon}{\mu}\right)\right]^{(i)}\frac{2\lambda_u\Delta\xi_{m+1}}{K(1+K)\Delta\zeta_n^2}\right.$$

$$\left.-\left[\left(\frac{1}{r^{\sigma}}\frac{\partial}{\partial\zeta}\left(r^{\sigma}\left(1+\frac{1}{Re_{REF}^{1/2}}\frac{\zeta}{R}\right)\left(1+\frac{\rho\varepsilon}{\mu}\right)\right)\right)+\frac{(\rho\varepsilon)}{Re_{REF}^{1/2}R}\right]^{(i)}\frac{\lambda_u}{(1+K)}\frac{\Delta\xi_{m+1}}{\Delta\zeta_n}\right\}$$

$$+ v_{m+1,n-1}\{0\}+v_{m+1,n}\left\{\left(\rho\frac{\partial u}{\partial\zeta}\right)^{(i)}\frac{\left(1+\frac{1}{Re_{REF}^{1/2}}\frac{\zeta}{R}\right)_{m+1,n}}{2}\Delta\xi_{m+1}\right.$$

$$\left.+\frac{\rho^{(i)}}{4Re_{REF}^{1/2}R}u_{m,n}\Delta\xi_{m+1}\right\}+v_{m+1,n+1}\{0\}$$

$$- T_{m+1,n-1}\left\{\frac{1}{Re_{REF}^{1/2}}\left(\frac{u}{R}\right)^{(i)}\left(\frac{\partial\mu}{\partial T}\right)^{(i)}\frac{\lambda_T\Delta\xi_{m+1}}{(1+K)\Delta\zeta_n}\right\}+T_{m+1,n}\{0\}$$

$$+ T_{m+1,n+1}\left\{\frac{1}{Re_{REF}^{1/2}}\left(\frac{u}{R}\right)^{(i)}\left(\frac{\partial\mu}{\partial T}\right)^{(i)}\frac{\lambda_T\Delta\xi_{m+1}}{(1+K)\Delta\zeta_n}\right\}+p_{m+1,n-1}\{0\}$$

$$+ p_{m+1,n}\{1\}+p_{m+1,n+1}\{0\}=(\rho u)^{(i)}u_{m,n}$$

$$- \left(\rho\frac{\partial u}{\partial\zeta}\right)^{(i)}\left(1+\frac{1}{Re_{REF}^{1/2}}\frac{\zeta}{R}\right)_{m,n}v_{m,n}\frac{\Delta\xi_{m+1}}{2}-\frac{dP_{EXT}(\xi)}{d\xi}\Delta\xi_{m+1}+P_{m,n}$$

$$+ \left[\left(1 + \frac{1}{Re_{REF}^{1/2}} \frac{\zeta}{R}\right)\mu\left(1 + \frac{\rho\varepsilon}{\mu}\right)\right]^{(i)} 2(1-\lambda_u) \frac{(u_{m,n+1} + Ku_{m,n-1} - (1+K)u_{m,n})}{K(1+K)\Delta\zeta_n^2} \Delta\xi_{m+1}$$

$$+ \left[\left(\frac{1}{r^\sigma} \frac{\partial}{\partial\zeta}\left(r^\sigma\left(1 + \frac{1}{Re_{REF}^{1/2}} \frac{\zeta}{R}\right)\mu\left(1 + \frac{\rho\varepsilon}{\mu}\right)\right)\right) + \frac{(\rho\varepsilon)}{Re_{REF}^{1/2} R}\right]^{(i)} \frac{(1-\lambda_u)\Delta\xi_{m+1}}{(1+k)\Delta\zeta_n}(u_{m,n+1} - u_{m,n-1})$$

$$- \frac{\mu^{(i)}}{Re_{REF}^{1/2} Rr^\sigma}\left(\frac{\partial r^\sigma}{\partial\zeta}\right)^{(i)} \frac{u_{m,n}}{2} \Delta\xi_{m+1}$$

$$- \frac{1}{Re_{REF}^{1/2}}\left(\frac{u}{R}\right)^{(i)} \left(\frac{\partial\mu}{\partial T}\right)^{(i)} \frac{(1-\lambda_T)\Delta\xi_{m+1}}{(1+K)\Delta\zeta_n}(T_{m,n+1} - T_{m,n-1}) - \frac{\rho^{(i)}}{2Re_{REF}^{1/2} R} u_{m,n} v_{m,n} \qquad \text{(F-8)}$$

Equation (F-8) in coefficient form becomes

$$A_{2n} u_{m+1,n-1} + B_{2n} u_{m+1,n} + C_{2n} u_{m+1,n+1} + D_{2n} v_{m+1,n-1} + E_{2n} v_{m+1,n}$$

$$+ F_{2n} v_{m+1,n+1} + G_{2n} T_{m+1,n-1} + H_{2n} T_{m+1,n} + I_{2n} T_{m+1,n+1}$$

$$+ J_{2n} p_{m+1,n-1} + K_{2n} p_{m+1,n} + L_{2n} p_{m+1,n+1} = S_{2n} \qquad \text{(F-9)}$$

where

$$A_{2n} = \frac{\lambda_u \Delta\xi_{m+1}}{(1+K)\Delta\zeta_n}\left\{-\frac{2}{\Delta\zeta_n}\left[\left(1 + \frac{1}{Re_{REF}^{1/2}} \frac{\zeta}{R}\right)\mu\left(1 + \frac{\rho\varepsilon}{\mu}\right)\right]^{(i)}\right.$$

$$\left. + \left[\left(\frac{1}{r^\sigma} \frac{\partial}{\partial\zeta}\left(1 + \frac{1}{Re_{REF}^{1/2}} \frac{\zeta}{R}\right)\mu\left(1 + \frac{\rho\varepsilon}{\mu}\right)\right)\right) + \frac{(\rho\varepsilon)}{Re_{REF}^{1/2} R}\right]^{(i)}\right\}$$

$$B_{2n} = (\rho u)^{(i)} + \left[\left(1 + \frac{1}{Re_{REF}^{1/2}} \frac{\zeta}{R}\right)\mu\left(1 + \frac{\rho\varepsilon}{\mu}\right)\right]^{(i)} \frac{2\lambda_u}{K} \frac{\Delta\xi_{m+1}}{\Delta\zeta_n^2}$$

$$+ \frac{\Delta\xi_{m+1}}{2Re_{REF}^{1/2} R}\left[\frac{\rho^{(i)} v_{m,n}}{2} + \frac{\mu^{(i)}}{r^\sigma}\left(\frac{\partial r^\sigma}{\partial\zeta}\right)^{(i)}\right]$$

$$C_{2n} = -\frac{\lambda_u \Delta\xi_{m+1}}{(1+K)\Delta\zeta_n}\left\{\frac{2}{K\Delta\zeta_n}\left[\left(1+\frac{1}{Re_{REF}^{1/2}}\frac{\zeta}{R}\right)\mu\left(1+\frac{\rho\varepsilon}{\mu}\right)\right]^{(i)}\right.$$

$$\left.+\left[\left(\frac{1}{r^{\sigma}}\frac{\partial}{\partial\zeta}\left(r^{\sigma}\left(1+\frac{1}{Re_{REF}^{1/2}}\frac{\zeta}{R}\right)\mu\left(1+\frac{\rho\varepsilon}{\mu}\right)\right)\right)+\frac{\rho\varepsilon}{Re_{REF}^{1/2}R}\right]^{(i)}\right\}$$

$$D_{2n} = 0$$

$$E_{2n} = \frac{\Delta\xi_{m+1}}{2}\left(\rho\frac{\partial u}{\partial\zeta}\right)^{(i)}\left(1+\frac{1}{Re_{REF}^{1/2}}\frac{\zeta}{R}\right)_{m+1,n}+\frac{\rho^{(i)}u_{m,n}}{2Re_{REF}^{1/2}}\frac{1}{R}\}$$

$$F_{2n} = 0$$

$$G_{2n} = -\frac{\lambda_T \Delta\xi_{m+1}}{(1+K)\Delta\zeta_n}\frac{1}{Re_{REF}^{1/2}}\left(\frac{u}{R}\right)^{(i)}\left(\frac{\partial\mu}{\partial T}\right)^{(i)}$$

$$H_{2n} = 0$$

$$I_{2n} = -G_{2n}$$

$$J_{2n} = 0$$

$$K_{2n} = 1$$

$$L_{2n} = 0$$

$$S_{2n} = (\rho u)^{(i)}u_{m,n}-\left(\rho\frac{\partial u}{\partial\zeta}\right)^{(i)}\left(1+\frac{1}{Re_{REF}^{1/2}}\frac{\zeta}{R}\right)_{m,n}v_{m,n}\frac{\Delta\xi_{m+1}}{2}$$

$$- \frac{dP_{EXT}(\xi)}{d\xi} \Delta\xi_{m+1} + P_{m,n} + \frac{2(1-\lambda_u)}{K(1+K)\Delta\zeta_n^2} \Delta\xi_{m+1}(u_{m,n+1} + Ku_{m,n-1}$$

$$- (1+K)u_{m,n})[(1 + \frac{1}{Re_{REF}^{1/2}} \frac{\zeta}{R})\ (1 + \frac{\rho\varepsilon}{\mu})]^{(i)}$$

$$+ [(\frac{1}{r^\sigma} \frac{\partial}{\partial\zeta}(r^\sigma(1 + \frac{1}{Re_{REF}^{1/2}} \frac{\zeta}{R})\mu(1 + \frac{\rho\varepsilon}{\mu})))$$

$$+ \frac{\rho\varepsilon}{Re_{REF}^{1/2}R}]^{(i)} \frac{(1-\lambda_u)}{(1+K)\Delta\zeta_n} \Delta\xi_{m+1}(u_{m,n+1} - u_{m,n-1})$$

$$- \frac{\mu^{(i)}}{Re_{REF}^{1/2}} \frac{1}{Rr^\sigma}(\frac{\partial r^\sigma}{\partial\zeta})^{(i)} \frac{u_{m,n}}{2} \Delta\xi_{m+1}$$

$$- \frac{1}{Re_{REF}^{1/2}}(\frac{u}{R})^{(i)}(\frac{\partial\mu}{\partial T})^{(i)} \frac{(1-\lambda_T)\Delta\xi_{m+1}}{(1+K)\Delta\zeta_n} (T_{m,n+1} - T_{m,n-1})$$

$$- \frac{\rho^{(i)} u_{m,n} v_{m,n}}{2Re_{REF}^{1/2}R} \qquad \text{(F-10)}$$

ζ-momentum

The linearized ζ-momentum equation is:

$$\frac{(\rho u)^{(i)}}{Re_{REF}^{1/2}} \frac{\partial v}{\partial\xi} + [\frac{\rho v}{Re_{REF}^{1/2}}(1 + \frac{1}{Re_{REF}^{1/2}} \frac{\zeta}{R})]^{(i)} \frac{\partial v}{\partial\zeta} = - Re_{REF}^{1/2}(1 + \frac{1}{Re_{REF}^{1/2}} \frac{\zeta}{R})^{(i)} \frac{\partial p}{\partial\zeta}$$

$$+ \frac{4}{3Re_{REF}^{1/2}} \mu^{(i)} \frac{\partial^2 v}{\partial\zeta^2} + \frac{2}{Re_{REF}^{1/2}}(\frac{\partial v}{\partial\zeta})^{(i)}(\frac{\partial\mu}{\partial T})^{(i)} \frac{\partial T}{\partial\zeta}$$

$$+ \frac{2}{Re_{REF}^{1/2}}(\frac{\partial r^\sigma}{\partial\zeta})^{(i)} \frac{\mu^{(i)}}{r^\sigma} \frac{\partial v}{\partial\zeta} + \frac{1}{Re_{REF}^{1/2}} \frac{1}{r^\sigma}[\frac{\partial}{\partial\xi}(\mu r^\sigma(1 + \frac{\rho\varepsilon}{\mu}))]^{(i)} \frac{\partial u}{\partial\zeta}$$

$$+\frac{\mu^{(i)}}{Re_{REF}^{1/2}}\left(1+\frac{\rho\varepsilon}{\mu}\right)^{(i)}\frac{\partial^2 u}{\partial\xi\partial\zeta}-\frac{2}{3Re_{REF}^{1/2}}\left(\frac{\partial\mu}{\partial T}\right)^{(i)}\left[\frac{\partial u}{\partial\xi}+\frac{\partial v}{\partial\zeta}+\frac{\sigma\sin\theta_w}{r}u\right]^{(i)}\frac{\partial T}{\partial\zeta}$$

$$-\frac{2}{3Re_{REF}^{1/2}}\mu^{(i)}\frac{\partial^2 u}{\partial\zeta\partial\xi}-\frac{2}{3Re_{REF}^{1/2}}\sigma\mu^{(i)}\left(\frac{\sin\theta_w}{r}\right)^{(i)}\frac{\partial u}{\partial\zeta}$$

$$+\frac{2}{3Re_{REF}^{1/2}}\sigma\mu^{(i)}\left(\frac{1}{r^2}\frac{\partial r}{\partial\zeta}\right)^{(i)}u\sin\theta_w+\frac{(\rho u)^{(i)}u}{R} \qquad \text{(F-11)}$$

The difference equation written for point A (figure 18) is:

$$\frac{(\rho u)^{(i)}}{Re_{REF}^{1/2}}\frac{(v_{m+1,n}-v_{m,n})}{\Delta\xi_{m+1}}+\frac{1}{Re_{REF}^{1/2}}\{[\rho v(1+\frac{1}{Re_{REF}^{1/2}}\frac{\zeta}{R})]^{(i)}$$

$$-\frac{2}{r^\sigma}\left(\frac{\partial r^\sigma}{\partial\zeta}\right)^{(i)}\mu^{(i)}\}[\lambda_v\frac{(v_{m+1,n+1}-v_{m+1,n-1})}{(1+K)\Delta\zeta_n}$$

$$+\frac{(1-\lambda_v)(v_{m,n+1}-v_{m,n-1})}{(1+K)\Delta\zeta_n}]=-Re_{REF}^{1/2}(1+\frac{1}{Re_{REF}^{1/2}}\frac{\zeta}{R})^{(i)}$$

$$[\lambda_p\frac{(p_{m+1,n+1}-p_{m+1,n})}{K\Delta\zeta_n}+\frac{(1-\lambda_p)(p_{m,n+1}-p_{m,n})}{K\Delta\zeta_n}]$$

$$+\frac{4}{3Re_{REF}^{1/2}}\mu^{(i)}\{2\cdot\lambda_v\frac{(v_{m+1,n+1}+Kv_{m+1,n-1}-(1+K)v_{m+1,n})}{K(1+K)\Delta\zeta_n^2}$$

$$+\frac{2(1-\lambda_v)(v_{m,n+1}+Kv_{m,n-1}-(1+K)v_{m,n})}{K(1+K)\Delta\zeta_n^2}]\}$$

$$+\frac{1}{Re_{REF}^{1/2}}\left(\frac{\partial\mu}{\partial T}\right)^{(i)}\{\frac{4}{3}\left(\frac{\partial v}{\partial\zeta}\right)^{(i)}-\frac{2}{3}[\left(\frac{\partial u}{\partial\xi}\right)^{(i)}+\sigma\left(\frac{u\sin\theta_w}{r}\right)^{(i)}]\}[\frac{\lambda_T(T_{m+1,n+1}-T_{m+1,n-1})}{(1+K)\Delta\zeta_n}$$

$$+\frac{(1-\lambda_T)(T_{m,n+1}-T_{m,n-1})}{(1+K)\Delta\zeta_n}]+\frac{1}{Re_{REF}^{1/2}}\{-\frac{2}{3}\sigma\mu^{(i)}\left(\frac{\sin\theta_w}{r}\right)^{(i)}$$

$$+[\frac{\partial}{\partial\xi}(\mu(1+\frac{\rho\varepsilon}{\mu}))]^{(i)}+[\frac{\sigma}{r}\frac{\partial r}{\partial\zeta}\mu(1+\frac{\rho\varepsilon}{\mu})]^{(i)}\}$$

$$[\frac{\lambda_u(u_{m+1,n+1}-u_{m+1,n-1})}{\Delta\zeta_n(1+K)}+\frac{(1-\lambda_u)(u_{m,n+1}-u_{m,n-1})}{(1+K)\Delta\zeta_n}]$$

$$+ \frac{(\rho u)^{(i)}}{R} \frac{(u_{m+1,n} + u_{m,n})}{2} + \frac{1}{Re_{REF}^{1/2}}\{\mu^{(i)} (1 + \frac{\rho\varepsilon}{\mu})^{(i)}$$

$$- \frac{2}{3} \mu^{(i)} [\frac{u_{m+1,n+1} - u_{m+1,n-1} - u_{m,n+1} + u_{m,n-1}}{\Delta\xi_{m+1}\Delta\zeta_n(1+K)}]$$

$$+ \frac{2}{3} \frac{\sigma}{Re_{REF}^{1/2}} \mu^{(i)} (\frac{1}{r^2} \frac{\partial r}{\partial \zeta})^{(i)} \frac{\sin\theta_w (u_{m+1,n} + u_{m,n})}{2} \qquad \text{(F-12)}$$

Expanding equation (F-12) and multiplying by $\Delta\xi_{m+1}$ yields:

$$u_{m+1,n-1}\{\frac{1}{Re_{REF}^{1/2}}[- \frac{2}{3} \sigma\mu^{(i)} (\frac{\sin\theta_w}{r})^{(i)} + (\frac{\partial}{\partial\xi}(\mu(1 + \frac{\rho\varepsilon}{\mu})))^{(i)}$$

$$+ (\frac{\sigma}{r} \frac{\partial r}{\partial \zeta} \mu(1 + \frac{\rho\varepsilon}{\mu}))^{(i)}] \frac{\lambda_u \Delta\xi_{m+1}}{\Delta\zeta_n(1+K)}$$

$$+ \frac{1}{Re_{REF}^{1/2}} \frac{1}{\Delta\zeta_n(1+K)}[\mu^{(i)} (1 + \frac{\rho\varepsilon}{\mu})^{(i)} - \frac{2}{3} \mu^{(i)}]\}$$

$$+ u_{m+1,n}\{- \frac{(\rho u)^{(i)}}{2R} \Delta\xi_{m+1} - \frac{2\sigma}{3Re_{REF}^{1/2}} \Delta\xi_{m+1} \mu^{(i)} (\frac{1}{r^2} \frac{\partial r}{\partial \zeta})^{(i)} \frac{\sin\theta_w}{2}\}$$

$$- u_{m+1,n+1}\{\frac{1}{Re_{REF}^{1/2}}[- \frac{2}{3} \sigma\mu^{(i)} (\frac{\sin\theta_w}{r})^{(i)}$$

$$+ (\frac{\partial}{\partial\xi}(\mu(1 + \frac{\rho\varepsilon}{\mu})))^{(i)} + (\frac{\sigma}{r} \frac{\partial r}{\partial \zeta} \mu(1 + \frac{\rho\varepsilon}{\mu}))^{(i)}] \frac{\lambda_u \Delta\xi_{m+1}}{\Delta\zeta_n(1+K)}$$

$$+ \frac{[(\mu(1 + \frac{\rho\varepsilon}{\mu}))^{(i)} - \frac{2}{3} \mu^{(i)}]}{Re_{REF}^{1/2}\Delta\zeta_n(1+K)}\}$$

$$+ v_{m+1,n-1}\{- \frac{\lambda_v \Delta\xi_{m+1}}{(1+K)\Delta\zeta_n Re_{REF}^{1/2}}[(\rho v)^{(i)} (1 + \frac{1}{Re_{REF}^{1/2}} \frac{\zeta}{R})^{(i)}$$

$$- (\frac{2}{r^\sigma} \frac{\partial r^\sigma}{\partial \zeta} \mu)^{(i)} - \frac{2\lambda_v \Delta\xi_{m+1}}{(1+K)\Delta\zeta_n^2} \frac{4\mu^{(i)}}{3Re_{REF}^{1/2}}\}$$

$$+ v_{m+1,n}\{\frac{(\rho u)^{(i)}}{Re_{REF}^{1/2}} + \frac{2\lambda_v \Delta\xi_{m+1}}{K\Delta\zeta_n^2}\frac{4\mu^{(i)}}{3Re_{REF}^{1/2}}\}$$

$$+ v_{m+1,n+1}\{\frac{\lambda_v \Delta\xi_{m+1}}{(1+K)\Delta\zeta_n Re_{REF}^{1/2}}[(\rho v)^{(i)}(1 + \frac{1}{Re_{REF}^{1/2}}\frac{\zeta}{R})^{(i)} - (\frac{2}{r^\sigma}\frac{\partial r^\sigma}{\partial\zeta}\mu)^{(i)}]$$

$$- \frac{2\lambda_v \Delta\xi_{m+1}}{K(1+K)\Delta\zeta_n^2}\frac{4\mu^{(i)}}{3Re_{REF}^{1/2}}\} + T_{m+1,n-1}\{\frac{1}{Re_{REF}^{1/2}}(\frac{\partial\mu}{\partial T})^{(i)}[\frac{4}{3}(\frac{\partial v}{\partial\zeta})^{(i)}$$

$$- \frac{2}{3}((\frac{\partial u}{\partial\xi})^{(i)} + \sigma(\frac{u\sin\theta_w}{r})^{(i)})]\frac{\lambda_T \Delta\xi_{m+1}}{(1+K)\Delta\zeta_n} + T_{m+1,n}\{0\}$$

$$+ T_{m+1,n+1}\{-\frac{1}{Re_{REF}^{1/2}}(\frac{\partial\mu}{\partial T})^{(i)}\frac{\lambda_T \Delta\zeta_{m+1}}{(1+K)\Delta\zeta_n}[\frac{4}{3}(\frac{\partial v}{\partial\zeta})^{(i)} - \frac{2}{3}((\frac{\partial u}{\partial\xi})^{(i)}$$

$$+ \sigma(\frac{u\sin\theta_w}{r})^{(i)})]\} + p_{m+1,n-1}\{0\}$$

$$+ p_{m+1,n}\{-Re_{REF}^{1/2}(1 + \frac{1}{Re_{REF}^{1/2}}\frac{\zeta}{R})^{(i)}\frac{\lambda_p \Delta\xi_{m+1}}{K\Delta\zeta_n}\}$$

$$+ p_{m+1,n+1}\{Re_{REF}^{1/2}(1 + \frac{1}{Re_{REF}^{1/2}}\frac{\zeta}{R})^{(i)}\frac{\lambda_p \Delta\xi_{m+1}}{K\Delta\zeta_n}\}$$

$$= \frac{(\rho u)^{(i)}}{Re_{REF}^{1/2}} v_{m,n} - \frac{1}{Re_{REF}^{1/2}}\{[(\rho v)^{(i)}(1 + \frac{1}{Re_{REF}^{1/2}}\frac{\zeta}{R})^{(i)}$$

$$- \frac{2}{r^\sigma}(\frac{\partial r^\sigma}{\partial\zeta})^{(i)}\mu^{(i)}]\}\frac{(1-\lambda_v)(v_{m,n+1} - v_{m,n-1})}{\Delta\zeta_n(1+K)}\Delta\xi_{m+1}$$

$$-Re_{REF}^{1/2}\left(1+\frac{1}{Re_{REF}^{1/2}}\frac{\zeta}{R}\right)^{(i)}\frac{(1-\lambda_p)(p_{m,n+1}-p_{m,n})}{K\Delta\zeta_n}\Delta\xi_{m+1}$$

$$+\frac{4}{3Re_{REF}^{1/2}}\mu^{(i)}\left\{\frac{2(1-\lambda_v)\Delta\xi_{m+1}}{(1+K)K\Delta\zeta_n^2}(v_{m,n+1,}+Kv_{m,n-1}-(1+K)v_{m,n}]\right\}$$

$$+\frac{1}{Re_{REF}^{1/2}}\left(\frac{\partial\mu}{\partial T}\right)^{(i)}\left\{\frac{4}{3}\left(\frac{\partial v}{\partial\zeta}\right)^{(i)}-\frac{2}{3}\left[\left(\frac{\partial u}{\partial\xi}\right)^{(i)}+\sigma\left(\frac{usin\theta_w}{r}\right)^{(i)}\right]\right\}\frac{(1-\lambda_T)T_{m,n+1}-T_{m,n-1})\Delta\xi_{m+1}}{(1+K)\Delta\zeta_n}$$

$$+\frac{1}{Re_{REF}^{1/2}}\left\{-\frac{2}{3}\sigma\mu^{(i)}\left(\frac{sin\theta_w}{r}\right)+\left[\frac{\partial}{\partial\xi}\left(\mu\left(1+\frac{\rho\varepsilon}{\mu}\right)\right)\right]^{(i)}\right.$$

$$\left.+\left[\frac{\sigma}{r}\frac{\partial r}{\partial\zeta}\mu\left(1+\frac{\rho\varepsilon}{\mu}\right)\right]^{(i)}\right\}\frac{(1-\lambda_u)\Delta\xi_{m+1}}{(1+K)\Delta\zeta_n}(u_{m,n+1}-u_{m,n-1})$$

$$+\frac{(\rho u)^{(i)}}{R}\frac{u_{m,n}}{2}\Delta\xi_{m+1}+\frac{1}{Re_{REF}^{1/2}}\left\{\mu^{(i)}\left(1+\frac{\rho\varepsilon}{\mu}\right)^{(i)}\right.$$

$$\left.-\frac{2}{3}\mu^{(i)}\right\}\frac{(u_{m,n-1}-u_{m,n+1})}{\Delta\zeta_n(1+K)}$$

$$+\frac{2}{3}\frac{\sigma}{Re_{REF}^{1/2}}\mu^{(i)}\left(\frac{1}{r^2}\frac{\partial r}{\partial\zeta}\right)^{(i)}\frac{sin\theta_w u_{m,n}}{2}\Delta\xi_{m+1} \qquad \text{(F-13)}$$

Equation (F-13) in coefficient form is:

$$A_{3n}u_{m+1,n-1}+B_{3n}u_{m+1,n}+C_{3n}u_{m+1,n+1}+D_{3n}v_{m+1,n-1}+E_{3n}v_{m+1,n}$$

$$+F_{3n}v_{m+1,n+1}+G_{3n}T_{m+1,n-1}+H_{3n}T_{m+1,n}+I_{3n}T_{m+1,n+1}$$

$$+J_{3n}p_{m+1,n-1}+K_{3n}p_{m+1,n}+L_{3n}p_{m+1,n+1}=S_{3n} \qquad \text{(F-14)}$$

where:

$$A_{3n} = \frac{1}{Re_{REF}^{1/2}} \frac{}{\Delta\zeta_n(1+K)}\{[-\frac{2}{3}\sigma\mu^{(i)}(\frac{\sin\theta_w}{r})^{(i)}$$

$$+ (\frac{\partial}{\partial\xi}(1+\frac{\rho\varepsilon}{\mu})))^{(i)} + (\frac{\sigma}{r}\frac{\partial r}{\partial\zeta}\ \mu(1+\frac{\rho\varepsilon}{\mu}))^{(i)}]\lambda_u\Delta\xi_{m+1}$$

$$+ [\mu^{(i)}(1+\frac{\rho\varepsilon}{\mu})^{(i)} - \frac{2}{3}\ \mu^{(i)}]\}$$

$$B_{3n} = -\Delta\xi_{m+1}\{\frac{(\rho u)^{(i)}}{2R} + \frac{2}{3}\frac{\sigma\mu^{(i)}}{Re_{REF}^{1/2}}(\frac{1}{r^2}\frac{\partial r}{\partial\zeta})^{(i)}\frac{\sin\theta_w}{2}\}$$

$$C_{3n} = -A_{3n}$$

$$D_{3n} = -\frac{\Delta\xi_{m+1}\lambda_v}{Re_{REF}^{1/2}(1+K)\Delta\zeta_n}\{[(\rho v)^{(i)}(1+\frac{1}{Re_{REF}^{1/2}}\frac{\zeta}{R})^{(i)}$$

$$- (\frac{2}{r^\sigma}\frac{\partial r^\sigma}{\partial\zeta}\mu)^{(i)}] + \frac{8\mu^{(i)}}{3\Delta\zeta_n}\}$$

$$E_{3n} = \frac{1}{Re_{REF}^{1/2}}\{(\rho u)^{(i)} + \frac{8\lambda_v\Delta\xi_{m+1}}{3K\Delta\zeta_n^2}\mu^{(i)}\}$$

$$F_{3n} = \frac{\lambda_v\Delta\xi_{m+1}}{(1+K)\Delta\zeta_n Re_{REF}^{1/2}}\{[(\rho v)^{(i)}(1+\frac{1}{Re_{REF}^{1/2}}\frac{\zeta}{R})^{(i)}$$

$$- (\frac{2}{r^\sigma}\frac{\partial r^\sigma}{\partial\zeta}\mu)^{(i)}] - \frac{8\mu^{(i)}}{3K\Delta\zeta_n}\}$$

$$G_{3n} = \frac{\lambda_T\Delta\xi_{m+1}}{Re_{REF}^{1/2}(1+K)\Delta\zeta_n}(\frac{\partial\mu}{\partial T})^{(i)}[\frac{u}{3}(\frac{\partial v}{\partial\zeta})^{(i)} - \frac{2}{3}(\frac{\partial u}{\partial\xi})^{(i)} + (\frac{\sigma u\sin\theta_w}{r})^{(i)})]$$

$$H_{3n} = 0$$

$$I_{3n} = -G_{3n}$$

$$J_{3n} = 0$$

$$K_{3n} = -Re_{REF}^{1/2}\left(1 + \frac{1}{Re_{REF}^{1/2}}\frac{\zeta}{R}\right)^{(i)} \frac{\lambda_p \Delta\xi_{m+1}}{K\Delta\zeta_n}$$

$$L_{3n} = -K_{3n}$$

$$S_{3n} = \frac{(\rho u)^{(i)} v_{m,n}}{Re_{REF}^{1/2}} - \frac{(1-\lambda_v)\Delta\xi_{m+1}(v_{m,n+1} - v_{m,n-1})}{Re_{REF}^{1/2}(1+K)\Delta\zeta_n}[(\rho v)^{(i)}\left(1 + \frac{1}{Re_{REF}^{1/2}}\frac{\zeta}{R}\right)^{(i)}$$

$$- \left(\frac{2}{r^\sigma}\frac{\partial r^\sigma}{\partial\zeta}\mu\right)^{(i)}] - Re_{REF}^{1/2}\left(1 + \frac{1}{Re_{REF}^{1/2}}\frac{\zeta}{R}\right)^{(i)} \frac{(1-\lambda_p)(p_{m,n+1} - p_{m,n})}{K\Delta\zeta_n}\Delta\xi_{m+1}$$

$$+ \frac{8(1-\lambda_v)\Delta\xi_{m+1}}{3Re_{REF}^{1/2}(1+K)K\Delta\zeta_n^2}\mu^{(i)}[v_{m,n+1} + Kv_{m,n-1} - (1+K)v_{m,n}]$$

$$+ \frac{1}{Re_{REF}^{1/2}}\left(\frac{\partial\mu}{\partial T}\right)^{(i)} \frac{(1-\lambda_T)\Delta\xi_{m+1}}{(1+K)\Delta\zeta_n}(T_{m,n+1} - T_{m,n-1})\{\frac{4}{3}\left(\frac{\partial v}{\partial\zeta}\right)^{(i)}$$

$$- \frac{2}{3}[\left(\frac{\partial u}{\partial\xi}\right)^{(i)} + \sigma\left(\frac{u\sin\theta_w}{r}\right)^{(i)}]\}$$

$$+ \frac{(1-\lambda_u)\Delta\xi_{m+1}}{Re_{REF}^{1/2}(1+K)\Delta\zeta_n}(u_{m,n+1} - u_{m,n-1})\{-\frac{2}{3}\sigma\mu^{(i)}\left(\frac{\sin\theta_w}{r}\right)^{(i)}$$

$$+ [\frac{\partial}{\partial\xi}(\mu(1 + \frac{\rho\varepsilon}{\mu}))]^{(i)} + [\frac{\sigma}{r}\frac{\partial r}{\partial\zeta}\mu(1 + \frac{\rho\varepsilon}{\mu})]^{(i)}\}$$

$$+ \frac{(\rho u)^{(i)}}{2R}u_{m,n}\Delta\xi_{m+1} + \frac{(u_{m,n-1} - u_{m,n+1})}{Re_{REF}^{1/2}\Delta\zeta_n(1+K)}\{\mu^{(i)}\left(1 + \frac{\rho\varepsilon}{\mu}\right)^{(i)} - \frac{2}{3}\mu^{(i)}\}$$

$$+ \frac{2}{3Re_{REF}^{1/2}} \sigma\mu^{(i)} \left(\frac{1}{r^2} \frac{\partial r}{\partial \zeta}\right)^{(i)} \frac{\sin\theta\, w_{m,n}}{2} \Delta\xi_{m+1} \qquad \text{(F-15)}$$

energy

The linearized energy equation is:

$$(\rho u)^{(i)} \frac{\partial T}{\partial \xi} + \left(1 + \frac{1}{Re_{REF}^{1/2}} \frac{\zeta}{R}\right)^{(i)} v\left(\rho \frac{\partial T}{\partial \zeta}\right)^{(i)}$$

$$= (\gamma-1)M_{REF}^2 \left[u^{(i)} \frac{\partial p}{\partial \xi} + \left(1 + \frac{1}{Re_{REF}^{1/2}} \frac{\zeta}{R}\right)^{(i)} v^{(i)} \frac{\partial p}{\partial \zeta}\right]$$

$$+ (\gamma-1)M_{REF}^2 \mu^{(i)} \left[\left(1 + \frac{1}{Re_{REF}^{1/2}} \frac{\zeta}{R}\right)^{(i)} - \frac{2u^{(i)}}{Re_{REF}^{1/2} R}\right] \frac{\partial u}{\partial \zeta}$$

$$+ \left[\left(1 + \frac{\zeta}{Re_{REF}^{1/2} \zeta}\right) \frac{\mu}{Pr_{REF}^{1/2}} \left(1 + \frac{\rho\varepsilon}{\mu} \frac{Pr_{REF}}{Pr_t}\right)\right]^{(i)} \frac{\partial^2 T}{\partial \zeta^2}$$

$$+ \left\{\frac{1}{r^\sigma}\left[\frac{\partial}{\partial \zeta}\left(r^\sigma \left(1 + \frac{1}{Re_{REF}^{1/2}} \frac{\zeta}{R}\right) \frac{\mu}{Pr_{REF}} \left(1 + \frac{\rho\varepsilon}{\mu} \frac{Pr_{REF}}{Pr_t}\right)\right)\right]\right\}^{(i)} \frac{\partial T}{\partial \zeta} \qquad \text{(F-16)}$$

The difference form of equation (F-16) for point A (figure 18) is:

$$(\rho u)^{(i)} \frac{(T_{m+1,n} - T_{m,n})}{\Delta\xi_{m+1}} + \left(\rho \frac{\partial T}{\partial \zeta}\right)^{(i)} \left(1 + \frac{1}{Re_{REF}^{1/2}} \frac{\zeta}{R}\right)^{(i)} \frac{(v_{m+1,n} + v_{m,n})}{2}$$

$$= (\gamma-1)M_{REF}^2 u^{(i)} \left(\frac{dP_{EXT}(\xi)}{d\xi} + \frac{(p_{m+1n} - p_{m,n})}{\Delta\xi_{m+1}}\right)$$

$$+ (\gamma-1)M_{REF}^2 \left(1 + \frac{1}{Re_{REF}^{1/2}} \frac{\zeta}{R}\right)^{(i)} v^{(i)} \left\{\frac{\lambda_p (p_{m+1,n+1} - p_{m+1,n})}{K\Delta\zeta_n}\right.$$

$$\left. + (1-\lambda_p) \frac{(p_{m,n+1} - p_{m,n})}{K\Delta\zeta_n}\right\}$$

$$+ (\gamma-1)M^2_{REF}\mu^{(i)}[(1 + \frac{1}{Re^{1/2}_{REF}}\frac{\zeta}{R})^{(i)}(\frac{\partial u}{\partial \zeta})^{(i)}$$

$$- \frac{2u^{(i)}}{Re^{1/2}_{REF}R}][\frac{\lambda_u(u_{m+1,n+1} - u_{m+1,n-1})}{(1+K)\Delta\zeta_n} + \frac{(1-\lambda_u)(u_{m,n+1} - u_{m,n-1})}{(1+K)\Delta\zeta_n}]$$

$$+ [(1 + \frac{\zeta}{Re^{1/2}_{REF}R})\frac{\mu}{Pr_{REF}}(1 + \frac{\rho\varepsilon}{\mu}\frac{Pr_{REF}}{Pr_t})]^{(i)}$$

$$[\frac{\lambda_T 2}{K(1+K)\Delta\zeta^2_n}(T_{m+1,n+1} + KT_{m+1,n-1} - (1+K)T_{m+1,n})$$

$$+ \frac{(1-\lambda_T)2}{K(1+K)\Delta\zeta^2_n}(T_{m,n+1} + KT_{m,n-1} - (1+K)T_{m,n})]$$

$$+ \{\frac{1}{r^\sigma}[\frac{\partial}{\partial\zeta}(r^\sigma(1 + \frac{1}{Re^{1/2}_{REF}}\frac{\zeta}{R})\frac{\mu}{Pr_{REF}}(1 + \frac{\rho\varepsilon}{\mu}\frac{Pr_{REF}}{Pr_t}))]\}^{(i)}$$

$$[\frac{\lambda_T(T_{m+1,n+1} - T_{m+1,n-1})}{(1+K)\Delta\zeta_n} + \frac{(1-\lambda_T)(T_{m,n+1} - T_{m,n-1})}{(1+K)\Delta\zeta_n}] \qquad \text{(F-17)}$$

Expanding equation (F-17) and multiplying by $\Delta\xi_{m+1}$ yields:

$$u_{m+1,n-1}\{(\gamma-1)M^2_{REF}\mu^{(i)}[(1 + \frac{1}{Re^{1/2}_{REF}}\frac{\zeta}{R})^{(i)}(\frac{\partial u}{\partial\zeta})^{(i)}$$

$$- \frac{2u^{(i)}}{Re^{1/2}_{REF}R}]\frac{\lambda_u\Delta\xi_{m+1}}{(1+K)\Delta\zeta_n}\} + u_{m+1,n+1}\{-(\gamma-1)M^2_{REF}\mu^{(i)}[(1 + \frac{1}{Re^{1/2}_{REF}}\frac{\zeta}{R})^{(i)}(\frac{\partial u}{\partial\zeta})^{(i)}$$

$$- \frac{2u^{(i)}}{Re^{1/2}_{REF}R}]\frac{\lambda_u\Delta\xi_{m+1}}{(1+K)\Delta\zeta_n}\} + v_{m+1,n}\{(\rho\frac{\partial T}{\partial\zeta})^{(i)}(1 + \frac{1}{Re^{1/2}_{REF}}\frac{\zeta}{R})^{(i)}\frac{\Delta\xi_{m+1}}{2}\}$$

$$- T_{m+1,n-1}\{[(1 + \frac{\zeta}{Re^{1/2}_{REF}R})\frac{\mu}{Pr_{REF}}(1 + \frac{\rho\varepsilon}{\mu}\frac{Pr_{REF}}{Pr_t})]^{(i)}\frac{2\lambda_T\Delta\xi_{m+1}}{(1+K)\Delta\zeta^2_n}$$

$$- \left[\frac{1}{r^{\sigma}} \frac{\partial}{\partial \zeta}\left[r^{\sigma}\left(1 + \frac{1}{Re_{REF}^{1/2}} \frac{\zeta}{R}\right)\frac{\mu}{Pr_{REF}}\left(1 + \frac{\rho\varepsilon}{\mu} \frac{Pr_{REF}}{Pr_t}\right)\right)\right]^{(i)}$$

$$\frac{\lambda_T \Delta\xi_{m+1}}{(1+K)\Delta\zeta_n}\Big\} + T_{m+1,n}\ \{(\rho u)^{(i)}$$

$$+ \left[\left(1+ \frac{1}{Re_{REF}^{1/2}} \frac{\zeta}{R}\right) \frac{\mu}{Pr_{REF}}\left(1 + \frac{\rho\varepsilon}{\mu} \frac{Pr_{REF}}{Pr_t}\right]^{(i)} \frac{2\lambda_T \Delta\xi_{m+1}}{K\Delta\zeta_n^2}\right\}$$

$$+ T_{m+1,n+1}\left\{-\left[\left(1 + \frac{\zeta}{Re_{REF}^{1/2} R}\right)\frac{\mu}{Pr_{REF}}\left(1 + \frac{\rho\varepsilon}{\mu} \frac{Pr_{REF}}{Pr_t}\right)\right]^{(i)} \frac{2\lambda_T \Delta\xi_{m+1}}{K(1+K)\Delta\zeta_n^2}\right.$$

$$- \left[\frac{1}{r^{\sigma}} \frac{\partial}{\partial \zeta}\left(r^{\sigma}\left(1 + \frac{1}{Re_{REF}^{1/2}} \frac{\zeta}{R}\right)\frac{\mu}{Pr_{REF}}\left(1 + \frac{\rho\varepsilon}{\mu} \frac{Pr_{REF}}{Pr_t}\right)\right)\right]^{(i)} \frac{\lambda_T \Delta\xi_{m+1}}{(1+K)\Delta\zeta_n}\Big\}$$

$$+ P_{m+1,n}\ \left\{-(\gamma-1)M_{REF}^2 u^{(i)} + (\gamma-1)M_{REF}^2\left(1 + \frac{1}{Re_{REF}^{1/2}} \frac{\zeta}{R}\right)^{(i)}\right.$$

$$v^{(i)} \frac{\lambda_p \Delta\xi_{m+1}}{K\Delta\zeta_n}\Big\} + P_{m+1,n+1}\ \left\{-(\gamma-1)M_{REF}^2\left(1 + \frac{1}{Re_{REF}^{1/2}} \frac{\zeta}{R}\right)^{(i)} v^{(i)} \frac{\lambda_p \Delta\xi_{m+1}}{K\Delta\zeta_n}\right\}$$

$$= (\rho u)^{(i)} T_{m,n} - \gamma\left(\rho \frac{\partial T}{\partial \zeta}\right)^{(i)}\left(1 + \frac{1}{Re_{REF}^{1/2}} \frac{\zeta}{R}\right)^{(i)} \frac{v_{m,n} \Delta\xi_{m+1}}{2}$$

$$+ (\gamma-1)M_{REF}^2 u^{(i)}\left[\frac{dP_{EXT}}{d\xi} \Delta\xi_{m+1} - p_{m,n}\right]$$

$$+ (\gamma-1)M_{REF}^2\ ^{(i)}\left[\left(1 + \frac{1}{Re_{REF}^{1/2}} \frac{\zeta}{R}\right)^{(i)} \left(\frac{\partial u}{\partial \zeta}\right)^{(i)}\right.$$

$$- \left.\frac{2(u)^{(i)}}{Re_{REF}^{1/2} R}\right] \frac{(1-\lambda_u)(u_{m,n+1} - u_{m,n-1})\Delta\xi_{m+1}}{(1+K)\Delta\zeta_n} + (\gamma-1)M_{REF}^2\left(1 + \frac{1}{Re_{REF}^{1/2}} \frac{\zeta}{R}\right)^{(i)}$$

$$v^{(i)} \frac{(1-\lambda_p)}{K\Delta\zeta_n} \Delta\xi_{m+1}(p_{m,n+1} - p_{m,n})$$

$$+ \left[\left(1 + \frac{\zeta}{Re_{REF}^{1/2} R}\right)\frac{\mu}{Pr_{REF}}\left(1 + \frac{\rho\varepsilon}{\mu}\frac{Pr_{REF}}{Pr_t}\right)\right]^{(i)} \frac{2(1-\lambda_T)\Delta\xi_{m+1}}{K(1+K)\Delta\zeta_n^2}$$

$$(T_{m,n+1} + KT_{m,n-1} - (1+K)T_{m,n})$$

$$+ \left\{\frac{1}{r^\sigma}\left[\frac{\partial}{\partial\zeta}\left(r^\sigma\left(1 + \frac{1}{Re_{REF}^{1/2}}\frac{\zeta}{R}\right)\frac{\mu}{Pr_{REF}}\left(1 + \frac{\rho\varepsilon}{\mu}\frac{Pr_{REF}}{Pr_t}\right)\right)\right]\right\}^{(i)}$$

$$\frac{(1-\lambda_T)}{(1+K)\Delta\zeta_n}(T_{m,n+1} - T_{m,n-1})\Delta\xi_{m+1} \qquad \text{(F-18)}$$

Equation (F-18) in coefficient form is:

$$A_{2n}u_{m+1,n-1} + B_{4n}u_{m+1,n} + C_{4n}u_{m+1,n+1} + D_{4n}v_{m+1,n-1} + E_{4n}v_{m+1,n}$$

$$+ F_{4n}v_{m+1,n+1} + G_{4n}T_{m+1,n-1} + H_{4n}T_{m+1,n} + I_{4n}T_{m+1,n+1} + J_{4n}p_{m+1,n-1}$$

$$+ K_{4n}p_{m+1,n} + L_{4n}p_{m+1,n+1} = S_{4n} \qquad \text{(F-19)}$$

where:

$$A_{4n} = (\gamma-1)M_{REF}^2\,\mu^{(i)}\,\frac{\lambda_u\Delta\xi_{m+1}}{(1+K)\Delta\zeta_n}\left[\left(1 + \frac{1}{Re_{REF}^{1/2}}\frac{\zeta}{R}\right)^{(i)}\left(\frac{\partial u}{\partial\zeta}\right)^{(i)} - \frac{2u^{(i)}}{Re_{REF}^{1/2}R}\right]$$

$$B_{4n} = 0$$

$$C_{4n} = -A_{4n}$$

$$D_{4n} = 0$$

$$E_{4n} = \left(\rho\frac{\partial T}{\partial\zeta}\right)^{(i)}\frac{\Delta\xi_{m+1}}{2}\left(1 + \frac{1}{Re_{REF}^{1/2}}\frac{\zeta}{R}\right)^{(i)}$$

$$F_{4n} = 0$$

$$G_{4n} = -\left\{\left[\left(1 + \frac{\zeta}{Re_{REF}^{1/2}R}\right)\frac{\mu}{Pr_{REF}}\left(1 + \frac{\rho\varepsilon}{\mu}\frac{Pr_{REF}}{Pr_t}\right)\right]^{(i)}\frac{2}{\Delta\zeta_n}\right.$$

$$- \left[\frac{1}{r^{\sigma}} \frac{\partial}{\partial \zeta}\left(r^{\sigma}\left(1 + \frac{1}{Re_{REF}^{1/2}} \frac{\zeta}{R}\right) \frac{\mu}{Pr_{REF}}\left(1 + \frac{\rho \varepsilon}{\mu} \frac{Pr_{REF}}{Pr_t}\right)\right)\right]^{(i)} \frac{\lambda_T \Delta \xi_{m+1}}{(1+K)\Delta \zeta_n}$$

$$H_{4n} = (\rho u)^{(i)} + \left[\left(1 + \frac{1}{Re_{REF}^{1/2}} \frac{\zeta}{R}\right) \frac{\mu}{Pr_{REF}}\left(1 + \frac{\rho \varepsilon}{\mu} \frac{Pr_{REF}}{Pr_t}\right)\right]^{(i)} \frac{2\lambda_T \Delta \xi_{m+1}}{K \Delta \zeta_n^2}$$

$$I_{4n} = - \frac{\lambda_T \Delta \xi_{m+1}}{(1+K)\Delta \zeta_n} \left\{ \frac{2}{\Delta \zeta_n}\left[\left(1 + \frac{1}{Re_{REF}^{1/2}} \frac{\zeta}{R}\right) \frac{\mu}{Pr_{REF}}\left(1 + \frac{\rho \varepsilon}{\mu} \frac{Pr_{REF}}{Pr_t}\right)\right]^{(i)} \right.$$

$$\left. + \left[\frac{1}{r^{\sigma}} \frac{\partial}{\partial \zeta}\left(r^{\sigma}\left(1 + \frac{1}{Re_{REF}^{1/2}} \frac{\zeta}{R}\right) \frac{\mu}{Pr_{REF}}\left(1 + \frac{\rho \varepsilon}{\mu} \frac{Pr_{REF}}{Pr_t}\right)\right)\right]^{(i)} \right\}$$

$$J_{4n} = 0$$

$$K_{4n} = - (\gamma-1) M_{REF}^2 u^{(i)} + (\gamma-1) M_{REF}^2 \left(1 + \frac{1}{Re_{REF}^{1/2}} \frac{\zeta}{R}\right)^{(i)} v^{(i)} \frac{\lambda_p}{K} \frac{\Delta \xi_{m+1}}{\Delta \zeta_n}$$

$$L_{4n} = - (\gamma-1) M_{REF}^2 \left(1 + \frac{1}{Re_{REF}^{1/2}} \frac{\zeta}{R}\right)^{(i)} v^{(i)} \frac{\lambda_p \Delta \xi_{m+1}}{K \Delta \zeta_n}$$

$$S_{4n} = (\rho u)^{(i)} T_{m,n} - \left(\rho \frac{\partial T}{\partial \zeta}\right)^{(i)} \left(1 + \frac{1}{Re_{REF}^{1/2}} \frac{\zeta}{R}\right)^{(i)} \frac{v_{m,n}}{2} \Delta \xi_{m+1}$$

$$+ (\gamma-1) M_{REF}^2 u^{(i)} \left[\frac{dP_{EXT}(\xi)}{d\xi} \Delta \xi_{m+1} - p_{m,n}\right]$$

$$+ (\gamma-1) M_{REF}^2 \left(1 + \frac{1}{Re_{REF}^{1/2}} \frac{\zeta}{R}\right)^{(i)} v^{(i)} \frac{(1-\lambda_p)}{K \Delta \zeta_n} \Delta \xi_{m+1} (p_{m,n+1} - p_{m,n})$$

$$+ (\gamma-1) M_{REF}^2 \mu^{(i)} \left[\left(1 + \frac{1}{Re_{REF}^{1/2}} \frac{\zeta}{R}\right)^{(i)} \left(\frac{\partial u}{\partial \zeta}\right)^{(i)} - \frac{2u^{(i)}}{Re_{REF}^{1/2} R}\right]$$

$$\frac{(1-\lambda_u)(u_{m,n+1} - u_{m,n-1})}{(1+K)\Delta \zeta_n}$$

$$+ \left[\left(1 + \frac{\zeta}{Re_{REF}^{1/2} R}\right)\frac{\mu}{Pr_{REF}}\left(1 + \frac{\rho\varepsilon}{\mu}\frac{Pr_{REF}}{Pr_t}\right)\right]^{(i)} \frac{2(1-\lambda_T)}{K(1+K)\Delta\zeta_n^2}$$

$$(T_{m,n+1} + KT_{m,n-1} - (1+K)T_{m,n})$$

$$+ \left\{\frac{1}{r^\sigma}\left[\frac{\partial}{\partial\zeta}\left(r^\sigma\left(1 + \frac{1}{Re_{REF}^{1/2}}\frac{\zeta}{R}\right)\frac{\mu}{Pr_{REF}}\left(1 + \frac{\rho\varepsilon}{\mu}\frac{Pr_{REF}}{Pr_t}\right)\right)\right]\right\}^{(i)}$$

$$\frac{(1-\lambda_T)\Delta\xi_{m+1}}{(1+K)\Delta\zeta_n}\,(T_{m,n+1} - T_{m,n-1})$$

(F-20)

APPENDIX G

BOUNDARY CONDITIONS IN MATRIX FORM

For solving the system of equations, the boundary conditions must be incorporated in difference form in order to have a closed system. As an example a detailed description is given here for the adiabatic case. Writing equation (84) for $\underline{n = 2}$ the following is obtained:

$$\bar{M}_2 \bar{X}_2 + \bar{E}_3 \bar{X}_3 = \bar{g}_2 \tag{G-1}$$

Expressing $T_{m+1,1}$ in terms of $T_{m+1,2}$ and $T_{m+1,3}$ using three point forward differencing yields:

$$\bar{M}_2 = \begin{vmatrix} B_{12} & E_{12} & H'_{12} & K_{12} \\ B_{22} & E_{22} & H'_{22} & K_{22} \\ B_{32} & E_{32} & H'_{32} & K_{32} \\ B_{43} & E_{42} & H'_{43} & K_{42} \end{vmatrix} \qquad \bar{E}_2 = \begin{vmatrix} C_{12} & F_{12} & I'_{12} & L_{12} \\ C_{22} & F_{22} & I'_{22} & L_{22} \\ C_{32} & F_{32} & I'_{32} & L_{32} \\ C_{42} & F_{42} & I'_{42} & L_{42} \end{vmatrix}$$

and

$$\bar{g}_2 = \begin{vmatrix} S'_{12} \\ S'_{22} \\ S'_{32} \\ S'_{42} \end{vmatrix} \tag{G-2}$$

where the primed quantities

$$H'_{12} = H_{12} + \frac{G_{12}(1+K)^2}{(1+K)^2 - 1}$$

$$I'_{12} = I_{12} - \frac{G_{12}}{(1+K)^2-1}$$

$$S'_{12} = S_{12} - D_{12}v_{m+1,1}$$

are adjusted values of the matrix elements due to the three-point evaluation of wall temperature in the adiabatic case. Similarly for the other elements H'_{n_2}, I'_{n_2}, S'_{n_2} (n = 2,3,4).

For $2 < n < N-1$ equation (84) can be written as:

$$\bar{D}_n\bar{X}_{n-1} + \bar{M}_n\bar{X}_n + \bar{E}_n\bar{X}_{n+1} = \bar{g}_n \qquad \text{(G-3)}$$

For $\underline{n = N-1}$ equation (84) is:

$$\bar{D}_{N-1}\bar{X}_{N-2} + \bar{M}_{N-1}\bar{X}_{N-1} = \bar{g}_{N-1} \qquad \text{(G-4)}$$

Incorporating the boundary conditions at the edge of the boundary layer n = N it can be shown that $\bar{D}_{N-1}$ and $\bar{M}_{N-1}$ do not change and $\bar{g}_{N-1}$ can be written as follows:

$$\bar{D}_{N-1} = \begin{vmatrix} A_{1,N-1} & D'_{1,N-1} & G_{1,N-1} & J_{1,N-1} \\ A_{2,N-1} & D'_{2,N-1} & G_{2,N-1} & J_{2,N-1} \\ A_{3,N-1} & D'_{3,N-1} & G_{3,N-1} & J_{3,N-1} \\ A_{4,N-1} & D'_{4,N-1} & G_{4,N-1} & J_{4,N-1} \end{vmatrix}$$

$$\bar{M}_{N-1} = \begin{vmatrix} B_{1,N-1} & E'_{1,N-1} & H_{1,N-1} & K_{1,N-1} \\ B_{2,N-1} & E'_{2,N-1} & H_{2,N-1} & K_{2,N-1} \\ B_{3,N-1} & E'_{3,N-1} & H_{3,N-1} & K_{3,N-1} \\ B_{4,N-1} & E'_{4,N-1} & H_{4,N-1} & K_{4,N-1} \end{vmatrix} \qquad \bar{g}_{N-1} = \begin{vmatrix} S'_{1,N-1} \\ S'_{2,N-1} \\ S'_{3,N-1} \\ S'_{4,N-1} \end{vmatrix} \qquad \text{(G-5)}$$

Here $v_{m+1,N}$ was calculated using three point backward differencing using $\frac{\partial v}{\partial \zeta}\Big|_N$ calculated from the continuity at the edge of the boundary layer. Thus we get:

$$D'_{i,N-1} = D_{i,N-1} - \frac{K^2}{(1+2K)} F_{i,N-1}$$

$$E'_{i,N-1} = E_{i,N-1} + \frac{(1+K)^2}{(1+2K)} F_{i,N-1}$$

$$S'_{i,N-1} = S_{i,N-1} - C_{i,\,N-1} u_{m+1,N} - \frac{(1+K)}{(1+2K)} \Delta\zeta_N F_{i,N-1} \left(\frac{\partial v}{\partial y}\right)_N - I_{i,N-1} T_{m+1,N}$$

APPENDIX H

CALCULATION OF THE PRESSURE AT THE WALL

Some investigators that include the normal momentum equation tend to assume a zero pressure gradient in the ζ direction at the wall. Upon looking at the ζ-momentum equation and satisfying the equation at the wall i.e., applying the boundary conditions it can be shown that the normal pressure gradient at the wall is not zero. Apply the boundary condition to equation (F-11) the following equation is obtained:

$$\frac{(\rho v)_w^{(i)}}{Re_{REF}^{1/2}} \frac{\partial v}{\partial \zeta}\Big|_w = - Re_{REF}^{1/2} \frac{\partial p}{\partial \zeta}\Big|_w + \frac{4}{3Re_{REF}^{1/2}} (\mu_w)^{(i)} \frac{\partial^2 v}{\partial \zeta^2}\Big|_w$$
$$+ \frac{2}{Re_{REF}^{1/2}} \frac{\partial v}{\partial \zeta}\Big|_w^{(i)} \left(\frac{\partial \mu}{\partial T}\right)_w^{(i)} \left(\frac{\partial T}{\partial \zeta}\right)\Big|_w$$
$$+ \frac{2}{Re_{REF}^{1/2}} \frac{\sigma}{r} \frac{\partial r}{\partial \zeta}\Big|_w (\mu_w)^{(i)} \frac{\partial v}{\partial \zeta}\Big|_w$$
$$- \frac{2}{3Re_{REF}^{1/2}} \sigma \mu_w^{(i)} \left(\frac{\sin\theta_w}{r}\right)^{(i)} \left(\frac{\partial u}{\partial \zeta}\right)_w + \frac{(\mu_w)^{(i)}}{3Re_{REF}^{1/2}} \frac{\partial^2 u}{\partial \zeta \partial x}\Big|_w$$
$$- \frac{2}{3Re_{REF}^{1/2}} \left(\frac{\partial \mu}{\partial T}\right)_w^{(i)} \left(\frac{\partial v}{\partial \zeta}\right)_w^{(i)} \left(\frac{\partial T}{\partial \zeta}\right)\Big|_w + \frac{1}{Re_{REF}^{1/2}} \frac{1}{r^\sigma} \frac{\partial}{\partial \xi} (\mu r^\sigma)_w^{(i)} \frac{\partial u}{\partial \zeta}\Big|_w \qquad \text{(H-1)}$$

Solving for $Re_{REF}^{1/2} \frac{\partial p}{\partial \zeta}\Big|_w$ and condensing somewhat

$$\mathrm{Re}_{REF}^{1/2}\left.\frac{\partial p}{\partial \zeta}\right|_w = \frac{4}{3\mathrm{Re}_{REF}^{1/2}}(\mu_w)^{(i)}\left.\frac{\partial v^2}{\partial \zeta^2}\right|_w + \frac{4}{3\mathrm{Re}_{REF}^{1/2}}\left(\left.\frac{\partial v}{\partial \zeta}\right|_w\right)^{(i)}\left(\frac{\partial \mu}{\partial T}\right)_w^{(i)}\left.\frac{\partial T}{\partial \zeta}\right|_w$$

$$- \frac{(\rho v)_w^{(i)}}{\mathrm{Re}_{REF}^{1/2}}\left.\frac{\partial v}{\partial \zeta}\right|_w + \frac{2}{\mathrm{Re}_{REF}^{1/2}}\frac{\sigma}{r}\left(\frac{\partial r}{\partial \zeta}\right)_w(\mu_w)^{(i)}\left.\frac{\partial v}{\partial \zeta}\right|_w$$

$$+ \frac{(\mu_w)^{(i)}}{3\mathrm{Re}_{REF}^{1/2}}\left.\frac{\partial^2 u}{\partial \xi \partial \zeta}\right|_w - \frac{2}{3\mathrm{Re}_{REF}^{1/2}}\sigma\mu_w^{(i)}\left(\frac{\sin\theta}{r}_w\right)^{(i)}\left.\frac{\partial u}{\partial \zeta}\right|_w$$

$$+ \frac{1}{\mathrm{Re}_{REF}^{1/2}}\frac{1}{r^\sigma}\frac{\partial}{\partial \xi}(\mu r^\sigma)\Big|_w^{(i)}\left.\frac{\partial u}{\partial \zeta}\right|_w \qquad \text{(H-2)}$$

or

$$\left.\frac{\partial p}{\partial \zeta}\right|_w = \frac{1}{\mathrm{Re}_{REF}}\left\{\frac{4}{3}(\mu_w)^{(i)}\left.\frac{\partial^2 v}{\partial \zeta^2}\right|_w + \frac{4}{3}\left(\frac{\partial v}{\partial \zeta}\right)_w^{(i)}\left(\frac{\partial \mu}{\partial T}\right)_w^{(i)}\left.\frac{\partial T}{\partial \zeta}\right|_w\right.$$

$$+ \left[2\frac{\sigma}{r_w}\left(\frac{\partial r}{\partial \zeta_w}\right)(\mu_w)^{(i)} - (\rho v)_w\right]\left.\frac{\partial v}{\partial \zeta}\right|_w + \frac{(\mu_w)^{(i)}}{3}\left.\frac{\partial^2 u}{\partial \xi \partial \zeta}\right|_w$$

$$\left. + \left[\frac{1}{r_w^\sigma}\left(\frac{\partial}{\partial \xi}(\mu r^\sigma)\right)_w^{(i)} - \frac{2}{3}\sigma_w^{(i)}\mu_w\left(\frac{\sin\theta}{r}_w\right)^{(i)}\right]\left.\frac{\partial u}{\partial \zeta}\right|_w\right\} \qquad \text{(H-3)}$$

Using two-point differencing the pressure at the wall is obtained by:

$$p(m+1,1) = p(m+1,2) - \left.\frac{\partial p}{\partial \zeta}\right|_w \Delta\zeta_1 \qquad \text{(H-4)}$$

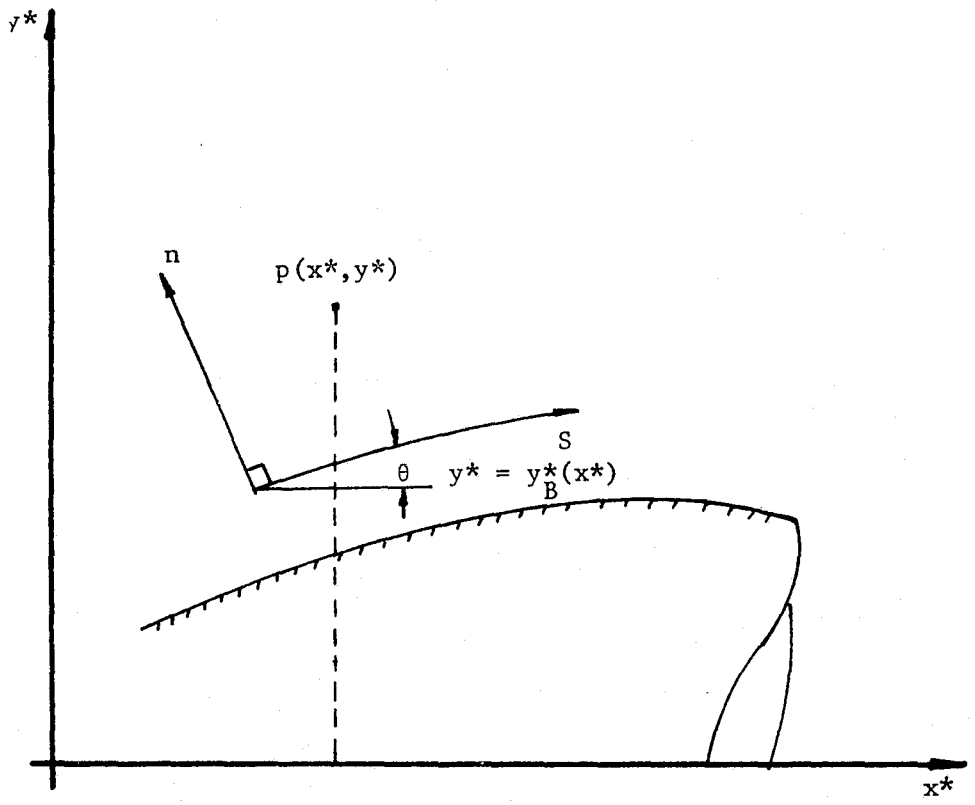

Figure 1 Coordinate System for Outer Region

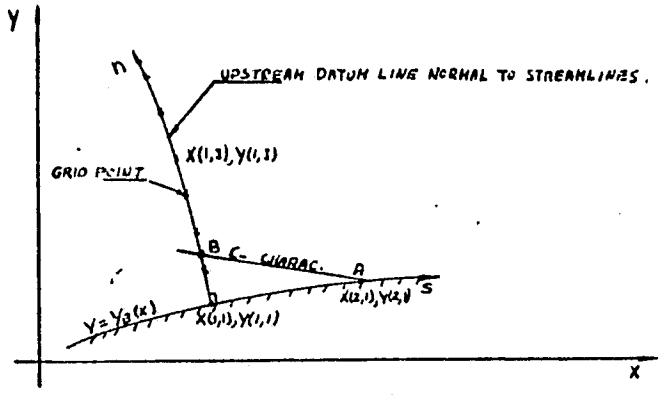

Figure 2 Boundary Point Calculation

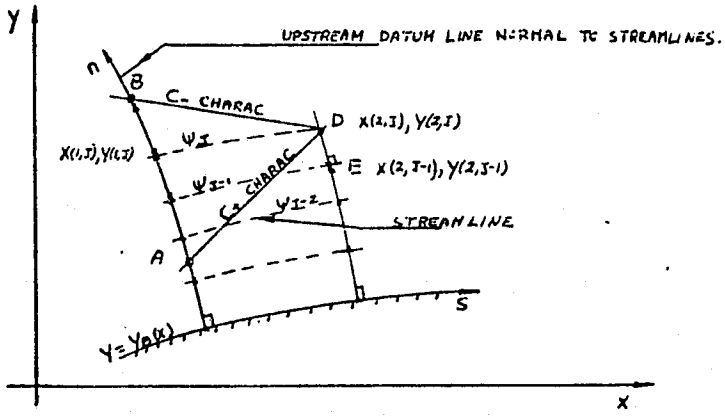

Figure 3 Field Point Calculation

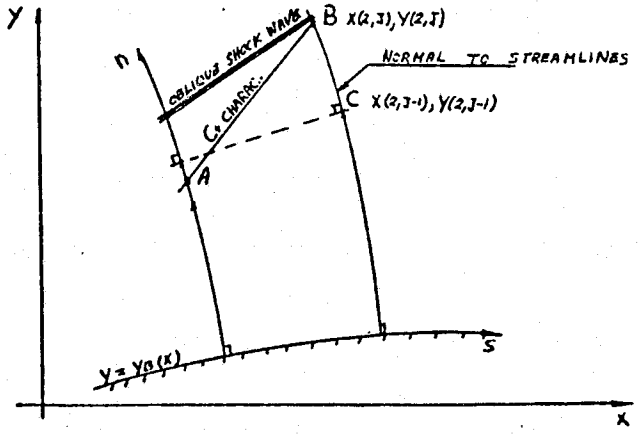

Figure 4 Shock Point Calculation

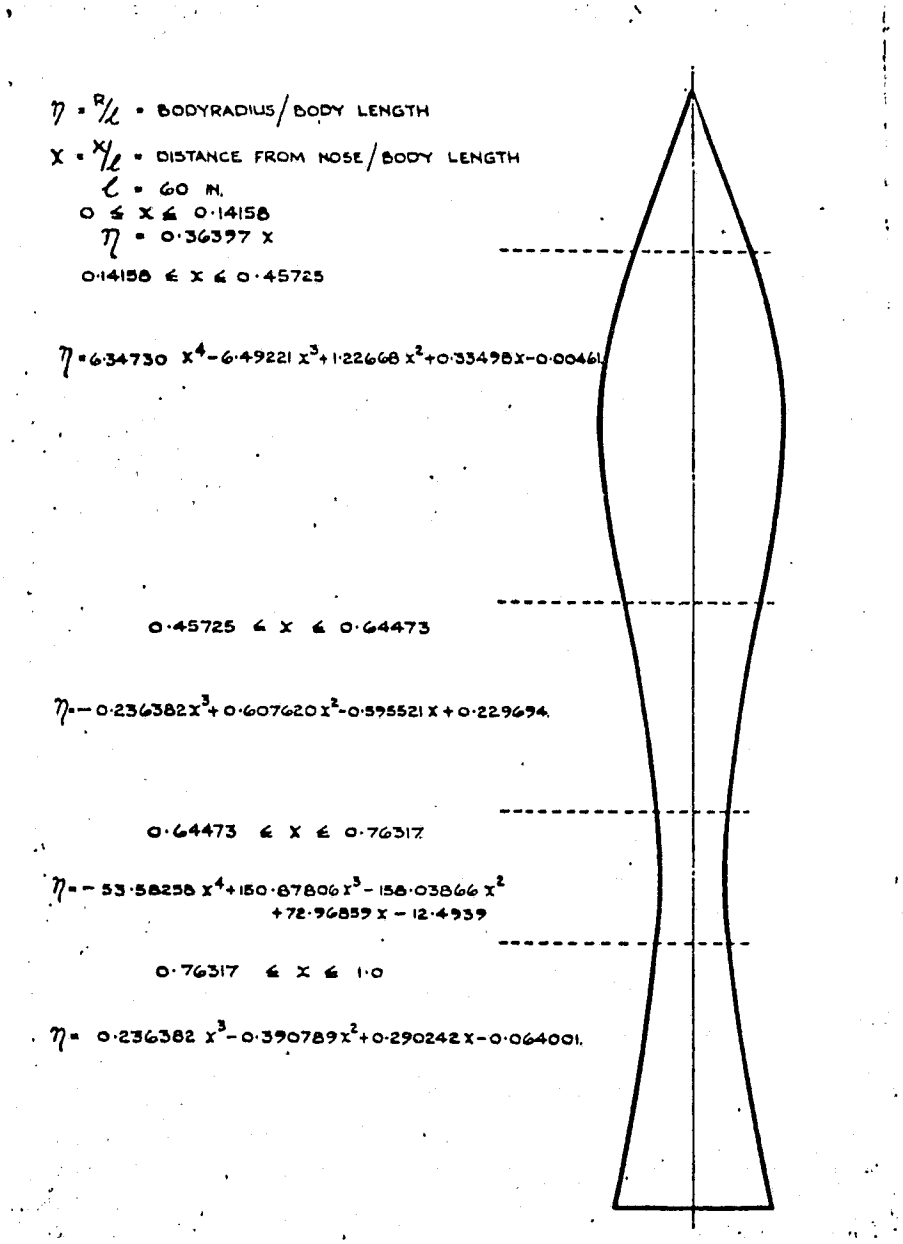

Figure 5 Geometry of Waisted Body

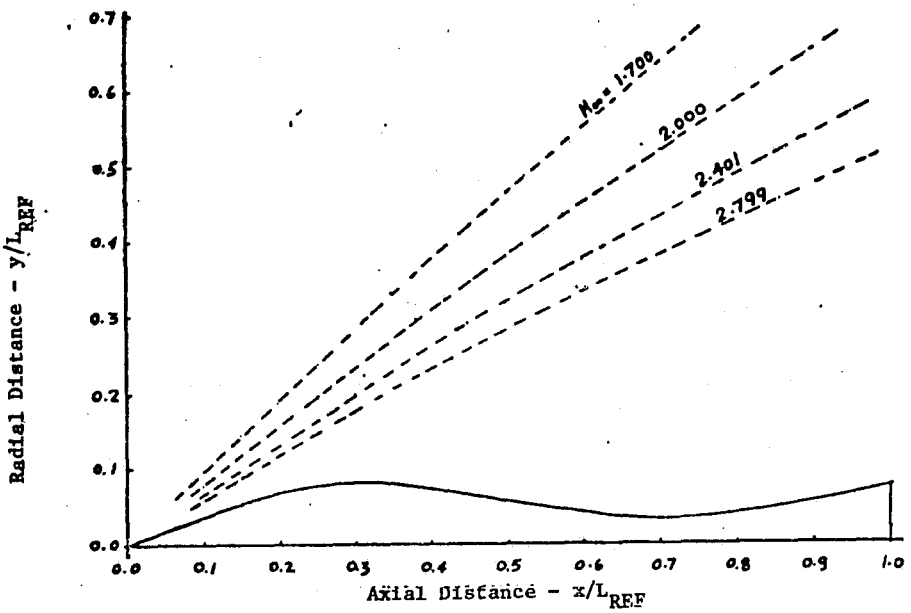

Figure 6 Calculated Shock Shape for Waisted Body of Winter, Smith and Rotta (Ref. 8)

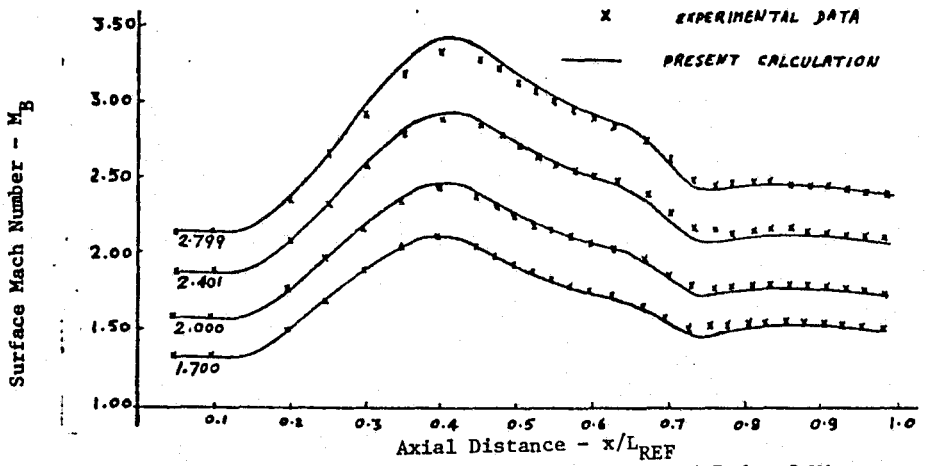

Figure 7 Mach Number Distribution for Waisted Body of Winter, Smith and Rotta (Ref. 8)

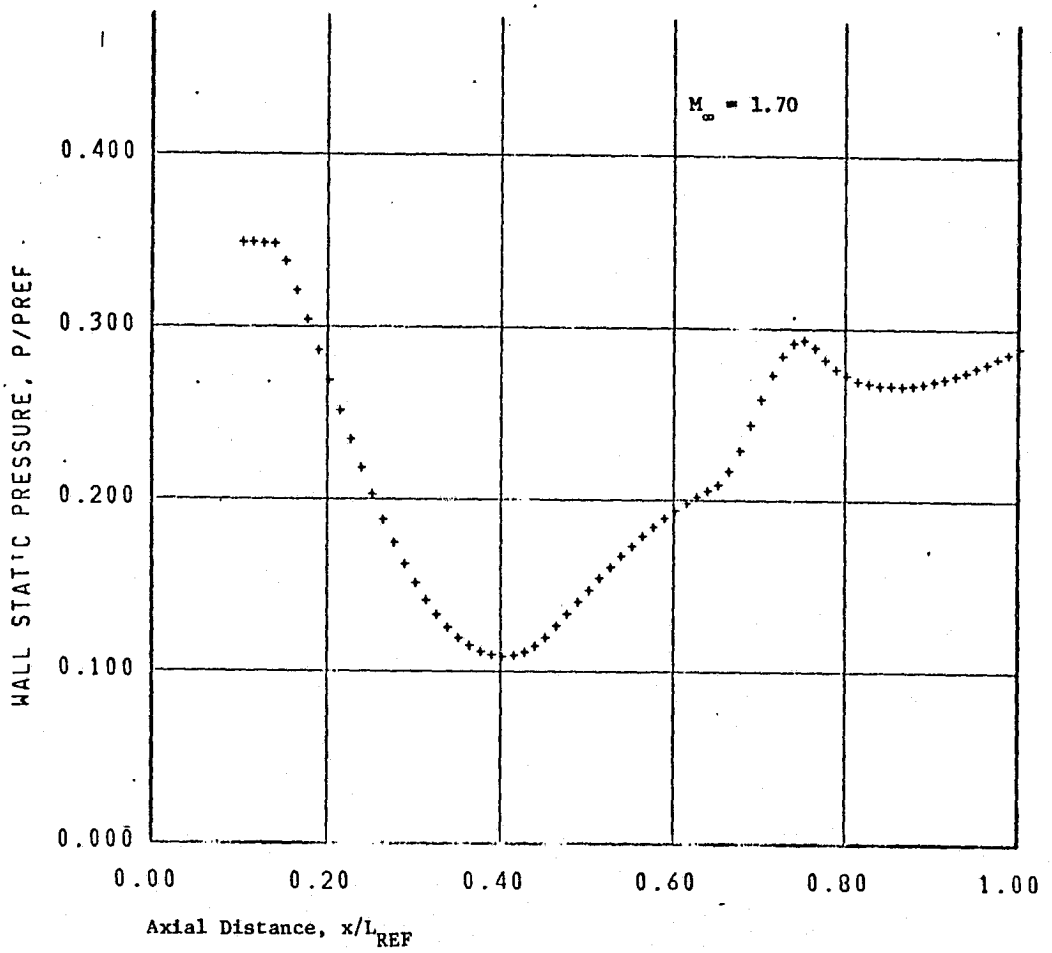

Figure 8(a) Wall Static Pressure Distribution for Waisted Body of Winter, Smith and Rotta (reference 8)

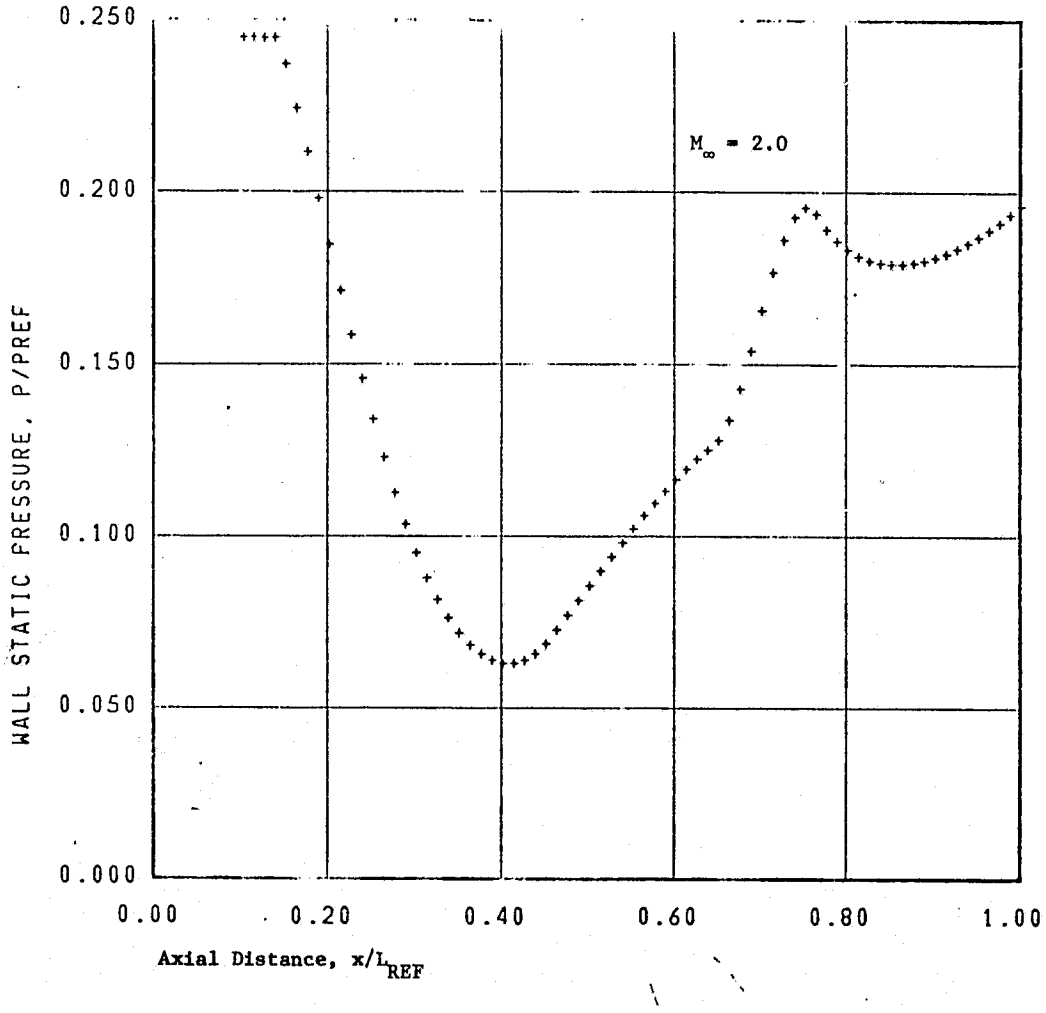

Figure 8(b) Wall Static Pressure Distribution for Waisted Body of Winter, Smith and Rotta (reference 8)

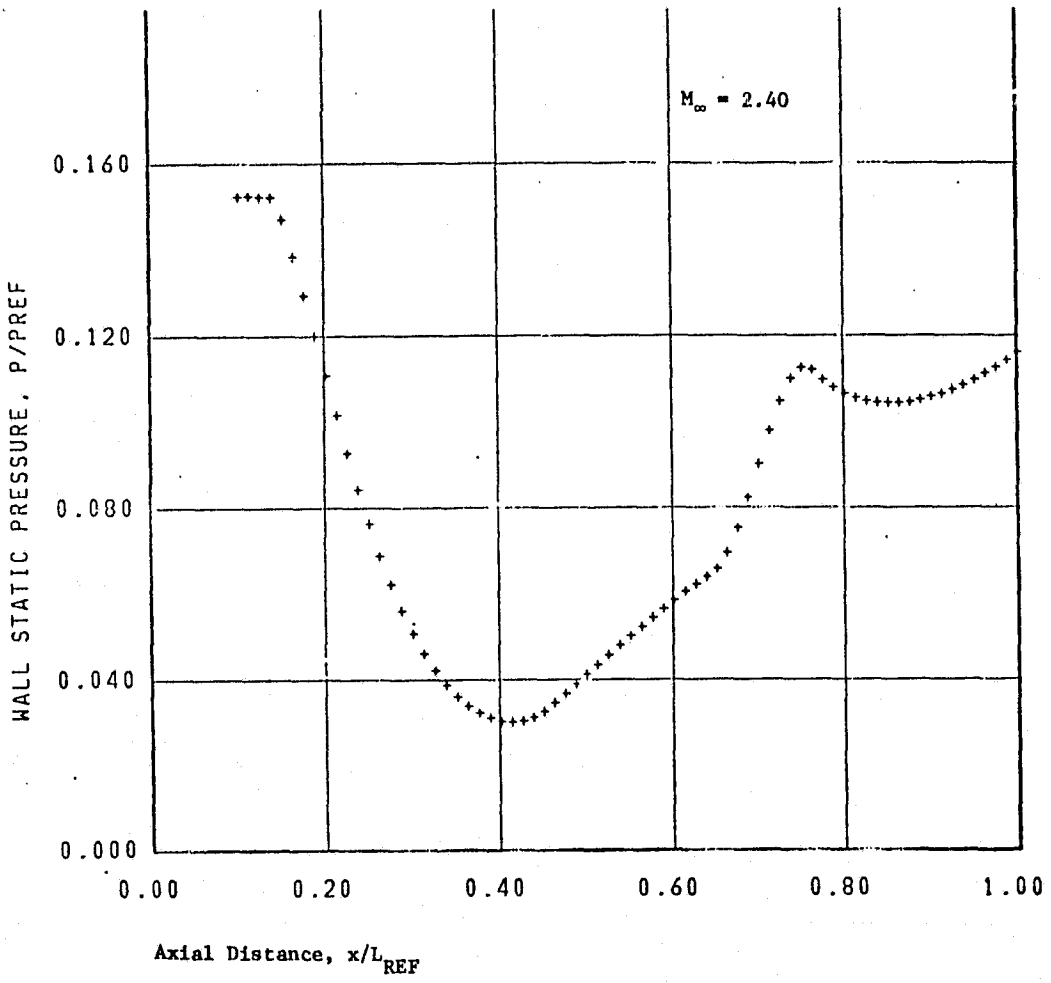

Figure 8(c) Wall Static Pressure Distribution for Waisted Body of Winter, Smith and Rotta (reference 8)

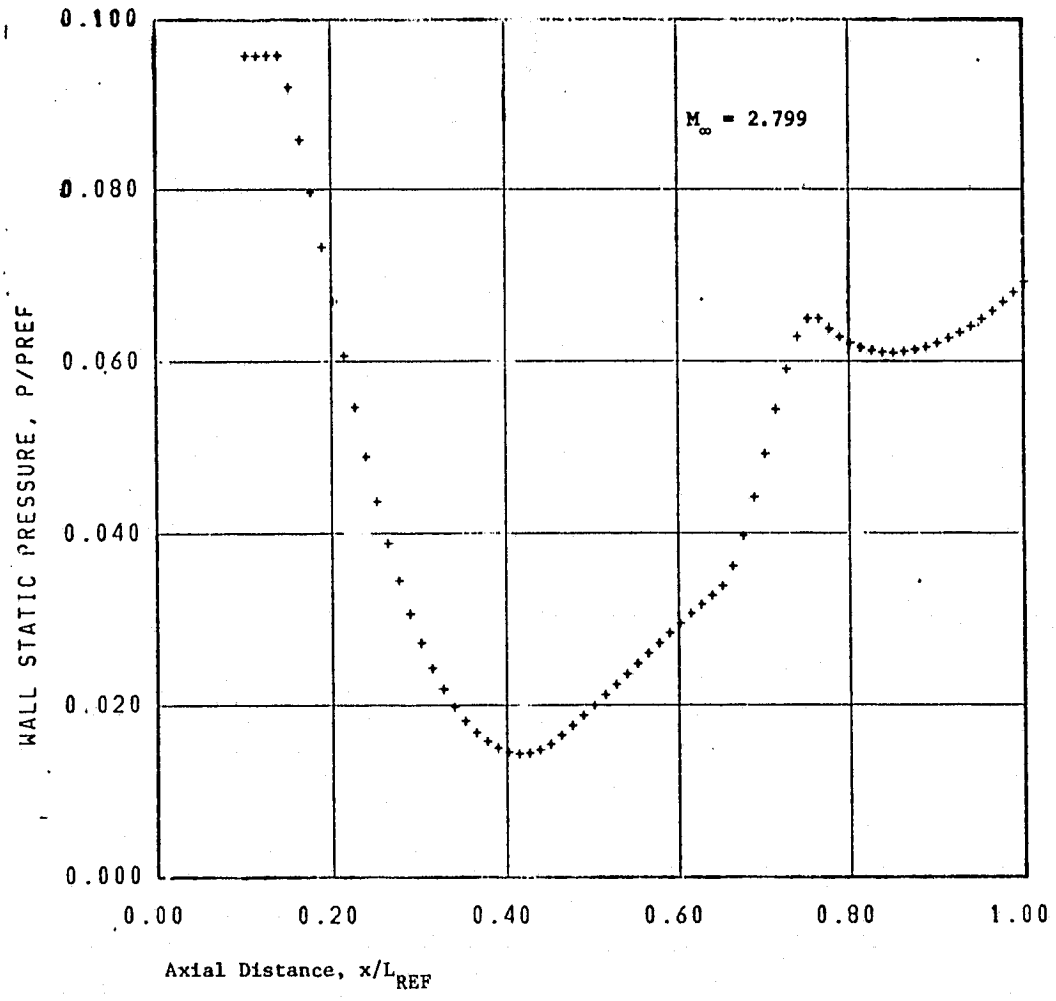

Figure 8(d) Wall Static Pressure Distribution for Waisted Body of Winter, Smith and Rotta (reference 8)

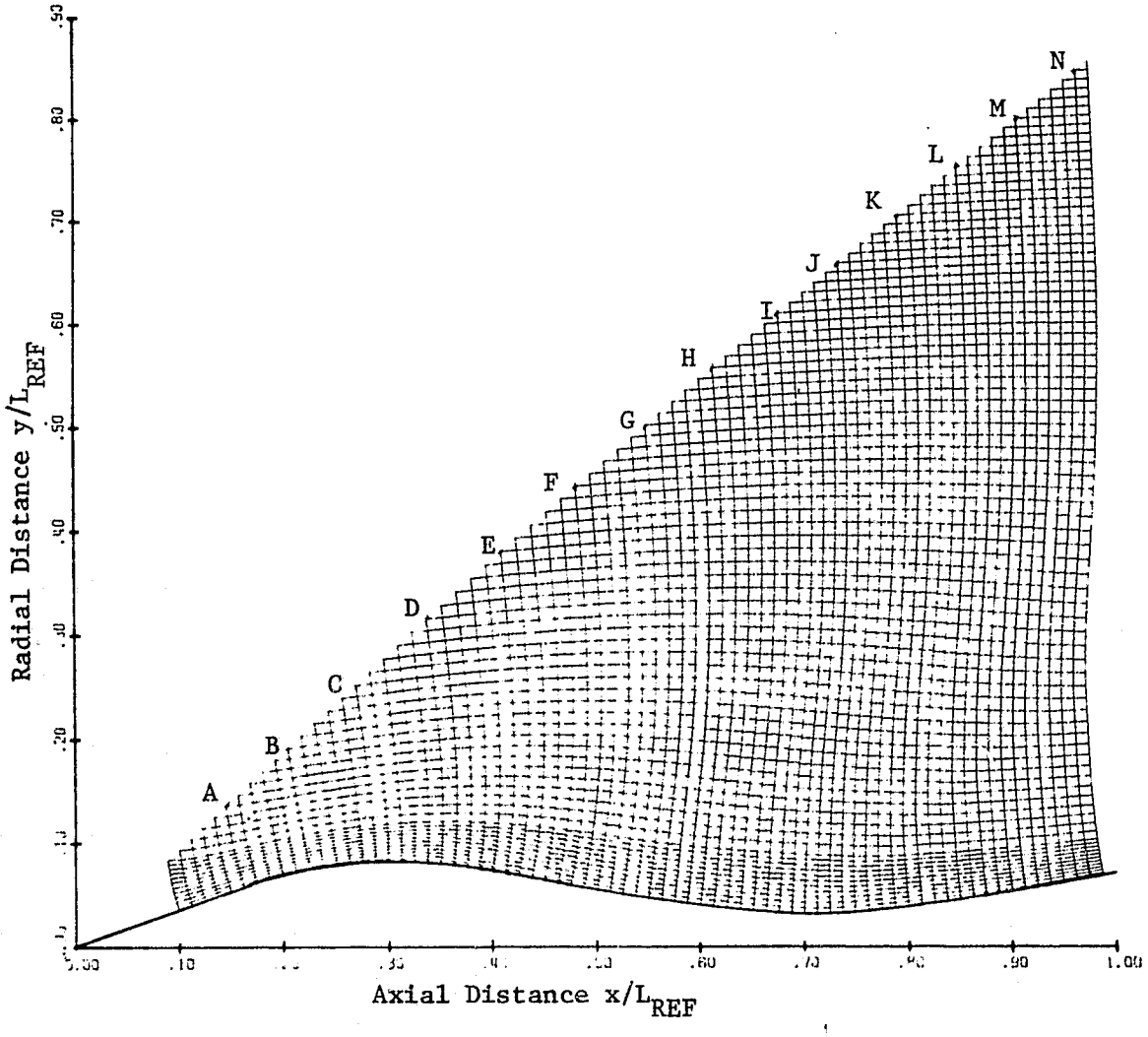

Figure 9 Streamline Patterns for the Waisted Body of Winter, Smith and Rotta (Ref. 8) at $M_\infty = 1.70$

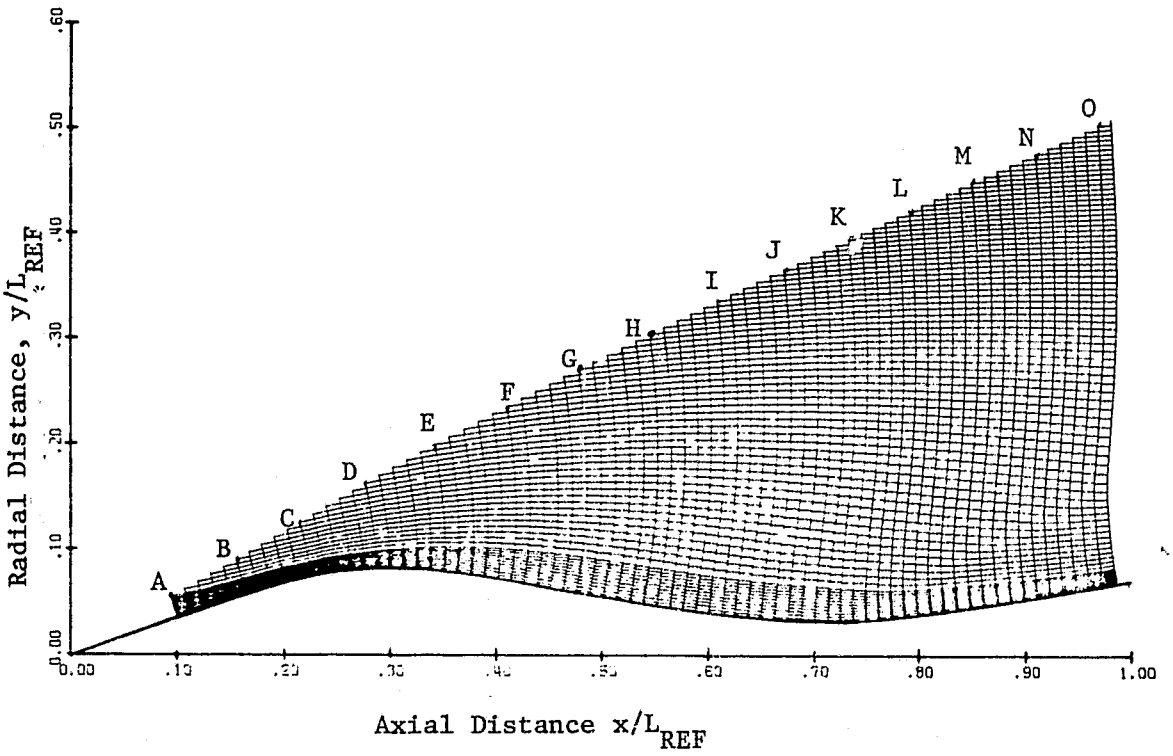

Figure 10 Streamline Patterns for the Waisted Body of Winter, Smith and Rotta (Ref. 8) at $M_\infty = 2.799$

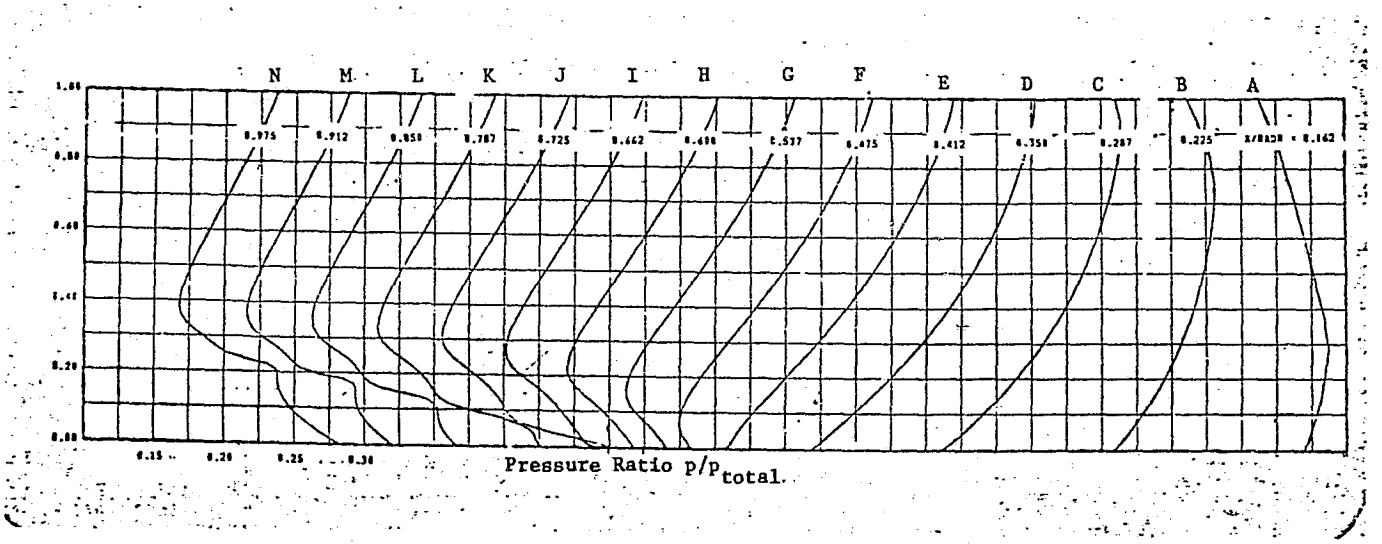

Figure 11(a) Static Pressure Distribution Across the Flowfield at M_∞ = 1.70

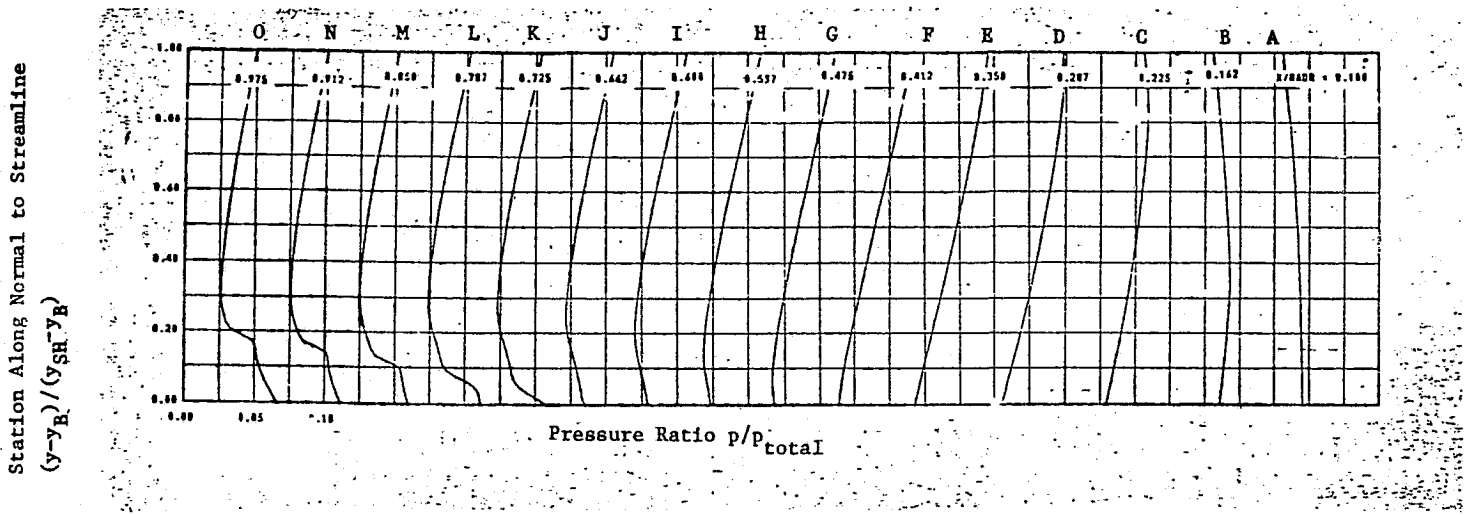

Figure 11(b) Static Pressure Distribution Across the Flowfield at $M_\infty = 2.799$

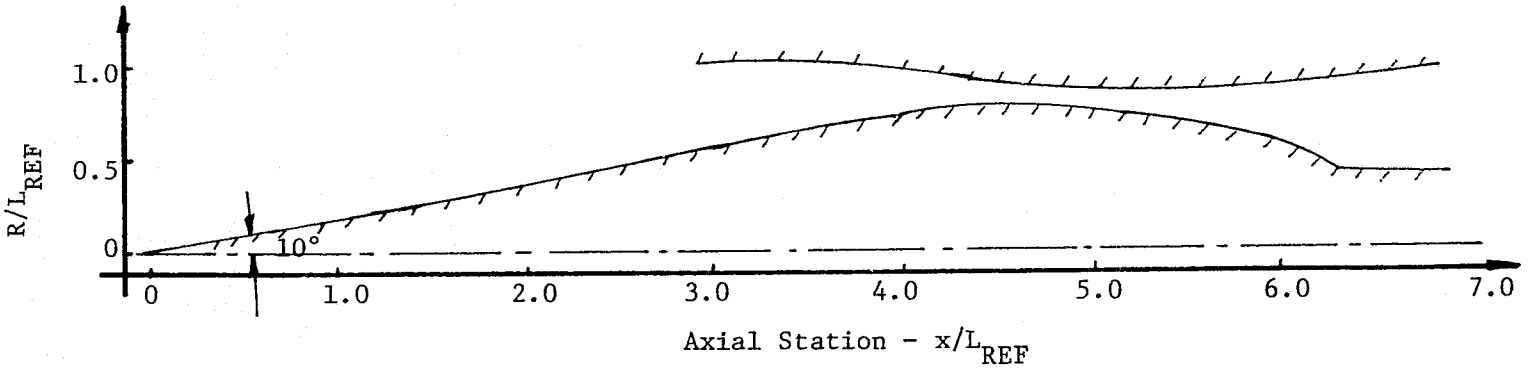

Figure 12 Geometry of Mach 3.5 Mixed Compression Inlet (Ref. 9)

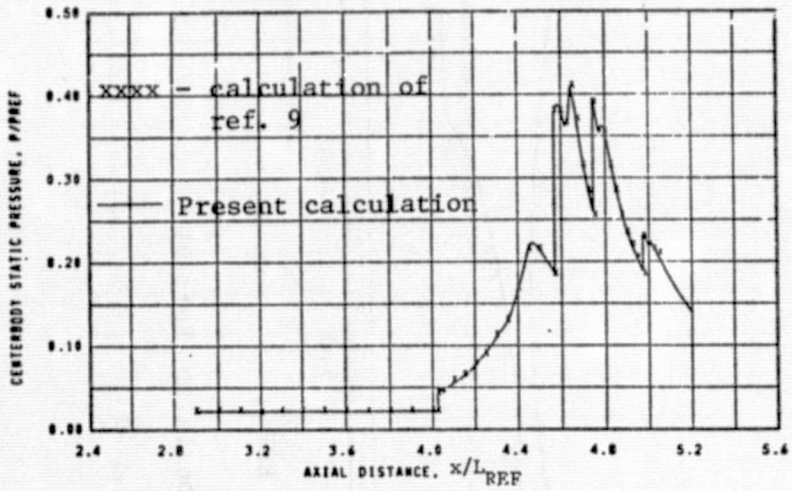

Figure 13 Static Pressure Distribution Along the Centerbody Surface at $M_\infty = 3.5$

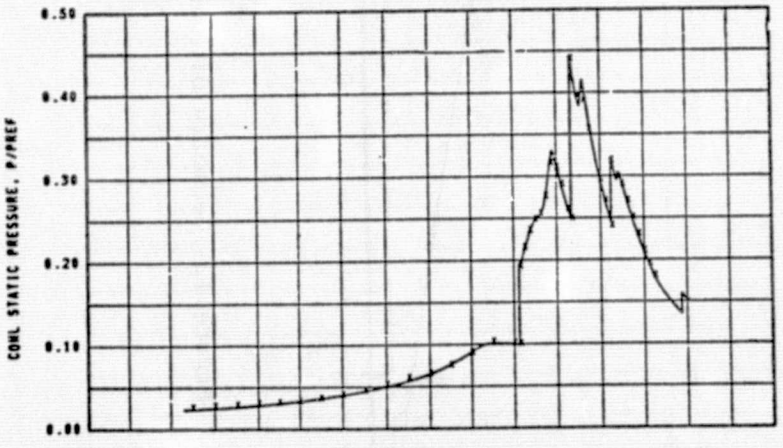

Figure 14 Static Pressure Distribution Along the Cowl Surface at $M_\infty = 3.5$

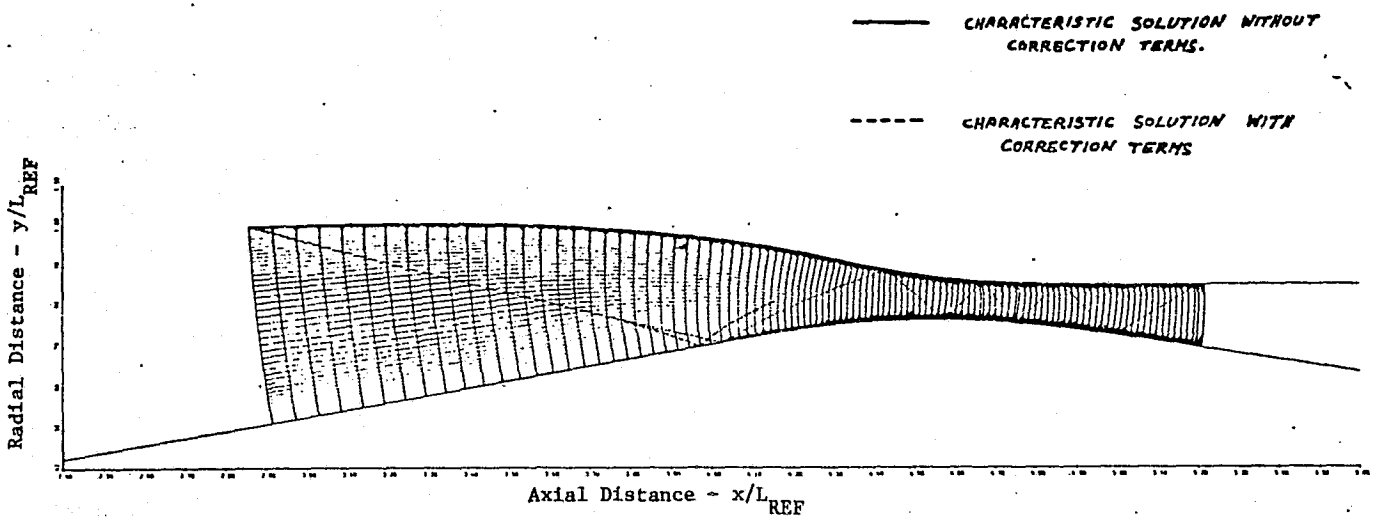

Figure 15 Outer Region Solution for the Mixed Compression Inlet (Ref. 9) at $M_\infty = 3.5$

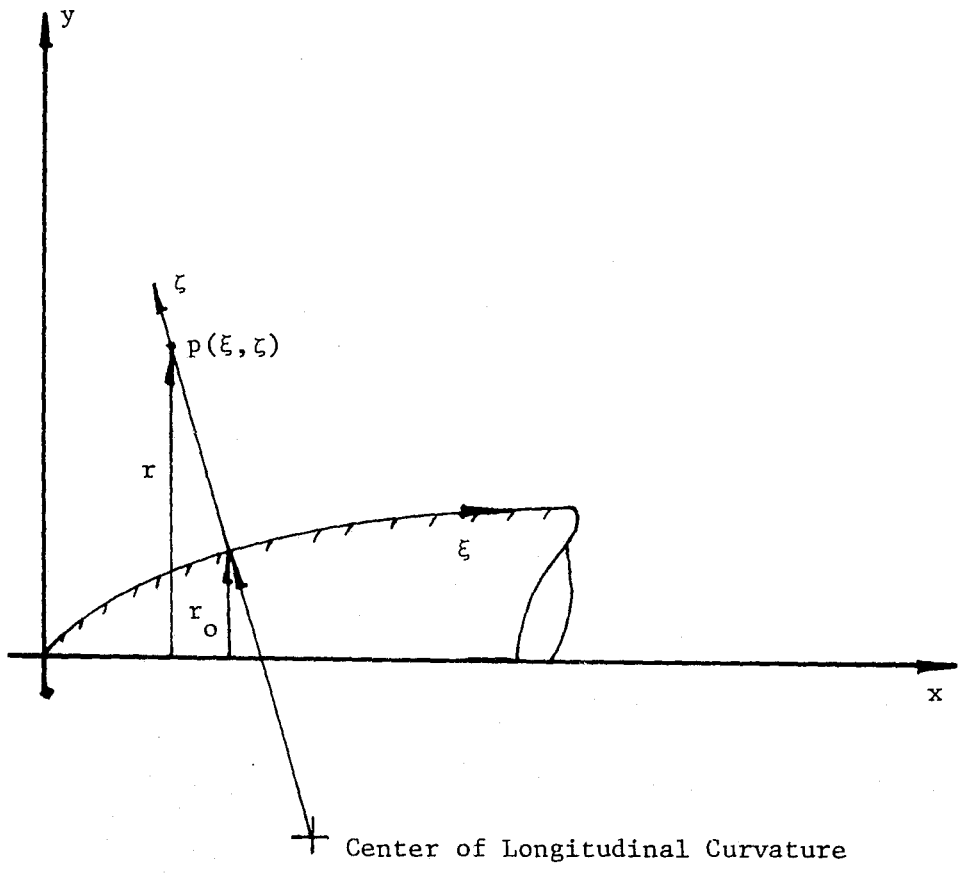

Figure 16 Coordinate System for Inner Region

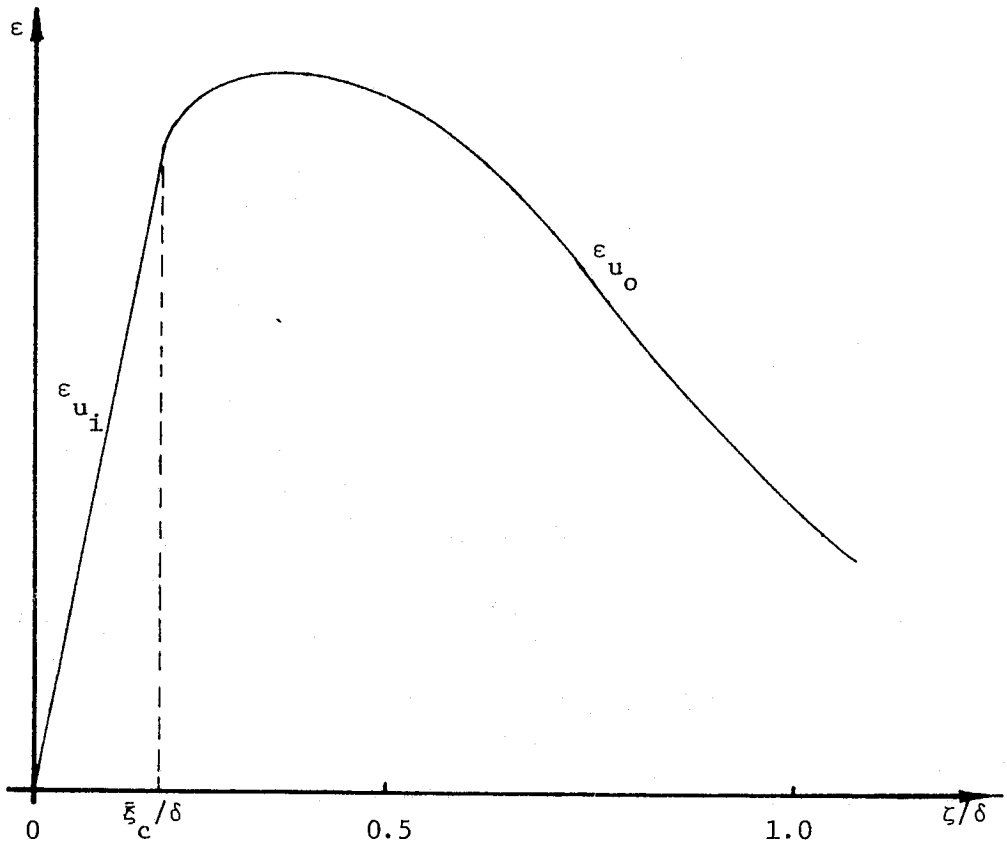

Figure 17 Scalar Eddy Viscosity Distribution

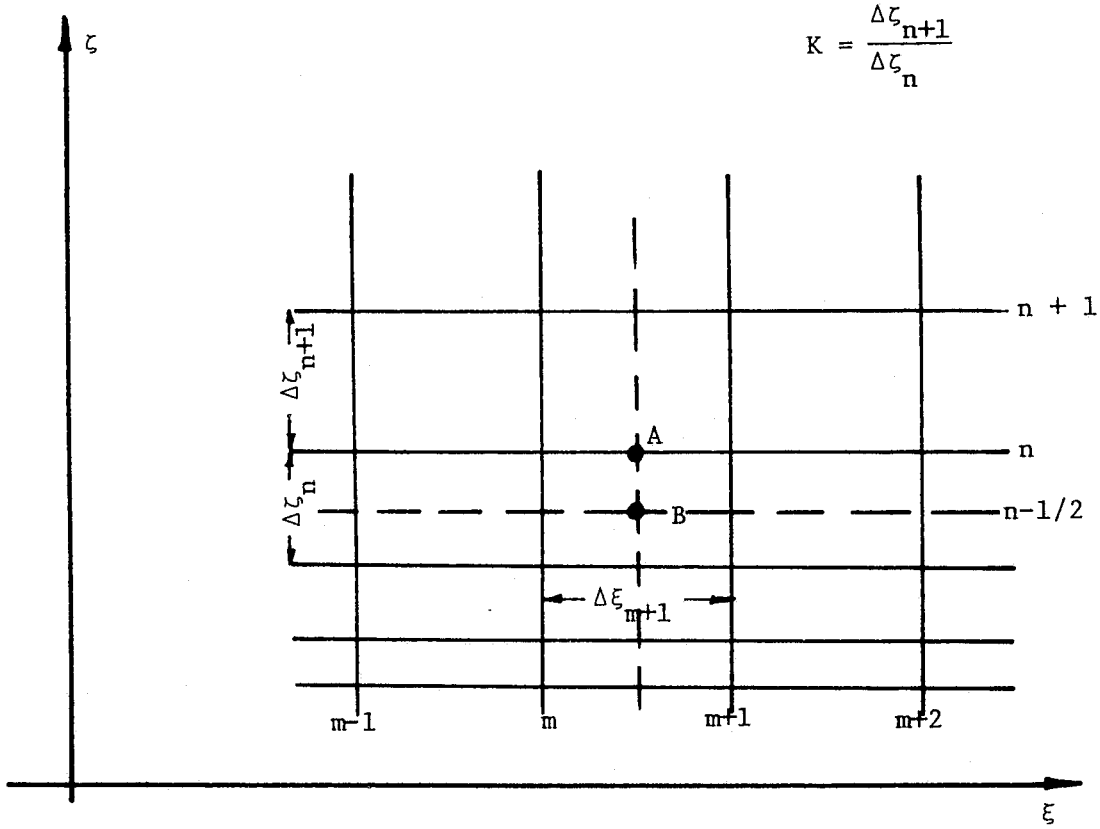

Figure 18 Computational Grid Scheme for Inner Region

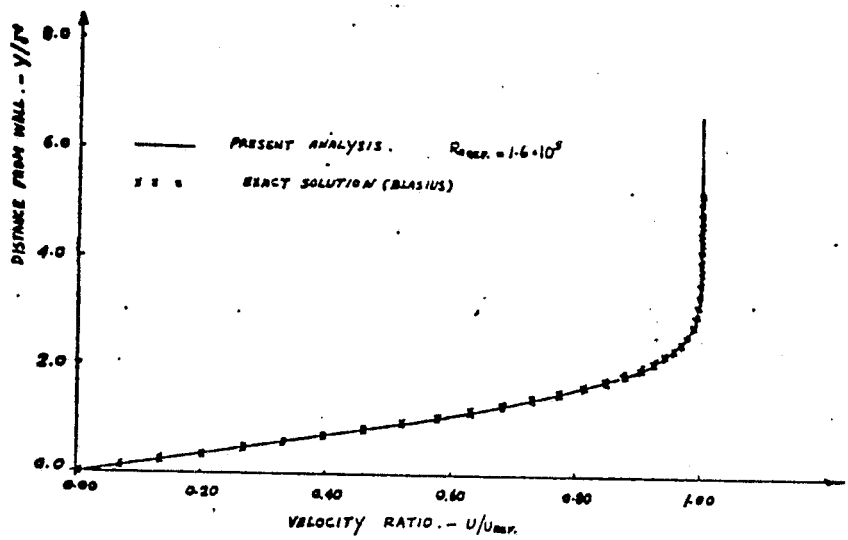

Figure 19 Longitudinal Velocity Profile for Flat Plate Laminar Boundary Layer at $M_\infty = 0$

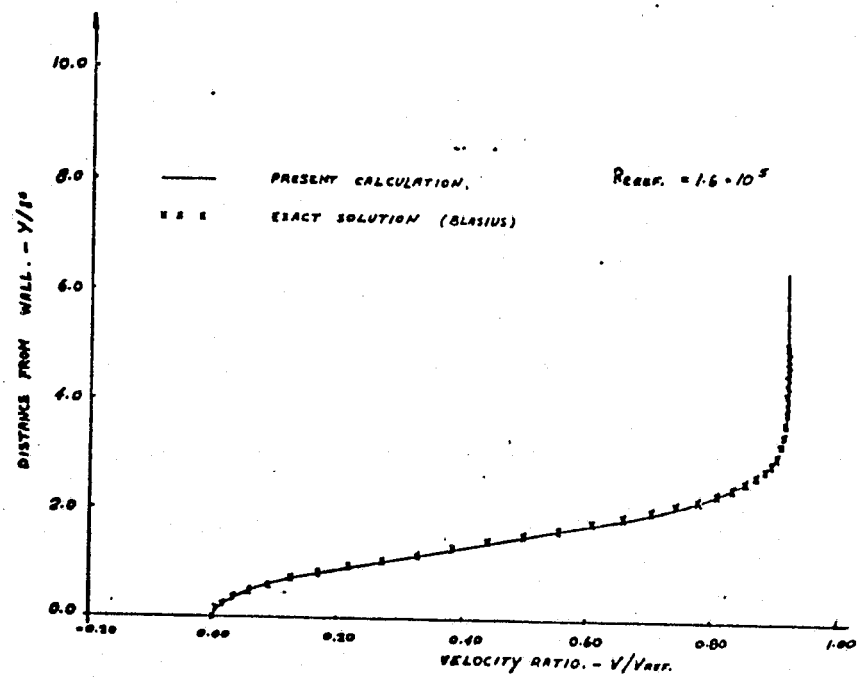

Figure 20 Normal Velocity Profile for Flat Plate Laminar Boundary Layer at $M_\infty = 0$

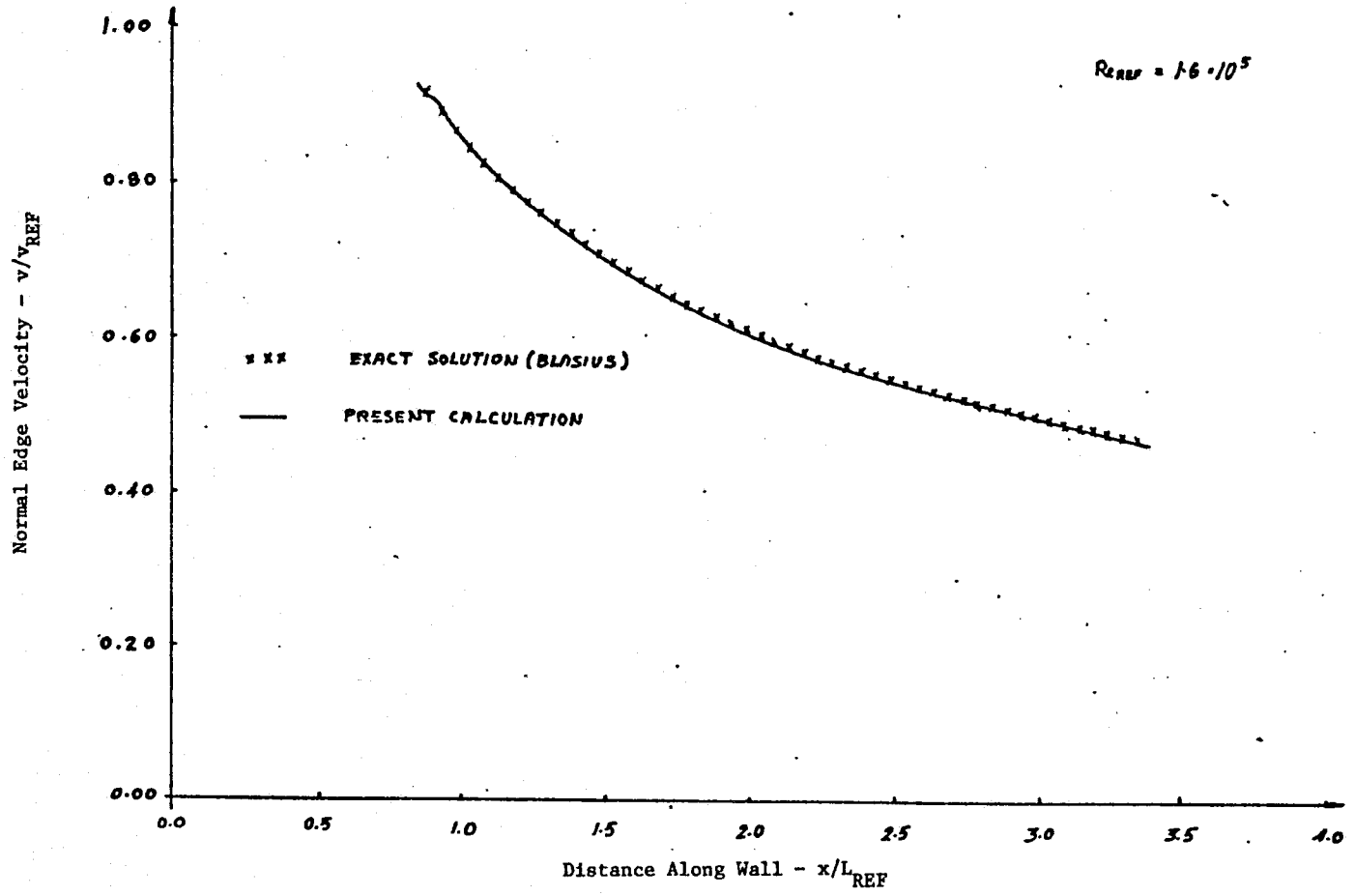

Figure 21 Normal Velocity Distribution at the Edge of Flat Plate Laminar Boundary Layer at $M_\infty = 0$

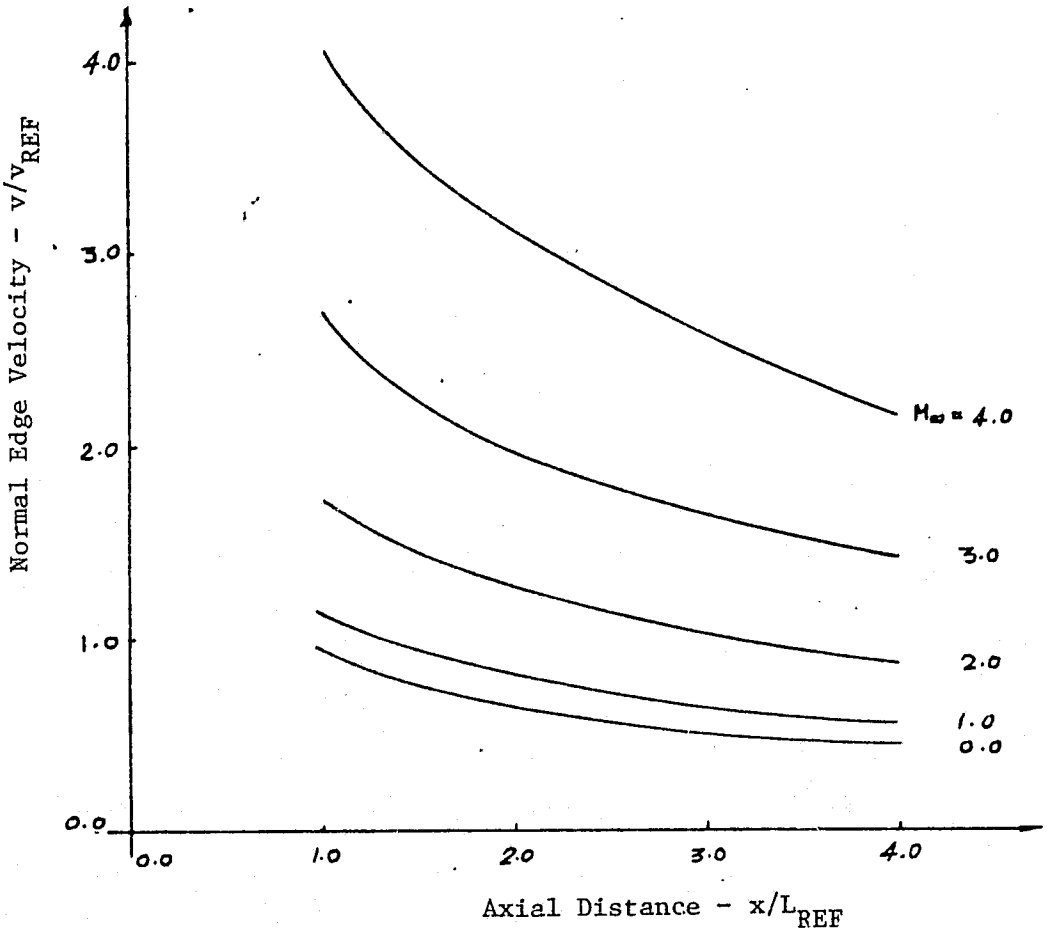

Figure 22 Normal Distribution at the Edge of Compressible Flat Plate Boundary Layer

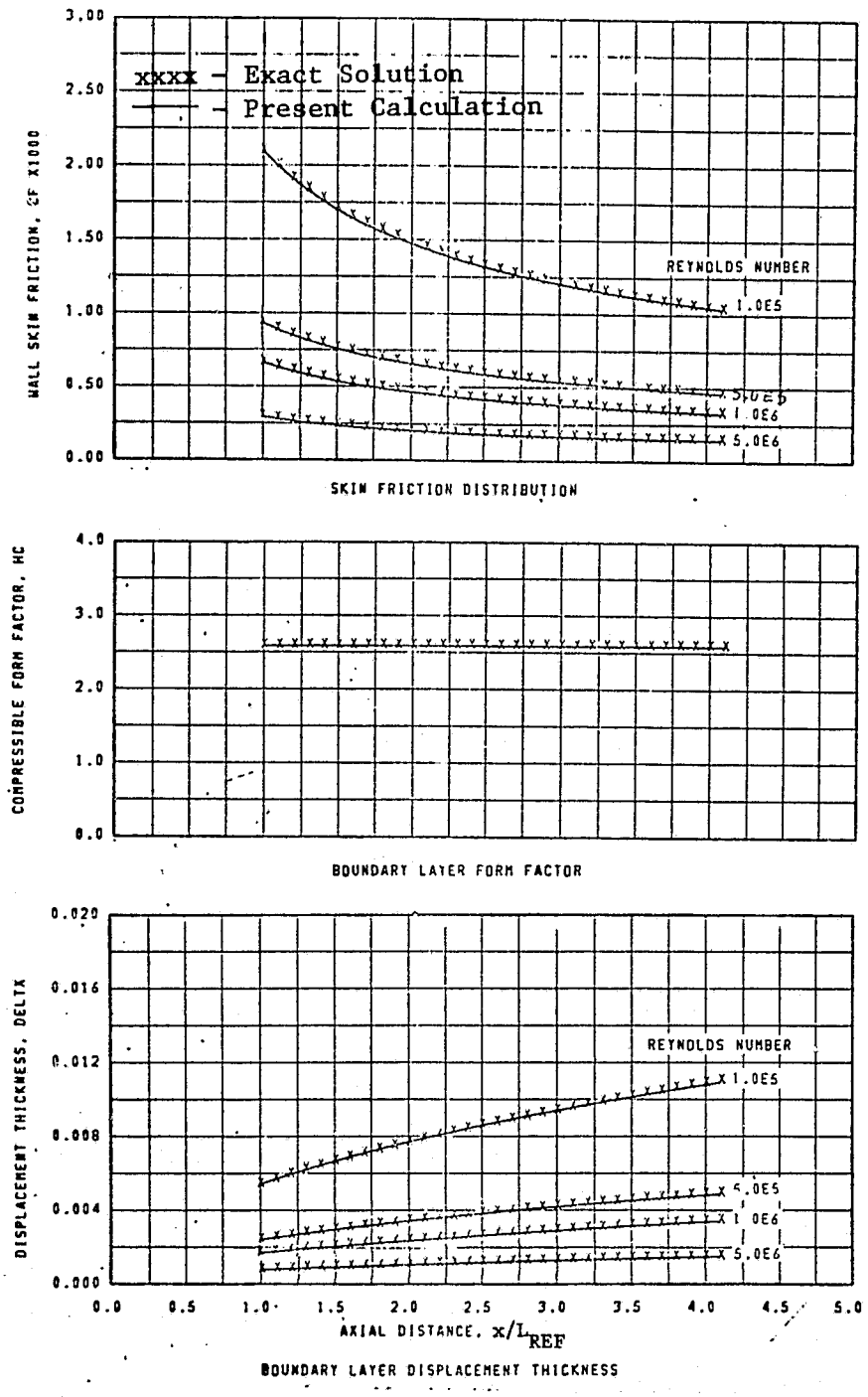

Figure 23 Displacement Thickness, Form Factor and Skin Friction Distribution for Flat Plate Boundary Layer at $M_\infty = 0$

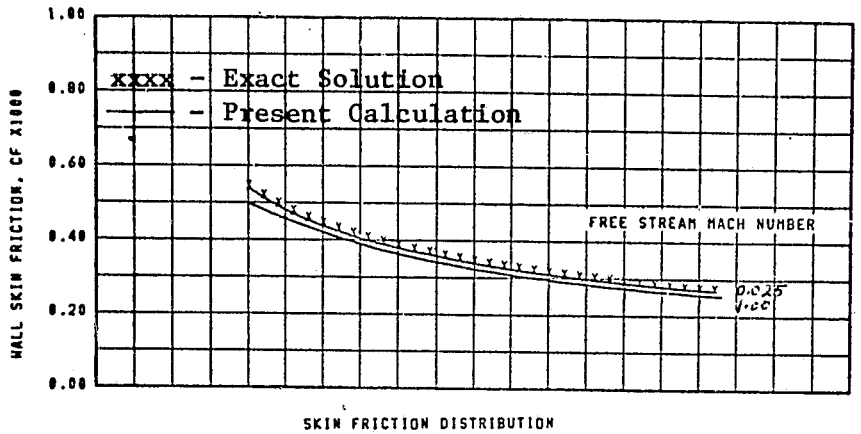

SKIN FRICTION DISTRIBUTION

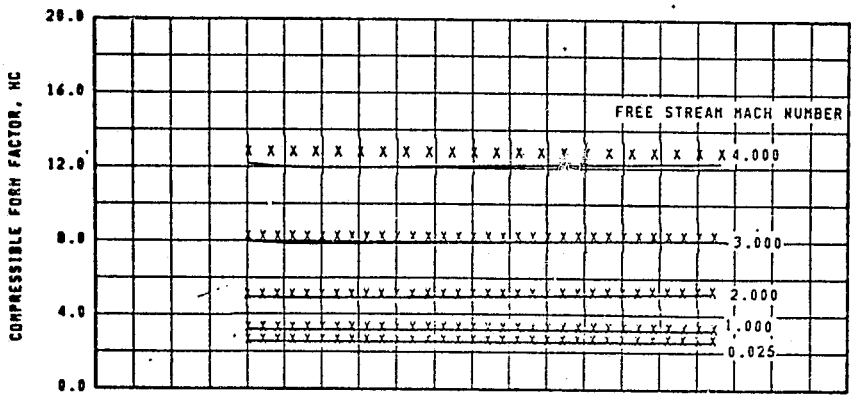

BOUNDARY LAYER FORM FACTOR

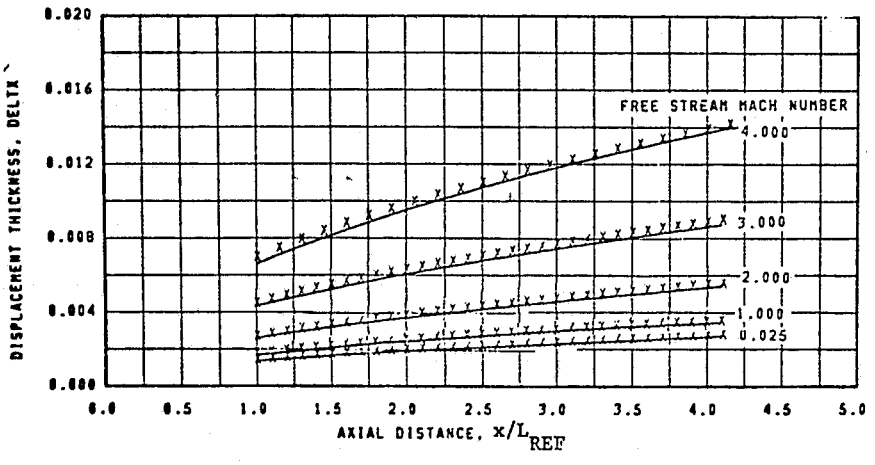

BOUNDARY LAYER DISPLACEMENT THICKNESS

Figure 24 Displacement-Thickness, Form Factor and Skin Friction. Distribution for Flat Plate Compressible Boundary Layer at $Re_{REF} = 1.5.\ 10^6$

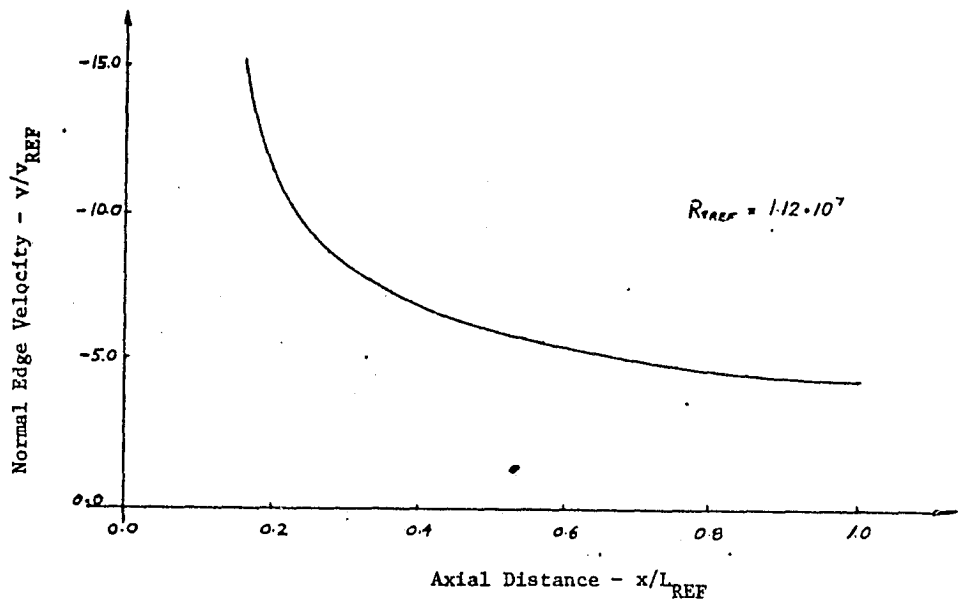

Figure 25 Normal Velocity Distribution at the Edge of Compressible Laminar Boundary Layer Over 20 Degree Half Angle Cone at $M_\infty = 2.80$

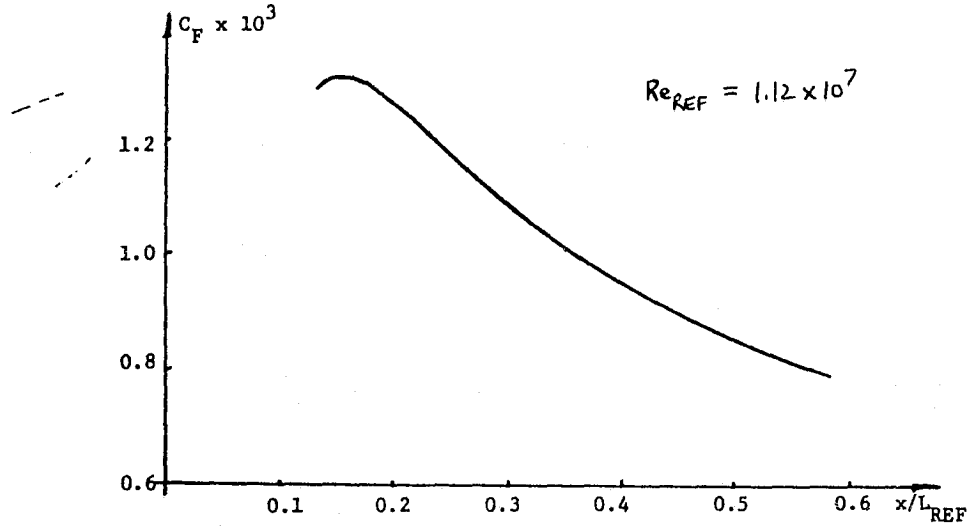

Figure 26 Skin Friction Distribution of Compressible Laminar Boundary Layer Over 20 Degree Half Angle Cone at $M_\infty = 2.799$

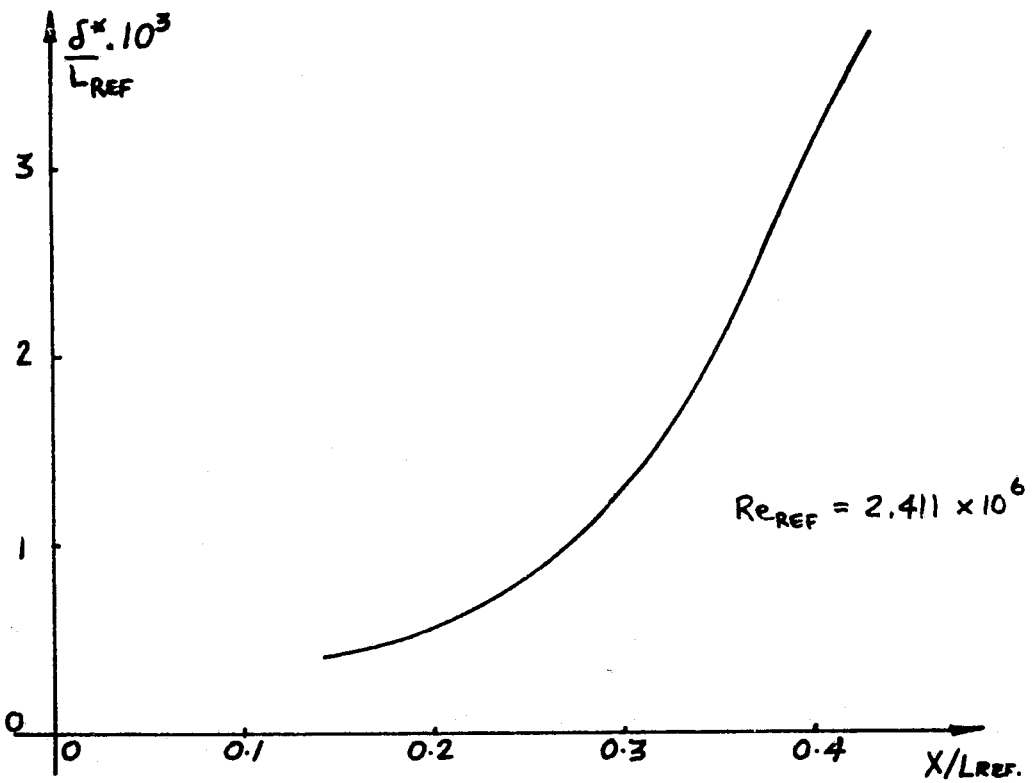

Figure 27 Displacement Thickness Distribution over Waisted Body at $M_\infty = 2.799$

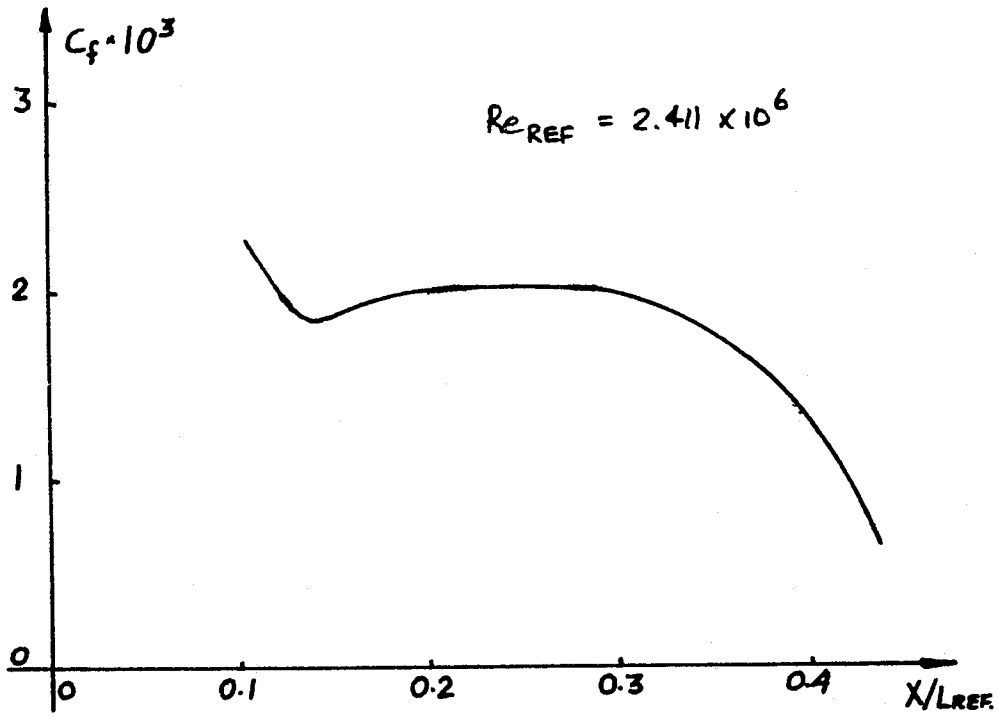

Figure 28 Skin Friction Distribution over Waisted Body at $M_\infty = 2.799$

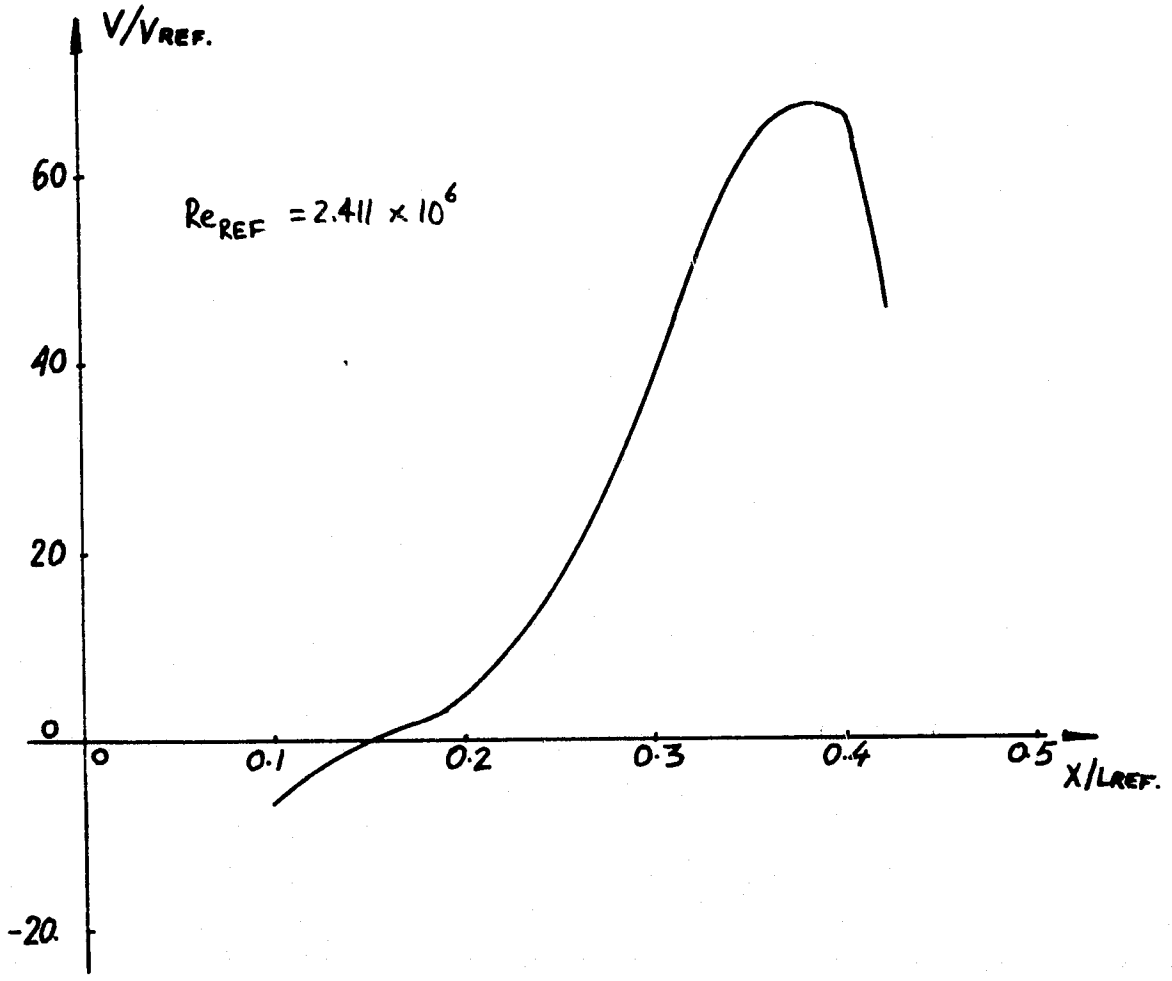

Figure 29 Normal Velocity at the Edge of the Boundary Layer Over Waisted Body at $M_\infty = 2.799$

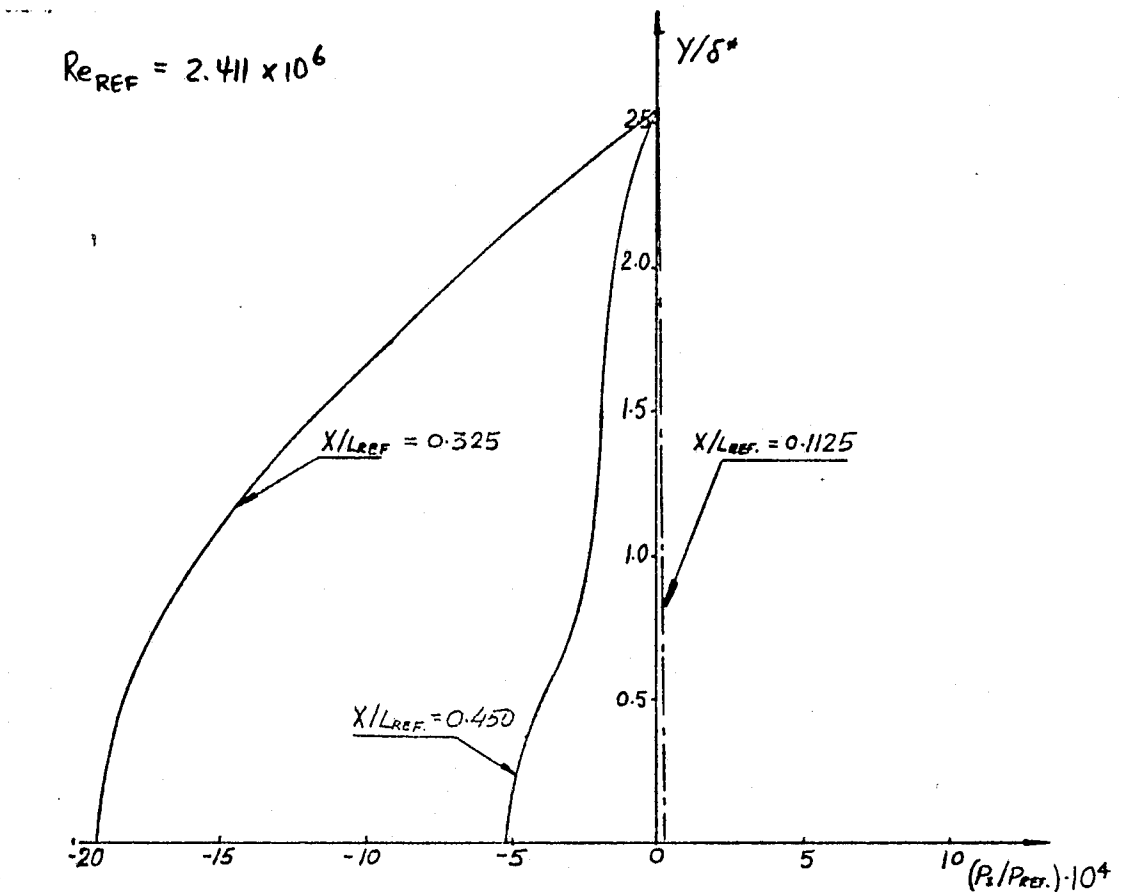

Figure 30 Pressure Distribution Across Boundary Layer Over Waisted Body at $M_\infty = 2.799$

$$\left|\frac{P_{IN} - P_{W_{INV}}}{P_{W_{INV}}}\right| \times 100 = 0.2 \quad \text{at } x/L_{REF} = 0.1125$$

$$\left|\frac{P_{IW} - P_{W_{INV}}}{P_{W_{INV}}}\right| \times 100 = 5.1 \quad \text{at } x/L_{REF} = 0.325$$

$$\left|\frac{P_{IW} - P_{W_{INV}}}{P_{W_{INV}}}\right| \times 100 = 1.0 \quad \text{at } x/L_{REF} = 0.450$$

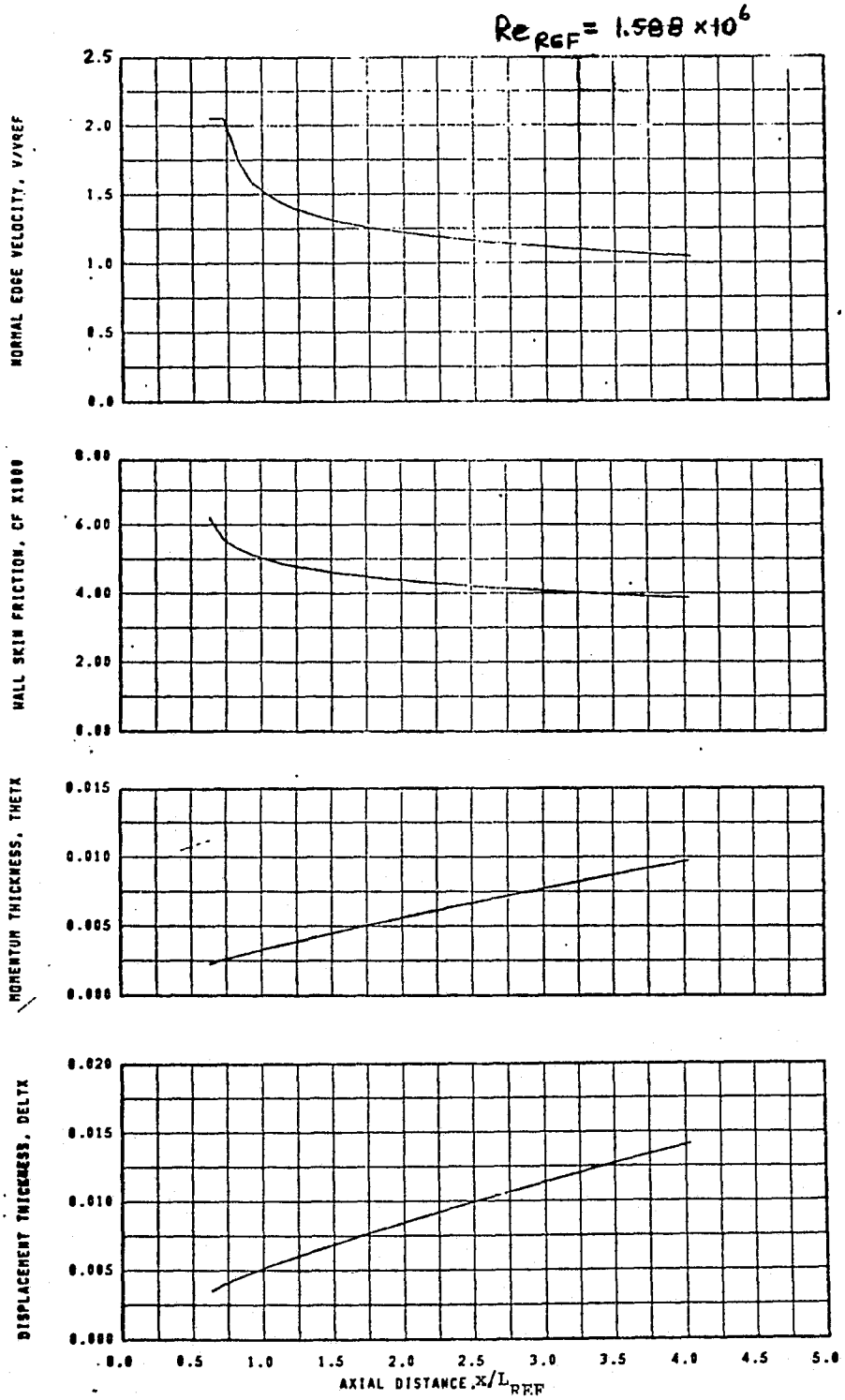

Figure 31 Displacement and Momentum Thicknesses, Skin Friction and Normal Edge Velocity Distributions for Turbulent Boundary Layer over Flat Plate at $M_\infty = 0$.

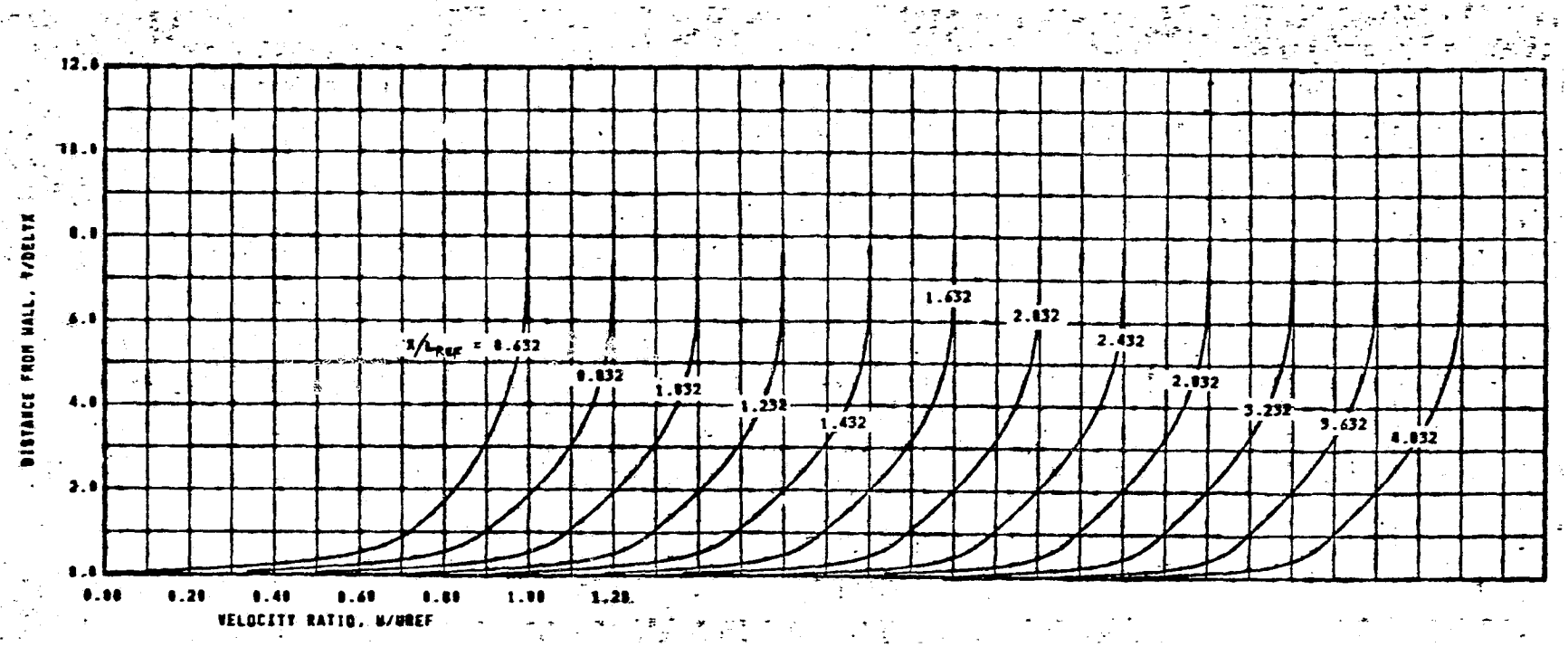

Figure 32(a) Longitudinal Velocity Profiles for Flat Plate Turbulent Boundary Layer at $M_\infty \approx 0$ and $Re_{REF} = 1.588 \times 10^6$

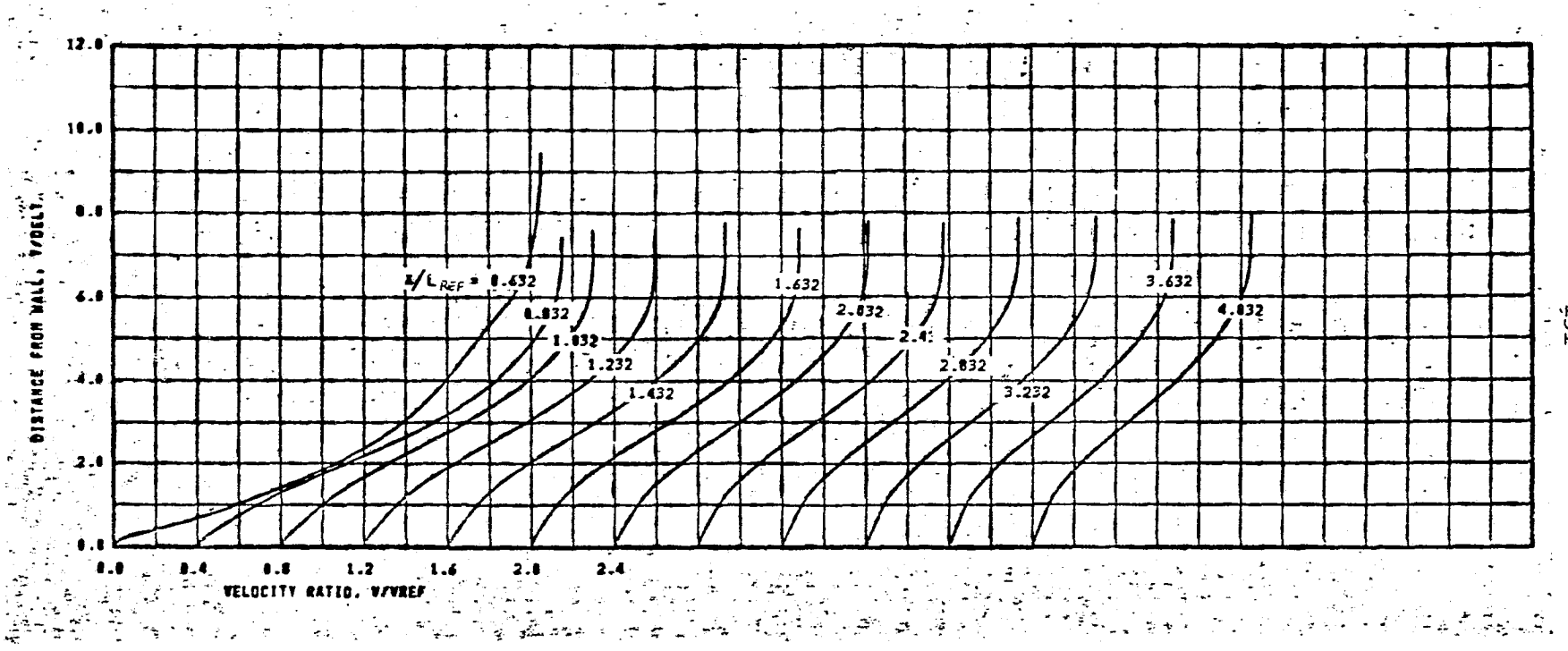

Figure 32(b) Normal Velocity Profiles for Flat Plate Turbulent Boundary Layer at $M_\infty \approx 0$ and $Re_{REF} = 1.588 \times 10^6$

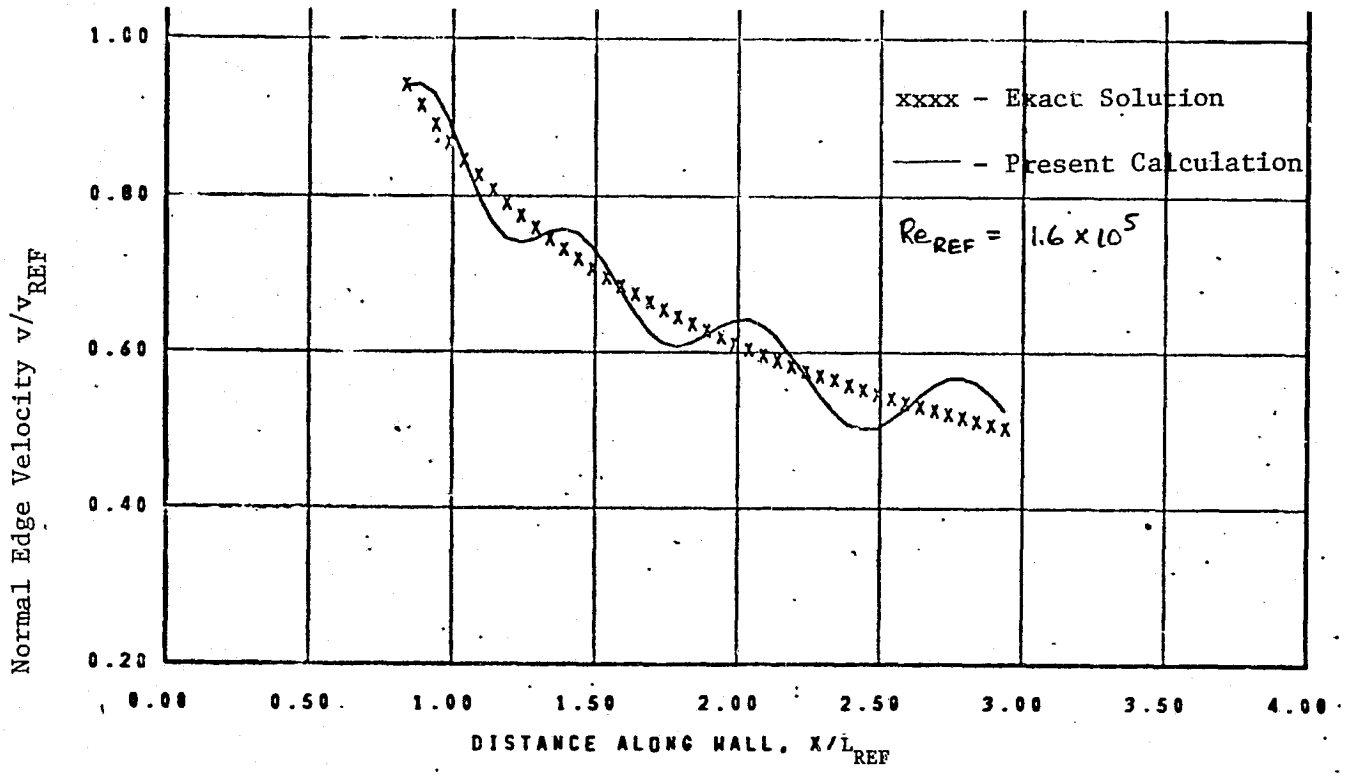

Figure 33 Normal Velocity Distribution at the Edge of Flat Plate Laminar Boundary Layer at $M_\infty \approx 0$ and $\lambda_c = 0.50$

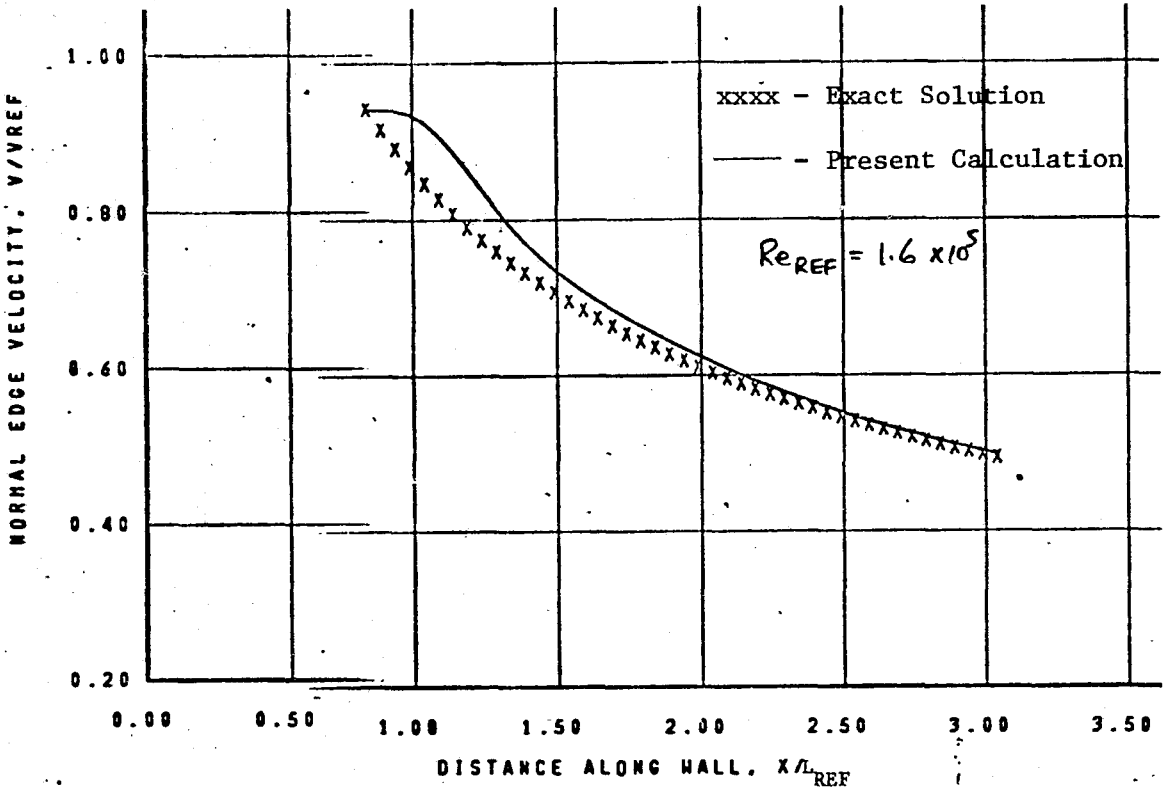

Figure 35 Normal Velocity Distribution at the Edge of Flat Plate Laminar Boundary Layer at $M_\infty \approx 0$ and $\lambda_c = 1.20$

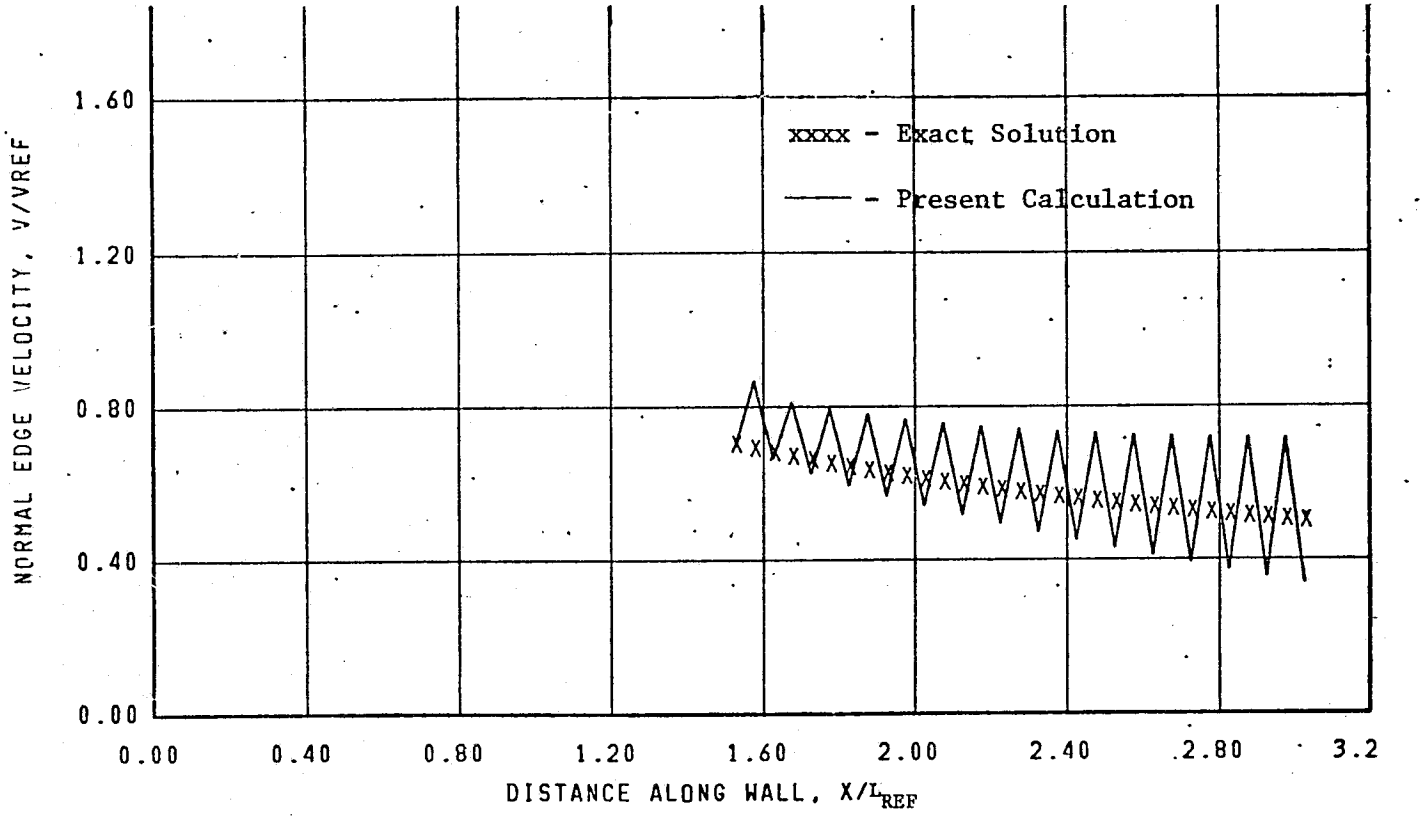

Figure 36 Normal Velocity Distribution at the Edge of Flat Plate Laminar Boundary Layer at $M_\infty = 0.50$ and $\lambda_c = 0.50$

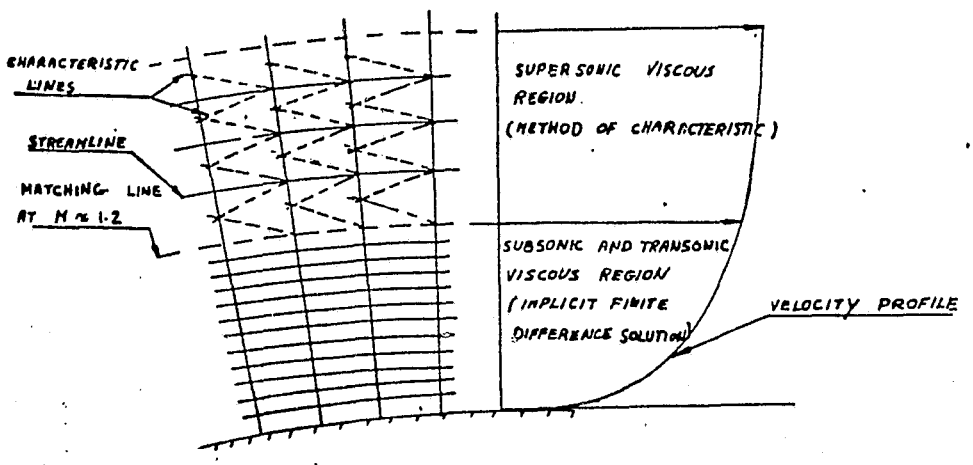

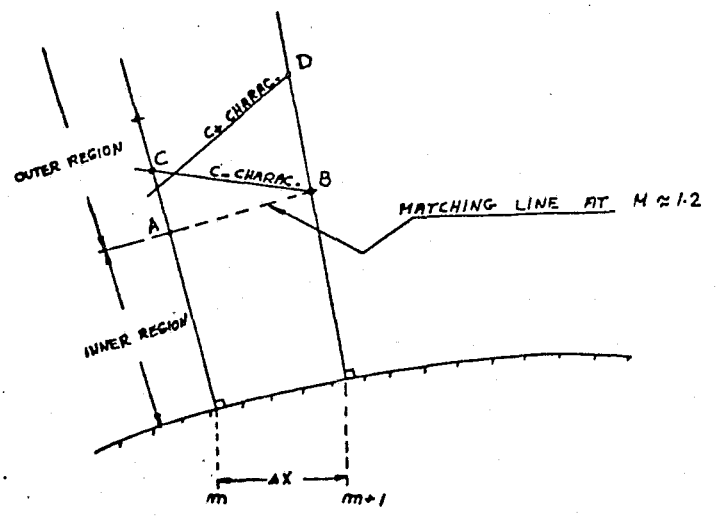

Figure 37 Schematic Illustration of Viscous-Inviscid Interaction Analysis

INTERACTIVE MODE - FLOW DIAGRAM

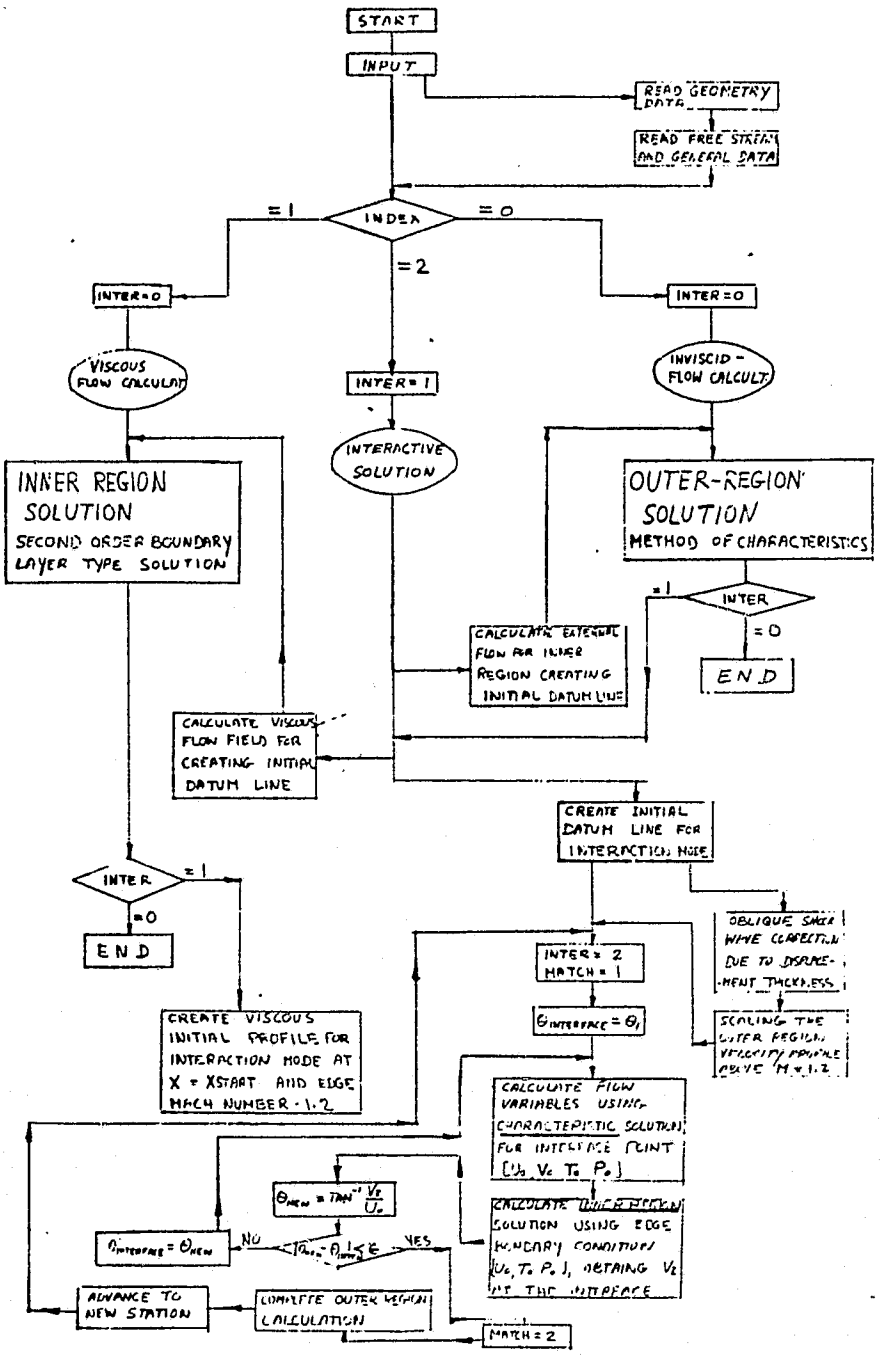

Figure 38 Flow Diagram for the Interactive Mode Computer Program

OUTER REGION - FLOW DIAGRAM

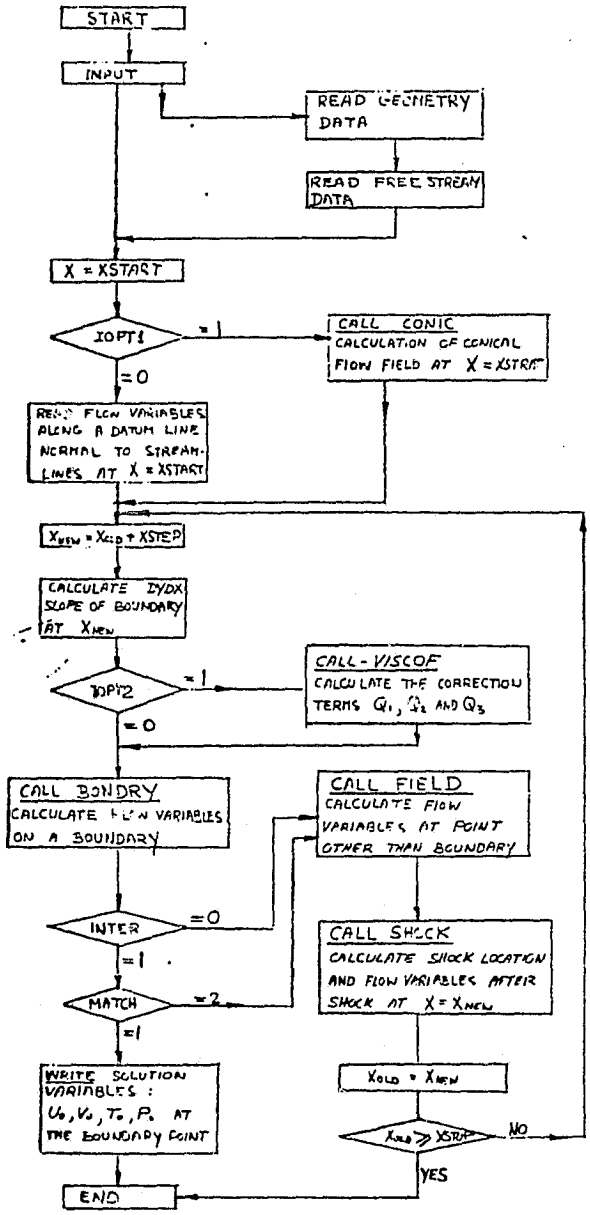

Figure 39 Flow Diagram for the Outer Region Computer Program

INNER REGION - FLOW DIAGRAM

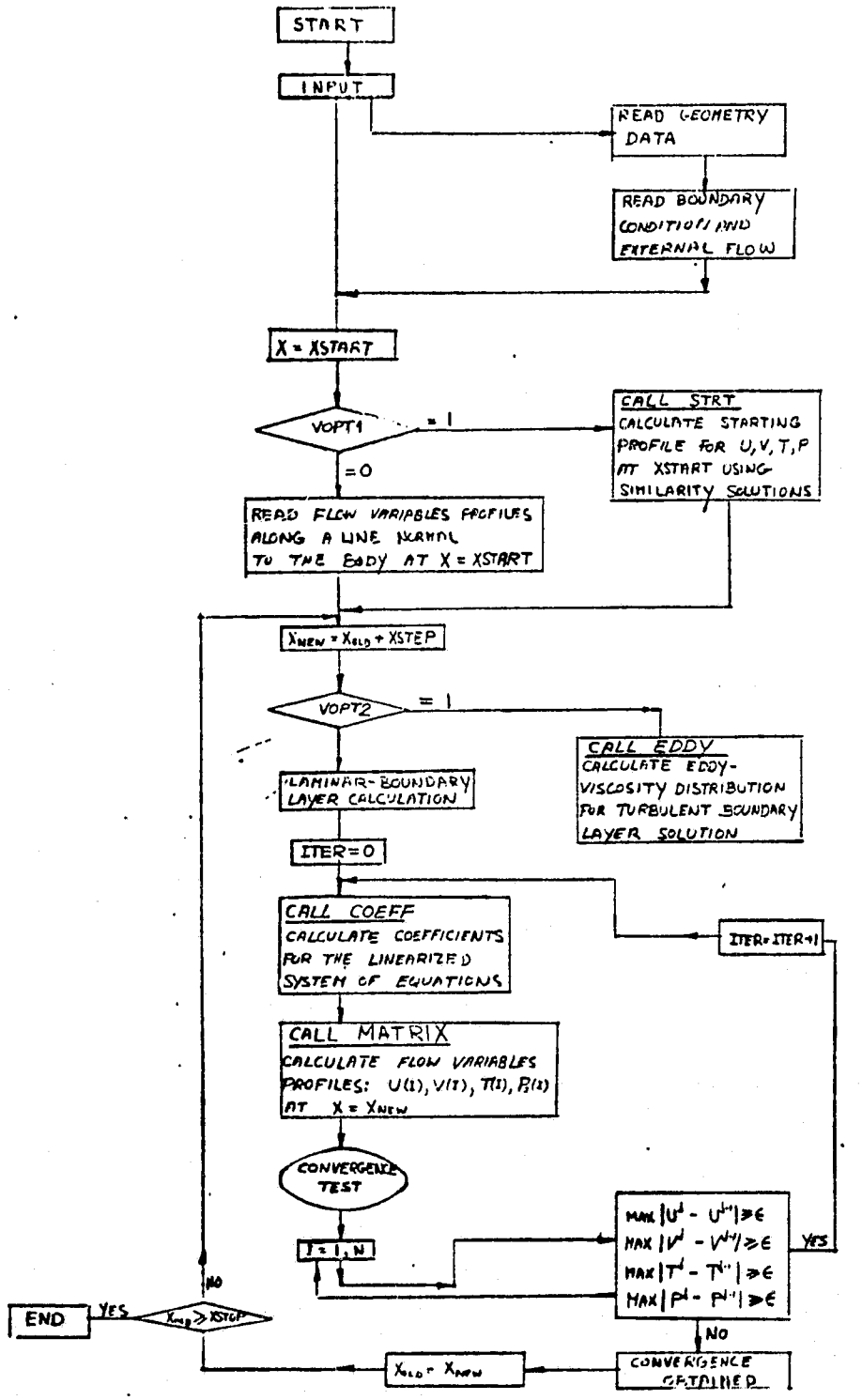

Figure 40 Flow Diagram for the Inner Region Computer Program

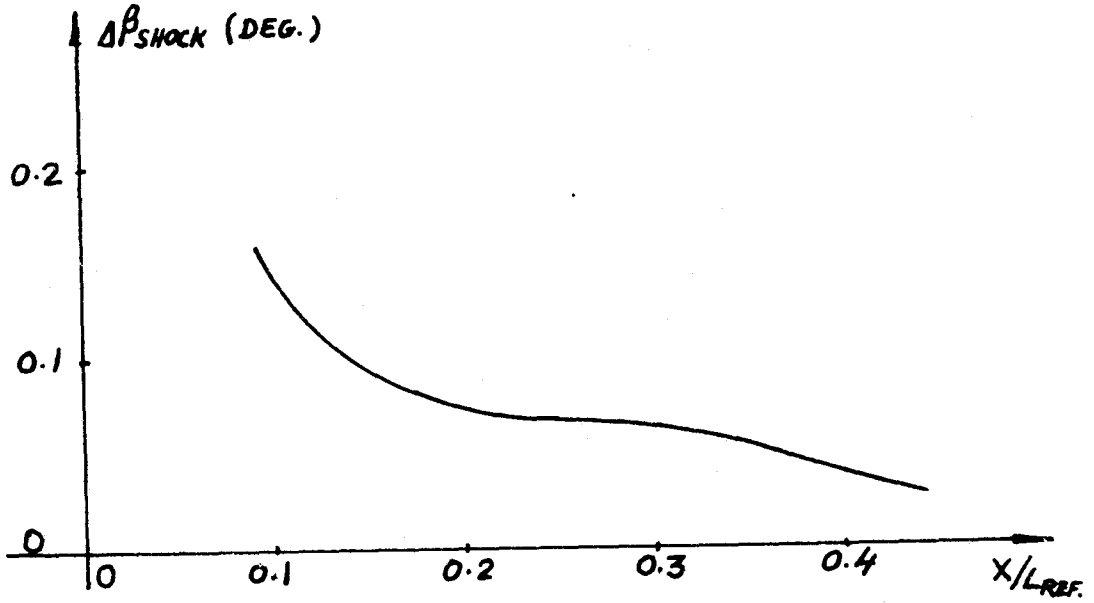

Figure 41 Shock Angle Difference Distribution for 20 Degree Half Cone Angle at $M_\infty = 2.80$

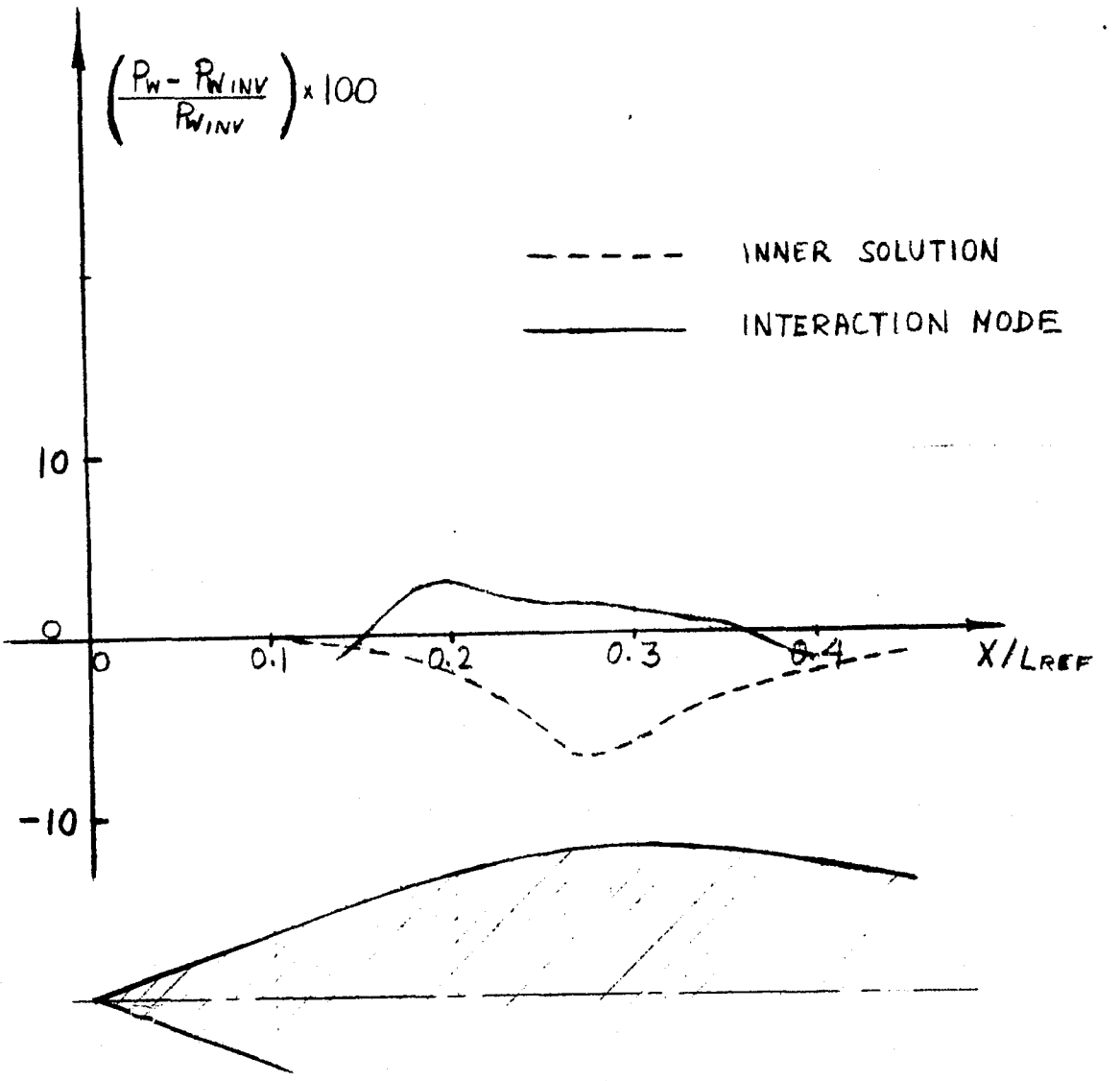

Figure 42 Wall Static Pressure Difference Along the Waisted Body of Winter, Smith and Rotta (reference 8) at $M_\infty = 2.80$.

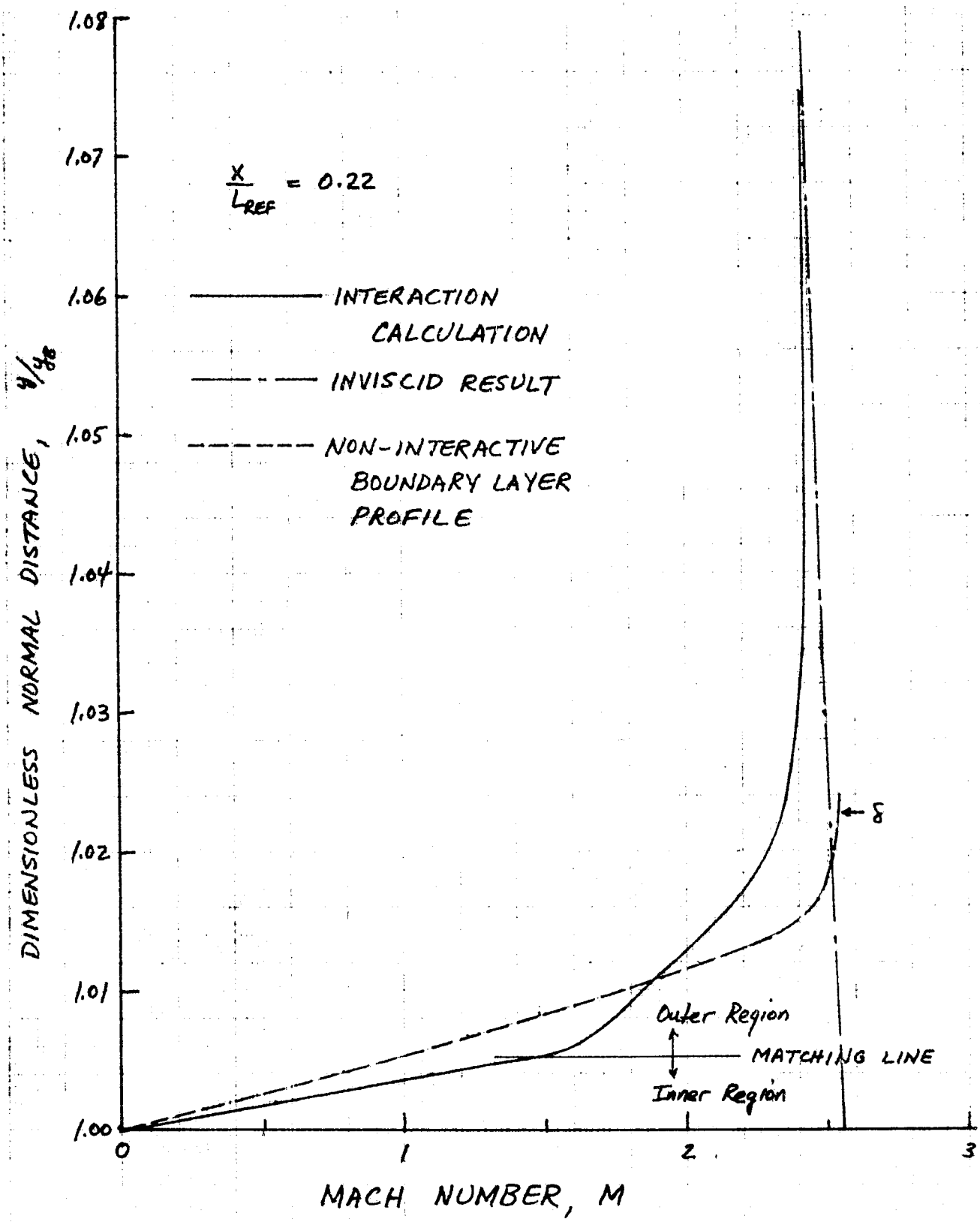

Figure 43 Mach Number Distribution Across the Two Regions for the Waisted Body of Winter, Smith and Rotta (ref. 8) at $M_\infty = 2.80$ ($y_{shock}/y_B = 1.67$)